MORPHOLOGICAL STABILIZATION OF LOWLAND RIVERS BY USING A SERIES OF GROYNES

MOHAMMED ALAUDDIN

Morphological Stabilization of Lowland Rivers by Using a Series of Groynes

A dissertation submitted in partial fulfillment of the requirements for the Degree of DOCTOR OF ENGINEERING

by

Mohammed ALAUDDIN

Supervised by

Professor Tetsuro TSUJIMOTO

DEPARTMENT OF CIVIL ENGINEERING
NAGOYA UNIVERSITY
JAPAN

September 2011

DEDICATION

This dissertation is dedicated to my parents, who introduced me to the joy of reading from birth, who not only tirelessly endured to lay down the foundation of but pursued my academic carrier with great moral support enabling such a study to take place today, whom I lost before this ending; also to all those who believe in the richness of learning.

TABLE OF CONTENTS

SYNOPSIS

Alluvial rivers at lowland as the Jamuna in Bangladesh are highly dynamic in nature; where huge landloss due to severe bank erosion at high flood as well as repeated interruptions of navigation system due to rapid sedimentation at low flow is very common. Groynes, revetments, and so on, are typically used to overcome these problems, but the suitable measure is yet to be accepted. In view of that, this study is aimed at improving the understanding in stabilization of lowland rivers.

Although the history of groynes is for long and their widespread use, the optimized design of new groynes is not attempted much, which is very important to treat the highly unstable lowland rivers. A completely blocked impermeable groyne suffers from instability of the structure itself; whereas, fully permeable structure can not divert the flow rightly. Recently, the concern about river environment has been added with groyne functions. Considering the present demands, the existing design of groynes is modified in both alignment and permeability to find the most suitable one for lowland river problems. Both numerical simulations and laboratory experiments are carried out in considering many aspects in the optimum design of groynes. Moreover, the large-scale sandbars resulted from the instability of loose sedimentary materials are very common features in lowland rivers. They make the channels highly unstable forming anabranches, influencing bank erosion, and so on. Thus the study on their formation processes, and their characteristics without and with groynes at natural scale becomes very urgent for better management of river engineering.

RIC-Nays, a two-dimensional model for flow and morphology, is utilized in this study upon confirmation through the detailed experimental data. The flow model is based on the depth-averaged shallow-water equations; the equations expressed in general coordinate system discretized by finite-difference method are solved on the boundary-

fitted structured grids for the unknown nodal values by an iterative process. Morphological computation involves a combination of flow fields, sediment transports, and channel-bottom changes along with bankline migration. Streamwise bed load is calculated by Ashida and Michiue formula; the effect of cross-gradient and the influence of secondary flow are then taken into account in accordance with Hasegawa and Engelund, respectively. In considering suspended sediment, an exponential profile of concentration is assumed. Itakura and Kishi's formula is utilized to calculate the entrainment rate, and the 2D advection-diffusion equations are used for planar distribution of depth-averaged concentration. Finally the bed deformation is determined using the 2D sediment continuity equation. In treating the bankline migration: when computations show that due to currents and scour, the cross-sectional slope angle of the riverbank exceeds the angle of repose, the sediment is assumed to be momentarily eroded up to the point of this angle, and bank erosion will progress. It is then included in the computation of the channel bed evolution as a supply of sediments from the banks.

Construction of a single groyne has only local effect on the flow and the river system. Therefore, the series of groynes are considered in this study to achieve better effect in both bank protection and navigation point of view; hence to increase the efficiency and enlarge the improved river stretch to be useful in engineering practices. To explore the most suitable design of groynes for lowland rivers, first, numerical investigations are made to examine the influence of various orientations and alignments of groynes. Schematized channel and flow parameters based on one of the subchannels of Jamuna are considered in the study. The channel responses from four different orientations and three different modified alignments are investigated to identify the most effective alignment.

Groynes are modified with various combinations of permeability for some selected alignments, and detailed laboratory experiments are conducted under clear-water scour condition to investigate the fluvial responses influenced by the structures. Including straight conventional design of groynes five different alternative configurations are investigated to find the most effective one. The experimental

investigations indicate that the functions of groynes are improved due to both alignment and permeability in the modified designs through minimizing separation of flow, hence minimizing local scour; maintaining bank-parallel flow as well as thalweg for navigation.

Utilizing the 2D numerical model, formation processes of alternate and multiple bars at experiment scale are studied first to verify the simulation results. The effects of initial and boundary conditions on the bar formation processes, and the cause of reduction of bar mode observed in experiments are also clarified. The multiple bar patterns present in the natural rivers are well reproduced by the numerical computation, where the evolution of bars is apparent with a pool-bar complex. As to their interactions with groynes, computation results reveal that accelerating flow due to intrusion of groynes triggers the sediment movement in the main channel, moves the bars reducing their scale, and finally disappears from the straight schematized channels. Thus, the groyne-system is useful to avoid the complexity in lowland rivers due to formation of bars, too.

CHAPTER 1

INTRODUCTION

1.1 Background

Bangladesh being an alluvial deltaic plain and the lowest riparian country of the three mighty river systems of the world—the Ganges, the Brahmaputra and the Meghna (**Fig. 1.1**), has become the natural outlet for an enormous amount of water and sediment over the annual cycle. This has made the country vulnerable to floods and pollution. Having the mild slope in this deltaic region, a part of the sediment load that passes through the country to the Bay of Bengal is deposited on the floodplains and streams, gradually changing its topography, and seriously reducing the carrying capacity and navigability of the drainage channels. Thus, flood waters attack the river

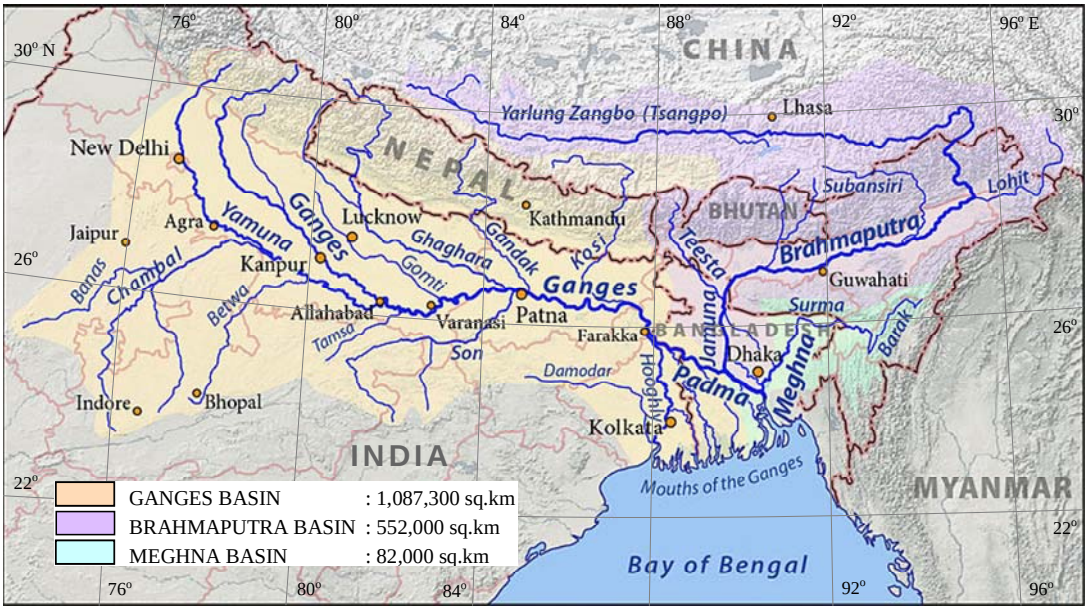

Fig. 1.1 The Brahmaputra, Ganges, and Meghna basins (Wikipedia, 2011)

banks, and substantial tracts of land are lost through bank erosion and the changing course of the swollen river channels every year, forcing dislocation of many people from the riverine areas. Devastating bank erosion inflicts damage on structures, such as houses, bridges, roads, boat ramps, and so on. This causes deleterious socio-economic impacts leading to loss of land and property, environmental degradation, and human hazards. Even the vulnerability of people increases further in the recent time.

Most of the rivers in Bangladesh are geomorphologically very active (Akter Hossain, 2004). As a consequence, these rivers erode large areas from floodplains as well as islands (*chars*, local name) every year. Among these rivers, the width of Jamuna is increasing substantially with time (CEGIS, 1997a); also channel shifting processes of Jamuna are rapid. The abandonment of large channels and the development of new channels in a few years are common features in this river. Thus the rapid changes in planform occurred. On the other hand, at low flow stage, water level within the river falls as much as 8.0 m (Bristow, 1987), and every year the depth in the river is found to be lower than the year before. This trend has remained for a long time, thus creating more and more hazards progressively in recent years. The interruptions of navigational routes in the lean season are very frequent, so that water-vehicles are forced to travel longer distances on the way towards their destinations, even sometimes they cannot move in the river for several hours to several days because of the rapid unknown sedimentation in the channels. The rivers are by far the cheapest routes for transport of goods in bulk, also a major means of travel for a large number of people. Thus, the important and economically favorable transports are greatly hampered.

Moreover, the bedforms of different scales are very common features in the Jamuna river caused by various factors such as less flow strength due to mild longitudinal slope, deposition of mid-channel bars at the downstream of node points initiated with some local condition, slack water developing in a reverse eddy or of some similar hydraulic factors (Coleman, 1967), huge sediment flux from upstream, bank erosion, and so on. They have significant roles in both engineering and ecological aspects in

fluvial processes: pools cause successive side bank erosion, while sandbars are important habitats for various species in the river ecosystem. Undue and rapid sedimentation resulted as large-scale bars in the river hampers the navigational routes in the lean season. Moreover, these structures make the channels highly unstable forming anabranches, influencing erosion of riverbanks, and so on. Thus the important characteristics of the Jamuna River causing problems can be summarized as below:

- widespread bank erosion
- widening of channels
- rapid changes in bed topographies
- lack of sufficient depth of flow and thalweg for navigation
- extremely unstable channel (westward movement due to continuous and severe erosion in the right bank)
- rapid planform changes

Bangladesh with its fragile state of economy which has strong linkage with well-managed river flow and fluvial systems needs an immediate sustainable solution against devastating river erosion to safeguard lives, properties and natural environment, and to keep the rivers navigable for the important transports as well.

1.2 Problem Definition

As described in the aforementioned section, due to very drastic nature of Jamuna river, apart from losing the homesteads of people in the riverine areas, the erosion and bank recession in monsoon have significantly limited agricultural and industrial developments. Besides, the problem of inland waterway transports in dry season is another big concern for the river management. To understand the dynamism of the river, and to develop and improve the techniques in stabilizing the channels, a large number of studies have been conducted in the past several decades (Coleman, 1969; Klaassen and Vermeer, 1988; Elahi, *et al.*, 1991; Thorne, *et al.*, 1993; Bristow, 1993; Halcrow, *et al.*, 1994; Zhou and Chen, 1998; CEGIS, 2004, 2005, 2006 and 2007).

Based on the research findings as well as engineering experiences and consultants' recommendations, some river training methods have been implemented, such as BRE (Brahmaputra Right Embankment), groynes, revetments, and recurrent dredging. But, the targeted goals are not achieved in many cases as expected, resulting failure of the structures due to local scour (Garde *et al.* 1961, Melville 1992, Halcrow and Haskoning, 1999; Klaassen *et al.*, 2002; Bharbhuiya and Dey 2004, Zhang *et al.* 2009); sudden and big responses from the groynes which make unstable the other regions away from the structures, such as the islands, where a number of people are living, etc.; attack to the same bank where the groynes are installed by some oblique flow reflected from the large sandbars, and so on. Even BRE has experienced multiple costly retirements. Thus the efficiency of the existing measures has been criticized (Klaassen, *et al.*, 2002; Rahman, *et al.*, 2004; Mosselman, 2006). Bandal-like structures are also practiced in the river for both bank protection and maintenance of thalweg for navigation; but, these are temporary measures, and their use for large variation in water stages are not evident yet.

Furthermore, recently the social needs for river environments have drawn much attention to improve the ecological values of the river landscapes. However, these issues are being addressed in advanced world like Japan, Europe, and so on for a long time. The area between groynes, the groyne fields, are the zones of sediment storage and are important elements for many aspects, erosion of which may affect the stability of the groynes, or even lead to the disappearance of the floodplains of fine sediments, a valuable habitat for riverine flora and fauna. The river environment which is severely affected by human activities can get relief by a series of groynes through ecosystem restoration (Tsujimoto *et al.* 2009). Thus, the way of overcoming all these problems is considered in the form of some modified designs of groyne structures, optimizing their configurations in both alignment and permeability that would act to guide the flow efficiently, so that it will minimize flow separation near groyne head and impact to other regions at monsoon flood, and will favor the deeper channel to form for navigation at dry season. Also, the fluvial responses will be in more natural way to allow for improvement of ecology and the quality of river landscape.

As the large sandbars are very common in lowland rivers like Jamuna in Bangladesh, and these, on one hand, cause bank erosion, the channels unstable, navigation problems, and so on; while on the other hand, are important habitats for the river ecosystem as well as are living ground (islands) by numbers of people inside the river. Therefore, their formation and characteristics without groynes, and their interactions with groynes are crucial to investigate for better management of river engineering.

1.3 Objectives and Approach

In view of the problems mentioned in the preceding section, the present study is mainly aimed at improving the understanding in stabilization of lowland rivers, and some specific objectives have been fixed to reach the targeted goals. They are:

- Orientations of straight groynes for lowland rivers.
- Modified alignments of groynes for lowland rivers.
- Configurations of groynes modified with both alignment and permeability for the most suitable design for lowland river problems.
- Characteristics of sandbars in both experiment and prototype scales.
- Interactions of groynes with macroscale bedforms in lowland rivers.

Both numerical analyses and laboratory experiments are conducted to explore the best design of groynes for lowland river problems. As there are many cases to be dealt with because of many aspects in optimal design of groynes, we started with two-dimensional (2D) numerical analysis to recognize the more efficient alternative of alignments from various ones. Then various configurations including modified combined and modified bandals are considered for the limited numbers of alignments, like the derived alignment suitable for lowland rivers and also conventional straight one, for detailed laboratory observations of the channel responses to recognize which one is the most effective for better modification of fluvial processes. Further, alternate and multiple bars are simulated by utilizing 2D numerical model in experiment scale and in prototype scale as well, to clarify the bar formation processes and to know the

characteristics of bars. Then the interactions of groynes with the sandbars are studied with the same numerical model, to recognize the effects of a series of groynes on the bedforms in lowland rivers.

1.4 Dissertation Outlines

The contents described in this dissertation are the sequential explanations of different phases of the present research. This dissertation is composed of eight chapters in total from introduction in Chapter 1 through conclusion in Chapter 8, as described below:

Chapter 1 briefly introduces the present research including the motivation for this study, objectives, and approaches to achieve the defined goals.

Chapter 2 presents some background information. It describes the river systems and the existing river training methods in Bangladesh, some general aspects of groynes and modeling approaches necessary to analyze the alluvial river problems.

Chapter 3 describes a numerical investigation on an alluvial channel with a series of groynes. From several alternatives of groyne angles an optimum orientation is explored and presented in this chapter. The excerpts from this chapter were published as a technical paper in the *9th International Conference on Hydro-Science and Engineering (ICHE 2010)* (Alauddin and Tsujimoto, 2010a).

Chapter 4 gives a description on the effect of groynes modified in alignment based on the outcome from that of straight orientations as discussed in Chapter 3, and the selection of a suitable alignment of groynes from several modified ones is made for lowland rivers by numerical investigation. The works described in this chapter have been published as technical papers in the *Annual Journal of Hydraulic Engineering* (Alauddin and Tsujimoto, 2011a) and in the *International Journal of Sediment Research* (Alauddin and Tsujimoto, 2011b).

Chapter 5 deals with the laboratory experiments for several configurations of groyne models. Groyne designs are further modified here with the combination of permeable and impermeable components in one structure. The alignment is maintained as found as the optimum one described in Chapter 4, also straight one is considered to

investigate its functions and to compare with the modified ones. They are placed on one side of the model channel in a series and run to investigate the channel responses against them to identify the most effective design of a groyne for lowland river problems. The works described in this chapter are to be published in the *Advances in River Engineering, JSCE* (Alauddin *et al.*, 2011c) and in the *Journal of Applied Mechanics, JSCE* (Alauddin *et al.*, 2011d).

Chapter 6 discusses the formation of sandbars in both experiment and prototype scales, and their characteristics. Formation processes of alternate and multiple bars are investigated first to verify the simulation results, then their characteristics are discussed for prototype scale. An excerpt from this chapter has been accepted to be published in the *International Review of Civil Engineering* (Alauddin *et al.*, 2011e).

In chapter 7, the interactions of groynes with macroscale bedforms in lowland rivers are described. An excerpt from this chapter was published in the *International Conference on Modern Hydraulic Engineering (CMHE 2010)* (Alauddin and Tsujimoto, 2010b).

Finally, we draw an overall conclusion of this research and some recommendations for further researches relating to this topic are made in Chapter 8. Concluding remarks are also made at the end of each chapter based on the results obtained in different phases of the research within the framework of the objectives.

The frame of the research phases presented in this dissertation with the relationship among them is delineated with a figure (**Fig. 1.2**).

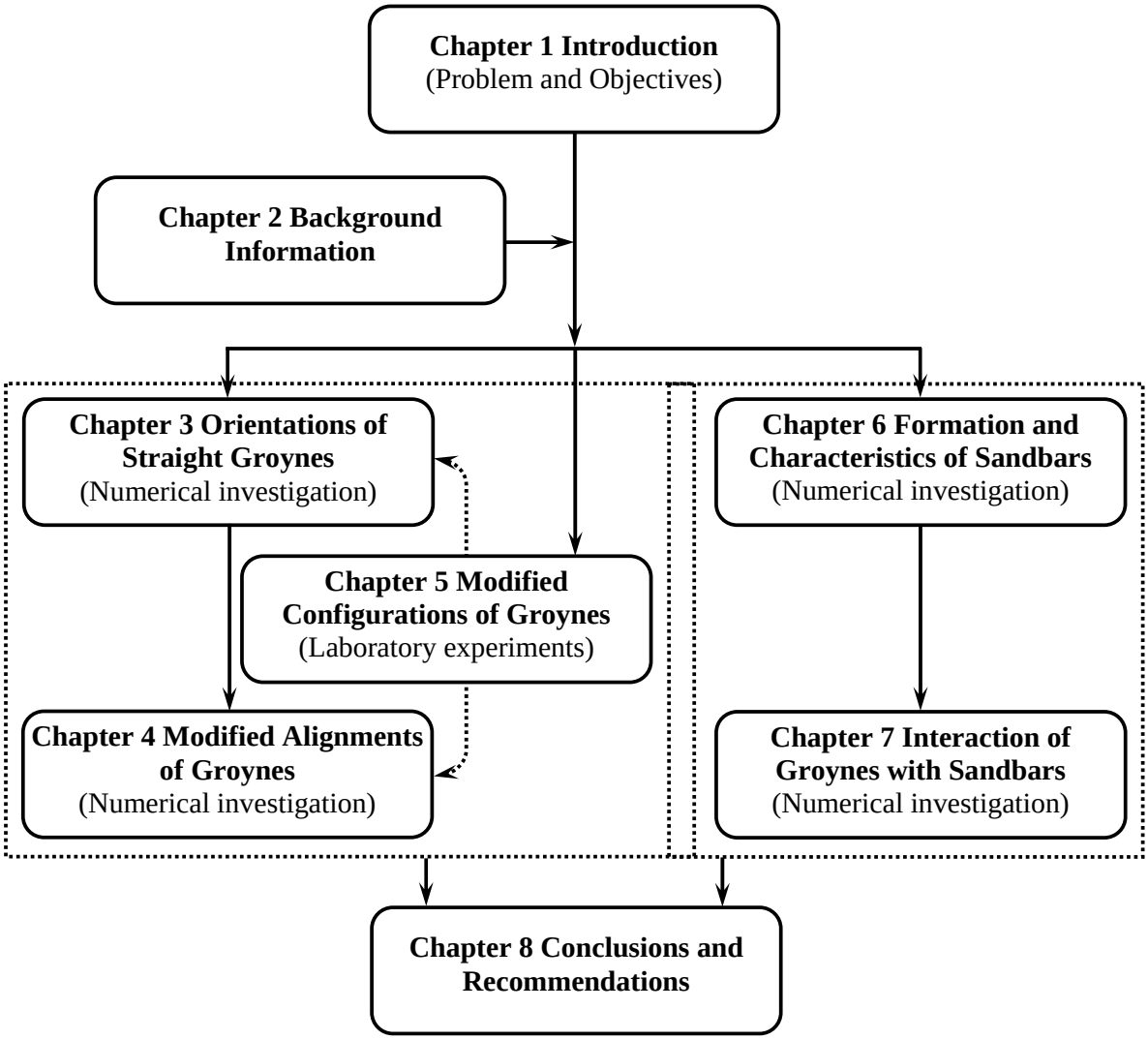

Fig. 1.2 Graphical representation of the dissertation framework

CHAPTER 2

BACKGROUND INFORMATION

2.1 General

In this chapter, we present some of the background information relevant to the present research that is useful in studying the effective approaches for stabilization of lowland rivers. In section 2.2, a brief discussion on the alluvial rivers, emphasizing Jamuna of Bangladesh; in 2.3, the river training methods practiced in Bangladesh; in 2.4, some general aspects of groynes are presented. Section 2.5 presents a brief overview on the modeling approaches to analyze the flow and sediment transports in alluvial river channels.

2.2 Alluvial River, Jamuna in Bangladesh

Jamuna is the downstream course of the Brahmaputra (**Fig. 2.1**) which avulsed due to devastating flood in 1787 and faulting. Presently the Brahmaputra continues southeast from Bahadurabad (Dewanganj upazila of Jamalpur district, Bangladesh) as the old Brahmaputra, and the river between Bahadurabad and Aricha (Manikganj, Bangladesh) is the Jamuna. The Hydrology Directorate of the Bangladesh Water Development Board (BWDB) refers to the whole stretch as the Brahmaputra-Jamuna. It originates in the Chemayung-Dung glacier, approximately at 31°30'N and 82°0'E, some 145 km from Parkha, an important trade centre between lake Manassarowar and Mount Kailas. The Brahmaputra is known as Tsangpo in Tibet and Dihang in Assam Himalayas (India) before it comes into the Great Plains of Bengal. It enters Bangladesh through Kurigram district (at the border of Kurigram Sadar and Ulipur

Upazilas). The total length of the Tsangpo-Brahmaputra-Jamuna river up to its confluence with the Ganges is about 2,740 km. Within Bangladesh territory, Brahmaputra-Jamuna is 276 km long, of which Jamuna is 205 km.

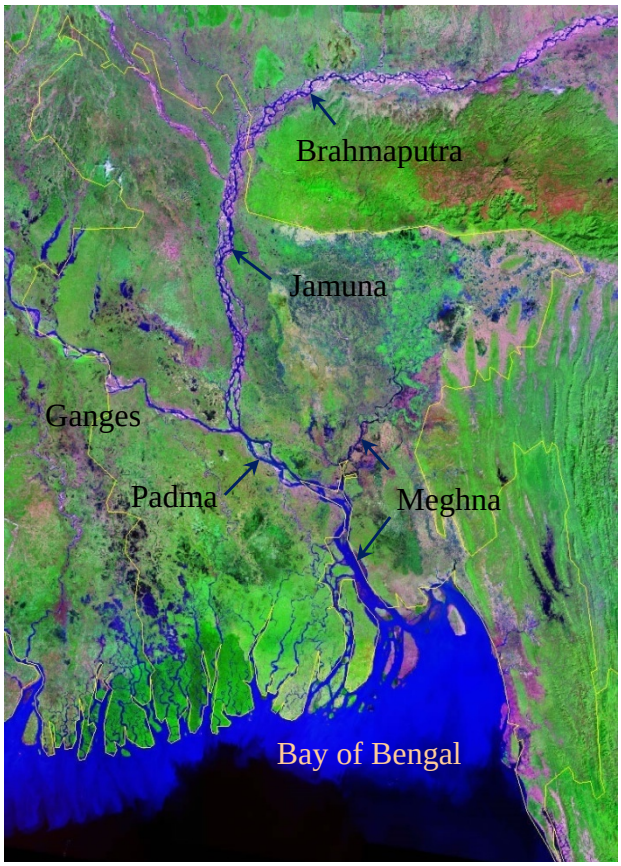

Fig. 2.1 River systems of Bangladesh (SOS-arsenic.net, 2006)

The width of the river varies from 3 km to 18 km with the average width is about 10 km. In the rainy season the river is nowhere less than five kilometres width. The stream flow in the river is in fact a multi-channel flow. The channels are of many different sizes, from hundreds of meters to kilometers wide, and of different patterns including braiding, meandering and anastomosing pattern. The width/depth ratios for individual channels of the river vary from 50:1 to 500:1, and the gradient is 0.000077, decreasing to 0.00005 near the confluence with the Ganges. Precipitation within the catchment varies widely; this also varies widely throughout the year. More than 80% of precipitation occurs in the five months of monsoon. The river starts rising in

March/April due to snowmelt in the Himalayas and reaches a peak in June. It rises again and reaches the annual peak in the late July to mid August. A widely varying discharge, easily eroded banks, and highly mobile bed materials cause response to fluvial processes quickly adopting and abandoning numerous anabranches at all levels within its braided system. A mean annual peak discharge of approximately 69,000 m^3/s (Delft Hydraulics & DHI, 1996) with a maximum of approximately 100,000 m^3/s (recorded during severe flooding in 1988) is known from the daily discharge data recorded at Bahadurabad, when the maximum flood level of 20.62 m is also recorded. An annual sediment transport is found up to $2{,}000 \times 10^6$ tons, the third highest alluvial sediment load in the world (Schumm & Winkley, 1994). Minimum flow in the river generally occurs at the end of February or beginning of March. The minimum discharge is recorded at 2,860 m3/s in March of 1971. The maximum range of WL variation in the Jamuna River is up to 8.0 m. A typical hydrograph of Jamuna has been added here, where huge variation of water discharges as well as water levels can be recognized (**Fig. 2.2,** personal communication to Executive Engineer, Flood Forecasting and Warning Centre (FFWC), Bangladesh).

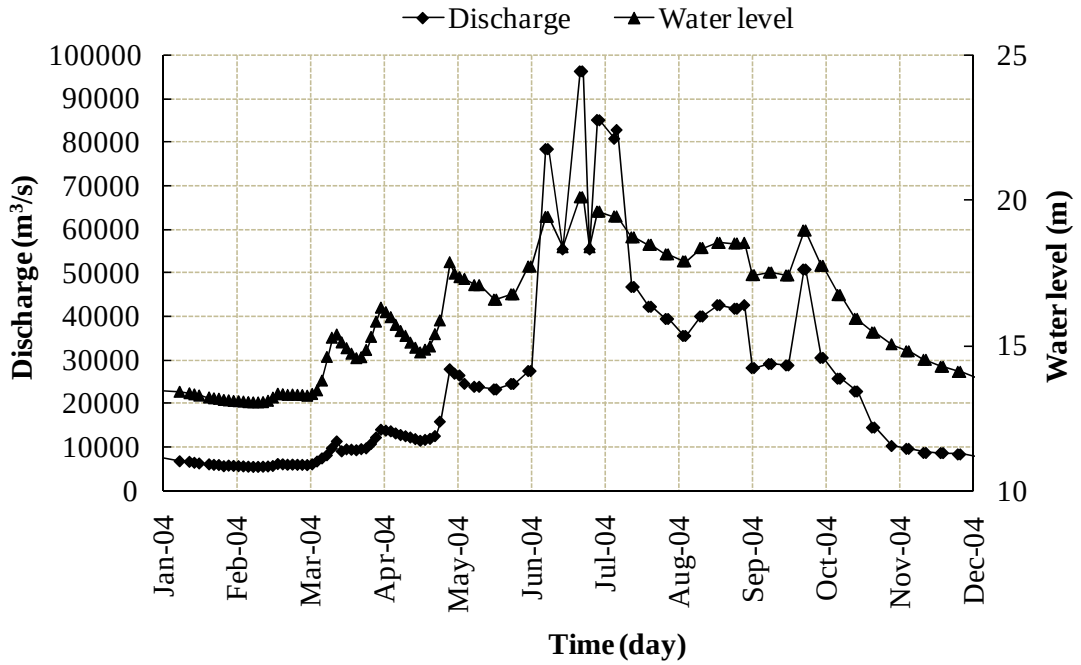

Fig. 2.2 Hydrograph of Jamuna River at Bahadurabad (Year, 2004) (FFWC, 2010)

The Jamuna has four major tributaries: the Dudhkumar, the Dharla, the Tista, and the Karatoya-Atrai system. The first three rivers are flashy in nature, rising from the steep catchment on the southern side of the Himalayas between Darjeeling in India and Bhutan. The river is braided in nature. Within the braided belt of the Jamuna, there are lots of chars of different sizes. An assessment of the 1992 dry season Landsat image shows that the Jamuna contained a total of 56 large island chars, each longer than 3.5 km. There were an additional number of 226 small island chars, varying in length between 0.35 and 3.5 km (Uddin, 2007).

The Ganges and the Padma rivers erode their banks locally, while the lower Meghna is extremely active at Chandpur and Eklaspur. The Ganges erodes its left bank severely for the last few years at Panka Narayanpur, Gudagari, Rajshahi, Sharda, Pakshi, and Pabna in Bangladesh. Erosion at Panka Narayanpur became very aggressive, where Bangladesh Water Development Board (BWDB) gave many efforts. The right bank of Padma is eroding with high rate near Faridpur and Munshiganj areas. The impact of erosion can be sudden and dramatic, even when the riverbank is protected. The Teesta is another braided river with behavior just like the Jamuna. Its both banks are eroding from many decades, and thousands of people lost their home and agricultural lands. The maximum discharge in the river is 12,500 m^3/s, whereas its width varies from 2 to 5 km. After construction of Teesta Barrage at Dalia (Nilphamari district), some protective measures have been constructed like solid spurs, reinforced cement concrete (RCC) spurs, revetment works, and so on. All the protective works are more or less effective in the Teesta River. The other rivers like Dharla, Dudkumar, Mohanada, Kushiyara, Gumti, Atrai, etc. are not so behind in the race of bank erosion.

The rivers sometimes cause massive riverbank erosion, engulf enormous amount of agricultural fields, destroy hundreds of homesteads (**Fig. 2.3**). Since time immemorial the most vulnerable and landless communities take shelter further inland if they have any other land there with constant risk from erosion; otherwise they either take shelter on the embankments or migrate to urban slum areas. These have serious economic

impacts and social implications including the breaking up of traditional life and families.

Fig. 2.3 Destructive consequences of bank erosion in Jamuna

2.3 River Training Works in Bangladesh

Natural processes and/or human interventions may disturb the equilibrium between the sediment supply to the channel and its transport capacity. Training structures are then necessary to protect the channel against the changes occurred due to these disturbances. The practices of major river-training measures in the low-lying delta, Bangladesh mainly started after the mid of nineteenth century driven by the demands for the safety due to continuous and severe erosion of river banks, and to increase navigability associated with the demand for very important transport system there. The river training works, which are more or less practiced in the country, can be listed as: revetment works, groynes or spurs, embankments or levees, cutoffs, closures of secondary channels, and miscellaneous methods like bandals, panels, and so on. Among the aforementioned methods, mostly used protection works are either solid spurs or revetment works to protect important locations like Kamarjani, Fulchari, Sariakandi, Kazipur, and Sirajganj in the Jamuna River. A brief description of the river training methods is made in this section.

2.3.1 Revetment Works

Riverbank erosion is a common feature for all alluvial rivers. Bank protection with revetment works is the method to reduce or stop this erosion process. The riverbank can be divided into an upper and a lower section. The lower part, the part below the low water level, acts as a foundation for the upper part. Erosion of this lower bank, especially at the toe, causes the failure of the bank. The upper part can be eroded by wave attack also. The condition is severe when the current directly attack the bank. Bank failure can also occur due to the piping (effluent) effect; during low stages piping may occur due to the motion of ground water towards the river. This ground water may carry finer material away from the soil causing the failure of the bank. Revetment work is a well known bank protection method, which is practiced all over the world and there is no exception in Bangladesh. A revetment is a structural protection against wave and current induced loads covering the existing river bank or an embankment. It is not an offensive structure like a groyne. It has several components such as cover layer, intermediate layers between cover and core material that are required for drainage and filtering to allow for a stable foundation of the overall system and the toe. The cover layer must resist the design impacts, mainly current and wave. Toe protection is required in case of currents and/or wave scour, and undermining the toe of a bank or an embankment, which are likely to result in sliding of the slope. Sliding of slope endangers the overall stability and function of the revetment which is commonly seen in Bangladesh. Normally the revetment works are done with CC blocks, boulders, mattresses, open asphalt concrete, and so on.

During revetment works the slope pitching is normally done with 1:2 to 1:3 slopes according to the soil characteristics and hydrological boundary conditions. Sometimes it is seen that the eroding bank is not uniform. Its slope varies along the bank and in certain locations it is seen very stiff. In that case it should be built with desired slope by using sand filled gunny bags. Otherwise the local scour along the bank will not uniform and in some locations the actual scour could be more than the anticipated value and the revetment will fail (**Fig. 2.4**).

Fig. 2.4 Failure scenery of revetment works

Bank protection with geobags

Geobags were introduced in Bangladesh mainly for emergency works to protect the river bank erosion. Now it is being used for a revetment works for protection of river bank from erosion, where sand-filled geobags are used instead of CC Blocks. Asian Development Board (ADB) financed a project through a foreign consultant for protection of bank erosion in the Jamuna and the Meghna Rivers; they would use better equipments and process to implement the project, as it was a new project to make the revetment works with geobags. The slope pitching and falling apron both were constructed with the geobags, with assorted geobags to build the falling apron.

2.3.2 Groynes or Spurs

Groynes are the structures extended from the riverbank into the river. There is a preferred angle between the groyne and the bank depending on the purpose of the groyne. Groynes are constructed with stone, gravel, rock, earth, or pile structures. Generally groynes are used to divert the river flow away from the critical zones of bank to protect it from the erosive action of the river; they are also used to constrict

the width of the river so that the river will increase its depth, which is important for navigation. The main design criteria to be considered are spacing of groynes, length of groynes, the crest level of groynes (i.e., either at flood plain level or at embankment level), and the possible scour at the head of the groyne. Stabilization of the river bank with a series of groynes is very effective. Bank protection with a single groyne is not effective; most of the time a single groyne creates adverse effect in the surrounding area. A series of groynes can make the flood flow line parallel to the bank which is not possible by a single groyne.

2.3.3 Embankment or Levees

An embankment or levee may be defined as an earthen embankment aligned generally parallel to the river channel and designed to protect the area behind it from being flooded by floodwater. The embankments or levees can be natural or man-made. In general the man-made levee consists of an earth-fill dyke with or without revetment. The main purposes of an embankment are to protect lives and properties from heavy floods. The important design parameters are alignment, crest level and slope, resistance to flow on the river side, and scour depth at the toe. The alignment of the embankment is generally determined by the development of land use on both sides of the embankment and by the river behavior. Generally, some space between riverbank and the embankment is allowed, which is called the set back distance. The flood level of the river determines the crest level of the embankment; which flood should be considered to determine the level depends on the degree of safety to be provided for the protected area.

2.3.4 Cutoffs

Cutoff processes are characteristic features of alluvial meandering river. When a river is flowing through a bend, under favourable condition this bend may become a large loop with narrow neck. With increased narrowing of the neck a short-cut channel can be created. So cutoffs are short channels across the neck of the river bends. By this

process a river straightens and shortens itself. Cutoffs can be natural and man-made. Though this process is a very characteristic feature of meandering river, it can also be observed in anabranches of braided rivers. This cutoff processes have some beneficial effects like reduction of flood levels, shortening of the river course, exclusion of reaches with excessive curvature along which training structures could be maintained to stop severe bank erosion, and so on. To achieve these beneficial effects, a cutoff can be used as a means of river training. Cutoff of bends can be initiated artificially by dredging a pilot channel of adequate dimension, so that flow can start to flow through this channel. This flow will adjust the channel to the required dimensions through further scour.

2.3.5 Closures of Secondary Channels

A wandering type of braided river always has a tendency to create a new channel abandoning its original one, but this new course may not be always in good position in view of river stabilization. Under such circumstances the flow of the main course can be forced through the original course by dredging and by closing the secondary channel. The soil-materials dredged from the main channel can be used to close the secondary channel, thus stabilizing the flow of the river. There are two types of closures: a complete closure or a partial closure; which one should be preferred depends on the purpose of the closing. In case of a complete closure of a secondary branch, a new condition will be reached where all the flow and sediment will follow the former one. This will adjust itself by changing its depth and slope to achieve a new equilibrium condition. When it is the intention to use only the main channel during the low flow and both channels during peak flow, then the secondary channel can be closed-off by a dam, which is overtopped during the high water level. This type of closing can be classified as partial closure.

2.3.6 Hard Points

In the concept of ‘Hard points’, the river is not directly modified, rather the aim is to

stabilize the present pattern of the river by limiting the boundaries of the local width of braid belt. Some important places on the bankline are protected by creating 'Hard points', which are isolated bank revetment works with upstream and downstream terminations. These hard points are connected with the flood embankment with the help of cross bar to prevent outflanking of the hard points. The function of the hard points is to limit the extent of erosion. The length and spacing of the hard points determines the extent of area protected from the erosion, and thus the maximum allowable depth of the embayment is permitted in the locations between the structures. After the devastating flood in 1988, River Survey Project (RSP), Flood Action Plan 21 (FAP21) and FAP22 studied river bank erosion problems of the major rivers of Bangladesh. FAP21 selected the critical locations for taking protection measures from erosion along the right bank of the Jamuna River (CEGIS report, 2005). Accordingly, during 1996 to 1998 some special protection measures are taken (Sariakandi and Mathurapara Hard points in Bogra, Sirajganj Hard point, and strengthening of Kalitola groyne in Sirajganj district).

2.3.7 Recurrent River Training Methods like Bandals, Panels, and so on.

Bandals

These are temporary types of river training works and their influence may exist for one or two years. Repeated dredging may be a similar example of temporary works

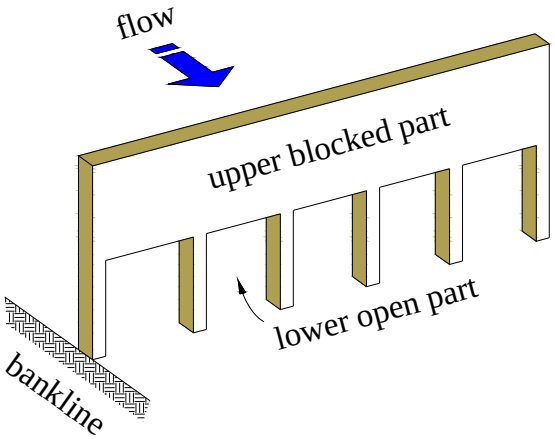

Fig. 2.5 Bandal-like structure

for navigation in an untrained river. Bandalling system has been developed locally in the Indian subcontinent for the improvement of channel navigability. Bandal may simply be described as a vertical screen mounted on a frame (**Fig. 2.5**), and can be placed on either sides of a channel that are required to be improved. They concentrate the flow into the channel, the velocity of the flow is increased, which results scouring of the channel. Bandals are placed in the riverbed in such a way that sediment can pass under the bandals and deposit behind them, where the velocity of the flow is relatively low. Their use is not so effective, where the large variation in water stages occurred.

Panels

Panels are of two types:

- surface panels, and
- bottom panels

Surface panels

The system of surface panels was developed in Russia in 1936 (Uddin, 2007). Surface panels are placed obliquely in the current which cause deviation of surface flow, and due to acceleration under the panel, deviation of bottom flow in another direction takes place. The result is the helical flow down of the panel, which causes increased sediment transport under the surface panels.

Bottom panels

The principle of bottom panels is also based on the generation of helical flow. The panels are placed at an angle of about 45^{o} to the current at the edge of the channel to be eroded; these are spaced by about two and a half times their own length for better functioning. The helical flow starts behind the panel and results in a movement of sediment along the panel. Bottom panels have not only been applied for creation of navigable channels but have also been used for the enclosure of secondary river branches (Jansen *et al.* 1979). Bottom panels may be left in the river even during floods.

2.4 River Training with Groynes

The groynes (as described earlier), or spur-dykes are small dams constructed at an angle to the flow extending from the bank to deflect the flowing water away from critical zones. They serve to maintain a desired channel for the purpose of flood control, improved navigation, and erosion control. They are made of stone, gravel, rock, earth, or piles, beginning at the riverbank with a root and ending at the regulation line with a head. Some modified combined groynes suitable for lowland rivers as explored through detailed experimental investigations under this research (explained next in Chapter 5) can be made with earthen shank for the first impermeable portion, and then with concrete piles or steel hollow pipes for the rest pervious ones of different permeability, considering both materials availability and technical feasibility.

Construction of a single groyne is generally not preferred in the river engineering practice. Prototype groynes are arranged in sequences in order to increase the efficiency and enlarge the improved stretch of the river system. The effect of a group of groynes to the flow and the river system is found to be quite different from that of a single groyne. With a single groyne, the local effect on the flow is the most important. However, a series of groynes are not only some kind of local obstructions, but also an artificial narrowing of the channel width. These two aspects lead to the final flow pattern and the bed morphology. Therefore, the present research deals with the effect of groynes in a series.

2.4.1 Types of Groynes

Various types of groynes can be distinguished according to their construction, action on stream flow, and appearance. Przedwojski *et al.* (1995) claim that the followings are necessary for a full description of groynes:

- Classification according to the methods and materials of construction:

Groynes may be permeable, allowing the water to flow through at reduced velocities, or impermeable, blocking and deflecting the current. Permeable groynes are made from piles, bamboo or timbers, whereas impermeable groynes (also called solid groynes) are constructed using rock, gravel, gabions, and so on.

- Classification according to submergence stage:

  Groynes may be designed either as submerged or as non-submerged under normal conditions. Which of the two types will be used is dictated by the design conditions. Usually impermeable groynes are designed to be non-submerged, since flow over the top of solid groynes may cause severe erosion along the shanks. Submerged groynes, on the other hand, may be designed permeable, depending on the degree of flow disturbance that is needed.

- Classification according to the action on the stream flow:

  Groynes may be classified as attracting, deflecting, or repelling. Attracting groynes point downstream, they serve to attract the stream flow towards themselves, and do not repel the flow towards the opposite bank. Deflecting groynes are generally short ones and used for local protection. They serve to change the direction of flow without repelling it. Repelling groynes point upstream. They serve to force the flow away from themselves.

- Classification according to their appearance in planview:

  Groynes may be built with different planview shapes. Examples are straight groynes, T-head, L-head, hocky stick, inverted hocky stick, straight groynes with pier head, wing or tail groynes.

2.4.2 Design Considerations of Groynes

The most important considerations involved in groyne design are planview shapes, length, spacing, orientation to the flow, crest elevation and slope, cross-section, and construction materials (Richardson *et al.*, 1975; Alvareg, 1989; and Przedwojski *et al.*, 1995).

Planview shape and orientation

Of the abovementioned types of groynes, the straight ones may be oriented perpendicular to the flow, or inclined upstream or downstream; the angle to the bank ranges from 70^o to 120^o (Klingeman *et al.*, 1984). Each orientation affects the flow in a different way and results in a different deposition of sediment in the vicinity of the groyne. The so-called attracting groynes are pointing downstream to attract the flow towards itself, repelling or deflecting groynes are pointing upstream. They have a rounded head to provide extra volume and area for scour protection at the outer end. T-head groynes are normally built under a right angle to the bank, and they have straight shanks with a perpendicular head at the outer end. L-head, wing or tail groynes have different structures at the end, which generally leads to larger sediment deposits between groynes, less scour at their head, and greater protection to the banks. L-head groynes are very effective in channelization for navigation when the length of the head closes 45% to 65% of the gap between groynes. Hocky stick groynes have scour holes that are more extensive in area than T-head groynes.

Spacing between groynes (S_g)

The spacing between groynes is measured at the riverbank between the groyne roots. It is related to river width, groyne length, flow velocity, angle to the bank, orientation to the flow, bank curvature, and purpose, but it is mostly expressed as a multiple of the groyne length. Richardson (1975) recommends a spacing of 1.5 to 6 times the upstream projected groyne length. In order to obtain a well-defined deep navigation channel, a spacing of 1.5 to 2 times the groyne length is recommended, whereas for bank protection the spacing is increased to 2 to 6 times the groyne length. There are, however, successful examples of bank protection with short groynes spaced at 10 to 100 times their length, but there the banks are protected with riprap or vegetation. If the spacing between groynes is too large, a meander loop may form between groynes. If the groynes are spaced too close together, on the other hand, construction costs will be higher and the system would work less efficiently, not making full use of each individual groyne.

Length of the groynes (L_g)

Groyne length depends on location, purpose, spacing, and economics of construction. The total length of the groyne includes the anchoring length, referring to the part embedded in the bank, and the working length, referring to the part protruding into the flow. The length can be established by determining the channel width and depth desired. The working length is usually around a quarter of the mean width of the free surface; the anchoring length is recommended to be less than a quarter of the working length.

The maximum length of groyne is equal to the distance between the bank and the river zone where no groyne encroachment is allowed. Such a zone should be determined in advance, as part of a river training strategy. Groyne intruding this zone may divert the river and trigger bank erosion at other locations over a large distance.

Crest elevation and base depth

The crest elevation of groynes depends on the purpose and possible problems due to overbank flow. For bank protection, the crest should be at least as high as the bank. Crests may be either level or sloping downwards from the bank towards the end of the groyne. For bank protection, sloping-crested groynes are recommended by Alvarez (1989), with a slope of 0.1 to 0.25. They have the advantages of reducing scour at the groyne tip, requiring less material for construction and faster deposition of sediment between them. For navigation channel control, level-crested groynes work best normal to the flow or angled downstream, whereas sloping-crested groynes work best normal or angled upstream (Richardson *et al.*, 1975). The expected scour depth should be taken into consideration when determining the base depth of the groynes.

2.4.3 Flow Near Groynes

The flow field differs significantly between the case of a single groyne and that of a series of groynes. This thesis focuses on groynes in series, for the flow pattern near a single groyne we refer to e.g. Ishi *et al.* (1983), Tingsanchali and Maheswarn (1990), Chen and Ikeda (1997), Ouillon and Dartus (1997).

Emerged Groynes

Under conditions where the groynes are not submerged, the groyne fields are not really part of the flow conveying cross-section of a river. Accordingly, the flow pattern in a groyne field does not directly contribute to the discharge in the main channel. Reducing the main stream velocity has little effect on the flow pattern itself, whereas lowering the water does affect the pattern (Uijttewaal *et al.*, 2001). Moreover, the flow pattern inside a groyne field may change with the change of its geometry, location along the river (inner bend, outer bend, straight part), and/or the groyne orientation (Przedwojski *et al.*, 1995). Flow pattern around a single groyne has been shown in **Fig. 2.6**.

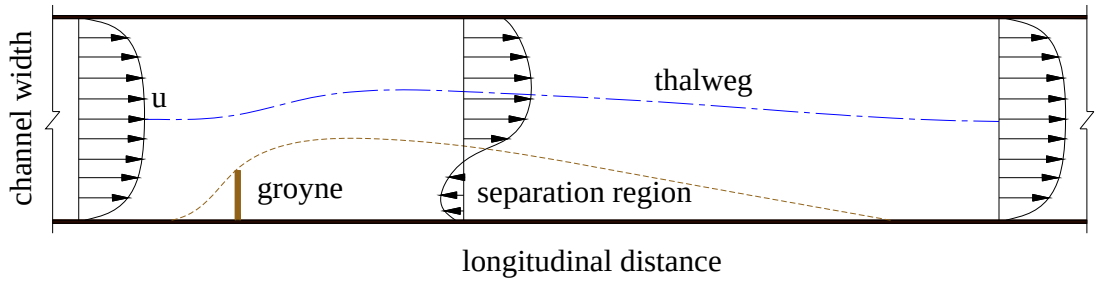

Fig. 2.6 Flow thalweg and separation around a single groyne

Length to width ratio of the groyne field determines the shape and number of eddies that emerge in the stagnant flow region (Uijttewaal, 1999; Muto *et al.*, 2000). An aspect ratio close to unity gives rise to a single eddy. A larger aspect ratio gives room for two stationary eddies, a large one, called primary eddy, in the downstream part of the groyne field, and a smaller secondary eddy near the upstream groyne. In a long groyne field with length to width ratio of around six, the flow penetrates into the groyne field. The two eddies remain in a relatively stable position, while the main flow field starts to penetrate into the groyne field further downstream. In all cases, there is an eddy shedding intermittently from the tip of the groyne and migrating along the interfacial line between the main flow and the eddies. It eventually merges with the primary eddy. The flow field is unsteady, even in the case of a steady

discharge. Hence, there is a significant difference between the time-averaged and the instantaneous flow field.

Away from the tip of the groyne, the flow pattern between emerged groynes is predominantly two-dimensional. The small-scale three-dimensional turbulence plays a minor role in the mass and momentum exchange process between the groyne field and the main channel. Strong large-scale three-dimensional structures cannot develop due to shallowness of water. The flow near the tip of the groyne is strongly three-dimensional (Krebs *et al.*, 1999).

Submerged Groynes

Relatively a lack of researches is made on groynes in submerged conditions, which may be due to the fact that the groynes are mostly functioning under emerged conditions. Another reason might be the complexity and three-dimensionality of the problem, which require advanced measurement techniques and/or powerful three-dimensional computational methods. A few researchers have attempted to study the case of submerged groynes (e.g., Aya *et al.*, 1997; Peng *et al.*, 1997; Krebs *et al.*, 1999; Tominaga *et al.*, 2001). Aya *et al.* (1997) report a sharp decrease in the water level between the upstream and downstream sides of the groynes. By implication, the water surface slope between two successive groynes is less than the slope in the main channel region.

Peng *et al.* (1997) compare three-dimensional numerical results with experimental results and conclude that the flow pattern in the case of submerged groynes shows strongly three-dimensional features behind groynes. On the upstream face of the groyne, the flow shows an upward motion because of the blockage effect. When the groynes are spaced far apart, the separating flow over the groyne reattaches to the bed, whereas too closely spaced groynes will prevent flow reattachment to the bed, thus keeping the bed shear stress at a low value.

2.5 Modeling Approaches

Methods of predicting sediment transport and bar formation range from numerical to empirical with physical modeling lying between these two end points.

2.5.1 Computation of Sediment Transport

Flows in open channels are described by a set of partial differential equations for computer simulation of hydrodynamic and sediment processes. Analytical solutions for these equations are not available, except for simplified, one-dimensional cases. Therefore, these equations are solved using numerical methods. Mathematically represented simulations are an efficient way to estimate the time and space-dependent sediment processes (van Rijn, 1989). There are numerous mathematical models available to simulate sediment transport and erosion/depositions in one-dimension (1D), two-dimension (2D), and three-dimension (3D).

One-dimensional (1D) models

To achieve a practical solution of the governing equations in one-dimension, model parameters are horizontally and vertically averaged over a cross-section of the water body. In this representation, model parameters have the same value over the entire width of the cross section. A detailed review of one-dimensional models together with their numerical solution methods and applications can be found in Cunge *et al.* (1980), Jansen *et al.* (1979), or review of De Vries *et al.* (1989).

One-dimensional models are virtually the only numerical tool available to simulate morphological changes occurring over years in rivers (van Rijn, 1989). They are relatively easy to set up and calibrate quickly on desktop computers. But the assumptions of 1D flow may not be valid in many situations. Flow in a channel along varying cross-section, changing alignment, or complex tidal flow in the estuaries are some of these examples.

Two-dimensional (2D) models

Two-dimensional models can be laterally (width) or vertically (depth) integrated. A laterally integrated model solves the laterally integrated momentum and continuity equations for the flow and the sediment phases (Smith and O'Connor, 1977). In

depth-averaged models, all the model parameters are assumed to be uniform through the water column at each computational point. The depth-integrated equations of motion and continuity are linked to a depth-integrated sediment transport model. The water surface elevation, velocity, sediment concentration, erosion or deposition is computed at each of many points across the cross-section.

A 2D model is necessary if the problem involves complicated circulation patterns and unsteady flows within the model domain. However, these models are more time consuming to set up compare with 1D model, and require much more computer time to run. Therefore, careful planning and analysis is needed to develop the optimum trade-off between the density of the computational mesh or grid and the resulting run time, requirements for computer memory, and storage.

Three-dimensional (3D) models

3D models are based on the 3D mass balance equations or the convection-diffusion equations for suspended sediment transport (van Rijn, 1989). In these models, both the horizontal and the vertical components of the sediment transport processes are considered. 3D models provide the most complete, quantitative representation of hydrodynamic system. The calibration data requirements are more extensive and expensive (van Rijn, 1989), because a comprehensive field program is required to capture the complexities of flow in three directions. Three dimensional models can provide insight into the short-term effects of a proposed structure on a particular river management option, but lengthy simulations that model morphological evolution are not currently feasible.

Three-dimensional models should be used when flow and sediment transport are stratified (Martin and McCutcheon, 1999). An example might be where freshwater flows over a salt-water wedge, or warm water overrides colder waters (van Rijn, 1989). Many 3D models have been applied most frequently in the laboratory (O'Connor and Nicholson, 1988) to small area field sites (van Rijn *et al.*, 1989). Computations for larger model domains in estuaries or the continental shelf are typically lumped to a single day or one tidal cycle (O'Connor and Nicholson, 1988).

The application of a 3D model is most necessary near or around a hydraulic structure where flow separation and vortex characteristics are truly three-dimensional, and sedimentation processes are complex (van Rijn 1987; van Rijn *et al.*, 1989).

Whether the problem is solved in 1D, 2D or 3D; in solving the equations it is necessary to reduce them to a numerical form that could be understood by a computer. There are three main methods for doing this: Finite Difference Method (FDM); Finite Volume Method (FVM); and Finite Element Method (FEM). In FDM, discretization is based upon the differential form of the PDE to be solved. Each derivative is replaced with an approximate difference formula (that can generally be derived from a Taylor series expansion). A structured mesh is necessary for implementation of the FDM, which comprises six-sided cells arranged in a regular topology to form a cuboid, and the solution will be obtained at each nodal point. The configuration of a water body can be represented more accurately by using the boundary-fitted coordinate or finite difference curvilinear method. This discretizes along boundaries and contours, and then uses transform relations to map the discretizations to a rectangular grid for solution.

In FVM, the flow domain is divided into control volumes (defined using the cells of the mesh), and governing conservation equations are written in a form which can be solved for a given finite volume (or cell). The computational domain is discretized into finite volumes, and then for every volume the governing equations are solved. The resulting system of equations usually involves fluxes of the conserved variable, and thus the calculation of fluxes is very important in FVM. When using the FVM, values for pressure are calculated at the cell centres. Velocity components are then calculated either at cell faces (a staggered grid) or along with pressures, at the cell centres (a co-located grid). The later produces a more accurate results field, but requires the use of the Rhie and Chow interpolation algorithm (Rhie and Chow, 1983) to prevent pressure and velocity decoupling and the numerical oscillation.

The FEM uses a unique variation of the dependent variables for every cell, so that the method lends itself well to unstructured meshes, where the cells do not have to be six-sided and are often tetrahedral in shape. The elements need not be the same size or

shape, and their edges may be curved. Nodes are placed at vertices and midway between vertices. FVM and FDM provide discrete solutions, while FEM provides a continuous (up to a point) solution. Overall, however, calculation time can be significantly greater for a finite element model if a large number of fairly small elements are used to describe the geometry.

2.5.2 Physical Modeling

Physical models frequently offer an alternative approach to sediment transport problems that are difficult to simulate computationally. According to Dalrymple (1985), physical models integrate the appropriate equations governing the processes without the simplifications that are required for analytical or numerical models. Fixed and movable beds have been utilized for river and coastal studies. Scaling effects are reasonably understood for fixed-bed models (Dalrymple, 1985; Hudson *et al.*, 1979); less understood are the scaling effects inherent in the material used to represent sediment in a movable bed physical model. A common scaling problem arises when the prototype grain-size is diminutive; geometric scaling of the sediments results in selection of a model bed material below the diameter boundary between cohesive and non-cohesive sediment. Distortion of the scale model, i.e., stretching vertical or horizontal length scales, has been suggested as a means for overcoming the inability to reduce the sediment to model scale.

Although many scaling laws have been suggested that require model distortion, this practice is still viewed with skepticism by some. Dean (1985) reviewed several studies, and concluded that the state of knowledge on movable bed models was largely qualitative. There is a potential that artifacts of the laboratory setting can influence the process being simulated to the extent that suitable representation of the prototype is not possible. Other laboratory effects arise from the impact of boundaries on the process being simulated; resulting in an inability to reproduce realistic forcing conditions (Dalrymple, 1985).

CHAPTER 3

ORIENTATIONS OF STRAIGHT GROYNES

Summary

An alluvial channel at lowland as in Bangladesh is highly dynamic in nature, being exposed to severe bank erosion at high flood causing huge landloss as well as rapid sedimentation at low flow interrupting navigation. Groynes, revetments, and so on, are typically used to overcome these problems, but the targeted goals are not achieved as expected. This study investigates optimum orientation of groynes to improve their functions at high flow and low flow both. A 2D model for flow and morphology, RIC-Nays, is utilized in this study upon confirmation through the detailed experimental data. The channel and flow parameters are selected in conformity with a typical river channel of Bangladesh. Three main parameters are considered here to evaluate the performance of groynes – erosion in channel bed (thalweg), deposition in groyne field, and scour near groynes. Two types of groynes: non-permeable and permeable; and four alignments: 100^o, 90^o, 80^o, and 70^o to the direction of flow are considered. Computations reveal that smaller angled groynes function better in respect of deepening the channel bed, except that deposition near bank reduces.

3.1 General

Alluvial river channels are highly dynamic in nature as they pass through alluvium, which are loose sedimentary materials formed through entrainment, transportation and deposition throughout the channels. They involve diverse phenomena like turbulent flow, secondary flow, sediment transport, bank erosion process, and so on. As discussed in the preceding chapter, Bangladesh is a part of the Bengal delta and is formed by the complex influence of three mighty river systems of the world: the Ganges, the Brahmaputra, and the Meghna. It is the lowest riparian country of the

large combined basin area spread over China, India, Nepal, Bhutan, and Bangladesh. Thus it has been the natural outlet for enormous amount of water and sediment over the annual cycle.

Planform changes are particularly dramatic in the sand-bed braided Jamuna river (downstream part of Old Brahmaputra distributary). A widely varying discharge, easily eroded banks, and highly mobile bed materials cause response to fluvial processes quickly adopting and abandoning numerous anabranches at all levels within its braided system. Thus, Jamuna is reported for its very drastic nature. Severe bank erosion in monsoon there causes massive havoc in different areas devouring vast tract of lands, making further shrinkage in the cultivable areas, and rendering millions of people landless and homeless. On the other hand, rapid deposition in the streams and floodplains changes its topography and seriously reduces navigability of drainage channels at low flow. So that, the navigational routes are often hampered, and usually water-vehicles are forced to travel longer distances on the way towards their destinations in dry season, even sometimes they cannot move for several hours to several days. Large seasonal variations in river flow and the gradual shallowing of riverbeds cause bank erosion and channel migration, thus keep the channels unstable. So far, numbers of studies have been conducted to understand the dynamism of the river, and to develop and improve the techniques in stabilizing the channels (Coleman, 1969; Klassen and Vermeer, 1988; Elahi, *et al.*, 1991; Thorne, *et al.*, 1993; Bristow, 1993; Halcrow, *et al.*, 1994; Zhou and Chen, 1998; and CEGIS, 2004, 2005, 2006, and 2007). Based on research findings as well as engineering experiences, some river training measures have been implemented, such as BRE (Brahmaputra Right Embankment), groynes, revetment-like structures (hardpoints), and so on. Also repeated dredging is conducted to maintain navigability in dry season, which is only a temporary measure and is much expensive. Nevertheless, the targeted goals are not achieved as expected: sudden and big responses from the structure in one way, leave behind strong eddies near the head causing local scour responsible for instability of the structure itself (Halcrow and Haskoning, 1999; Klassen, *et al.*, 2002) and further, the diverted flow can affect the other regions such as islands where a large number of people are living or other bank, and so on, and make them unstable; attack to the same

bank where the structures are installed by some oblique flow; and so on. Besides, the desired regular channel for navigation is not influenced rightly, so that waterway transports are greatly interrupted at low flow period. Thus, the stable river course is not established yet. Compared to other restoration structures like bank covers, and so on, the groynes have been documented to be the most durable solution (Shields, *et al.*, 1995). However, in large rivers (in terms of width) like Jamuna, it is too expensive and impracticable to contract the total flow providing very large groynes on both sides. Thus, necessity arises to stabilize near-bank channels optimizing the deflection of flow from the bank to minimize high separation near groyne-head and guiding the flow smoothly, also to concentrate the flow for deepening the channel for navigation in dry season. In the present study the optimum orientation of groynes is explored to have their effective functioning at high flow and low flow conditions both.

So far experimental work led to a better understanding of the groyne-induced flow, such as Fazli *et al.* (2008), Ghodsian and Vaghefi (2009), Zhang *et al.* (2009), Yossef and Vriend (2010) and many others, but not to optimized design of new groynes. The possibilities of exploring alternative designs have come into sight with the availability of computer models. Depth-averaged two-dimensional (2D) models (Tingsanchali and Maheswaran, 1990; Jia and Wang, 1999; Zhang *et al.*, 2006; and some others) have been used to simulate hydrodynamic flow fields near groynes considering corrections for streamline curvature in momentum equations. Using large eddy simulation, McCoy *et al.* (2008) studied the flow hydrodynamics in a straight channel containing a series of groynes with shallow embayments. Separation of flow occurred near the groyne-head causes the formation of return currents towards the groyne-field area and often attacks the riverbank. Therefore, permeable groynes are, sometimes, preferred as a solution of the aforesaid problem (FAP 21, 2001); where a groyne acts as a roughness (resistance) to the flow, but does not block as the impervious groynes do. The loss of energy at the lee side of the groyne due to form drags reduces the flow velocity in the groyne region and hence influences deposition.

Despite the history of groynes is for long and their widespread use, there is still lack of knowledge about their effects in river. Even though local scour phenomena near a

single groyne has been discussed by many researchers (Tingsanchali & Maheswarn, 1990; Chen & Ikeda, 1997; Kuhnle 2002; Duan *et al.*, 2009; and others), discussions about the overall bed degradation in the main channel and aggradations in the groyne regions caused by a series of groynes are not sufficient yet. Usually, groynes are applied in a series, so as to achieve better effect from both bank protection and navigation point of view. The embayment region between successive groynes acts as a dead water zone, where the mean velocities are much smaller compared with the main channel and influences deposition there. Thus, this chapter presents the morphological impact of groynes with shallower embayments compared with the main channel, along with hydrodynamics behind these for the most optimal orientation to be identified for lowland rivers.

Therefore, the general goal of the numerical investigations presented in this chapter is to explore the suitable orientation of groynes to stabilize the main stream flow of an alluvial river channel through protecting the bank from erosion at high flood and maintaining thalweg for navigation at low flow as well. Keeping in view the above considerations, the associated sub-objectives are pointed out as follows:

- To investigate flow dynamics against various orientations of groynes in a sand-bed alluvial river channel.
- To investigate the sediment transport processes, and the changes in bed topographies in the far and near bank regions.
- To compare the performances of the groynes of various orientations to suggest the suitable one for field uses.

3.2 Numerical Model

The channel responses from a series of groynes with various orientations have been investigated with a numerical model. A 2D model for flow and morphology, RIC-Nays, is utilized in the present study. The governing equations involving flow dynamics in shallow water channels, and sediment transports in bed load as well as

suspended load mode, including the techniques in taking into consideration the bankline migration processes have been discussed in this section.

3.2.1 Hydrodynamic Equations

The shallow-water equations for two-dimensional unsteady flow expressed in a general coordinate system are calculated on the boundary-fitted structured grids using the finite-difference method. The system of equations governing the flow consists of the continuity and horizontal momentum equations. Assuming that the vertical component of velocity is negligible and that the pressure is hydrostatic, the two-dimensional equations, using a Cartesian coordinate system (x, y), can be given as follows:

Continuity equation:

$$\frac{\partial h}{\partial t}+\frac{\partial(hu)}{\partial x}+\frac{\partial(hv)}{\partial y}=0 \tag{01}$$

Momentum equations:

$$\frac{\partial(hu)}{\partial t}+\frac{\partial(hu^2)}{\partial x}+\frac{\partial(huv)}{\partial y}=-hg\frac{\partial H}{\partial x}-\frac{\tau_x}{\rho}+D_x \tag{02}$$

$$\frac{\partial(hv)}{\partial t}+\frac{\partial(huv)}{\partial x}+\frac{\partial(hv^2)}{\partial y}=-hg\frac{\partial H}{\partial y}-\frac{\tau_y}{\rho}+D_y \tag{03}$$

with:

Shear stresses

$$\frac{\tau_x}{\rho}=\frac{\tau_{bx}+\tau_{vx}}{\rho}=(C_d+K_v h)u\sqrt{u^2+v^2}\ ,\frac{\tau_y}{\rho}=\frac{\tau_{by}+\tau_{vy}}{\rho}=(C_d+K_v h)v\sqrt{u^2+v^2} \tag{04}$$

Diffusion terms

$$D_x=\frac{\partial}{\partial x}\left[\nu_t\frac{\partial(hu)}{\partial x}\right]+\frac{\partial}{\partial y}\left[\nu_t\frac{\partial(hu)}{\partial y}\right] \tag{05}$$

$$D_y=\frac{\partial}{\partial x}\left[\nu_t\frac{\partial(hv)}{\partial x}\right]+\frac{\partial}{\partial y}\left[\nu_t\frac{\partial(hv)}{\partial y}\right] \tag{06}$$

where h is depth of flow; H is water stage; u, v are depth-averaged velocity components in x and y directions, respectively; τ_x, τ_y are x and y components of resistance to flow, respectively; τ_{bx}, τ_{by} are x and y components of bottom-friction, respectively with C_d is bed friction coefficient; τ_{vx}, τ_{vy} are x and y components of vegetation drags, respectively, where $K_v = 1/2\, C_{dv} N_a d_v$ with C_{dv} is drag coefficient of vegetation, N_a vegetation density, and d_v is diameter; ρ is density of water; and ν_t is eddy viscosity. For considering turbulence in the flow phenomena, both zero- and two-equation turbulence models are available in the calculation framework. One of them is parabolic eddy viscosity model, $\nu_t = \kappa u_* z\left(1 - \frac{z}{h}\right)$; it is integrated over flow depth to get the depth-averaged one, $\nu_t = \frac{\kappa}{6} u_* h$; where u_* is bed shear velocity $= \sqrt{\frac{\tau_x^2 + \tau_y^2}{\rho}}$, and κ is Von Karman's constant (= 0.4). It is utilized in the present calculation; other available models are mixing length and k-ε turbulence models.

Transformation of flow equations from Cartesian coordinates (x,y) to General coordinates (ξ, η) system is as follows:

$$\frac{\partial}{\partial x} = \frac{\partial \xi}{\partial x}\frac{\partial}{\partial \xi} + \frac{\partial \eta}{\partial x}\frac{\partial}{\partial \eta}, \quad \frac{\partial}{\partial y} = \frac{\partial \xi}{\partial y}\frac{\partial}{\partial \xi} + \frac{\partial \eta}{\partial y}\frac{\partial}{\partial \eta}$$

or,

$$\begin{pmatrix} \frac{\partial}{\partial x} \\ \frac{\partial}{\partial y} \end{pmatrix} = \begin{pmatrix} \xi_x & \eta_x \\ \xi_y & \eta_y \end{pmatrix} \begin{pmatrix} \frac{\partial}{\partial \xi} \\ \frac{\partial}{\partial \eta} \end{pmatrix} \tag{07}$$

where;

$$\xi_x = \frac{\partial \xi}{\partial x},\ \xi_y = \frac{\partial \xi}{\partial y},\ \eta_x = \frac{\partial \eta}{\partial x},\ \eta_y = \frac{\partial \eta}{\partial y}$$

In the same manner,

$$\frac{\partial}{\partial \xi} = \frac{\partial x}{\partial \xi}\frac{\partial}{\partial x} + \frac{\partial y}{\partial \xi}\frac{\partial}{\partial y}, \quad \frac{\partial}{\partial \eta} = \frac{\partial x}{\partial \eta}\frac{\partial}{\partial x} + \frac{\partial y}{\partial \eta}\frac{\partial}{\partial y}$$

or,

$$\begin{pmatrix} \frac{\partial}{\partial \xi} \\ \frac{\partial}{\partial \eta} \end{pmatrix} = \begin{pmatrix} x_\xi & y_\xi \\ x_\eta & y_\eta \end{pmatrix} \begin{pmatrix} \frac{\partial}{\partial x} \\ \frac{\partial}{\partial y} \end{pmatrix} \tag{08}$$

where;

$$x_\xi = \frac{\partial x}{\partial \xi},\ x_\eta = \frac{\partial x}{\partial \eta},\ y_\xi = \frac{\partial y}{\partial \xi},\ y_\eta = \frac{\partial y}{\partial \eta}$$

Therefore,

$$\begin{pmatrix} \frac{\partial}{\partial \xi} \\ \frac{\partial}{\partial \eta} \end{pmatrix} = \frac{1}{\xi_x \eta_y - \xi_y \eta_x} \begin{pmatrix} \eta_y & -\eta_x \\ -\xi_y & \xi_x \end{pmatrix} \begin{pmatrix} \frac{\partial}{\partial x} \\ \frac{\partial}{\partial y} \end{pmatrix} = \begin{pmatrix} x_\xi & y_\xi \\ x_\eta & y_\eta \end{pmatrix} \begin{pmatrix} \frac{\partial}{\partial x} \\ \frac{\partial}{\partial y} \end{pmatrix} \tag{09}$$

with:

$$J = \xi_x \eta_y - \xi_y \eta_x,\ \frac{1}{J} \begin{pmatrix} \eta_y & -\eta_x \\ -\xi_y & \xi_x \end{pmatrix} = \begin{pmatrix} x_\xi & y_\xi \\ x_\eta & y_\eta \end{pmatrix} \tag{10}$$

$$x_\xi = \frac{1}{J}\eta_y,\ y_\xi = -\frac{1}{J}\eta_x,\ x_\eta = -\frac{1}{J}\xi_y,\ y_\eta = \frac{1}{J}\xi_x$$

or,

$$\eta_y = Jx_\xi,\ \eta_x = -Jy_\xi,\ \xi_y = -Jx_\eta,\ \xi_x = Jy_\eta$$

$$J = \xi_x \eta_y - \xi_y \eta_x = J^2 \left(x_\xi y_\eta - x_\eta y_\xi \right)$$

$$J = \frac{1}{\left(x_\xi y_\eta - x_\eta y_\xi \right)} \tag{11}$$

Contravariant components of flow velocity in (ξ, η) coordinates are defined as u^ξ and u^η (**Fig. 3.1**) by

$$u^\xi = \xi_x u + \xi_y v \tag{12}$$

$$u^\eta = \eta_x u + \eta_y v \tag{13}$$

or,

$$\begin{pmatrix} u^\xi \\ u^\eta \end{pmatrix} = \begin{pmatrix} \xi_x & \xi_y \\ \eta_x & \eta_y \end{pmatrix} \begin{pmatrix} u \\ v \end{pmatrix} \tag{14}$$

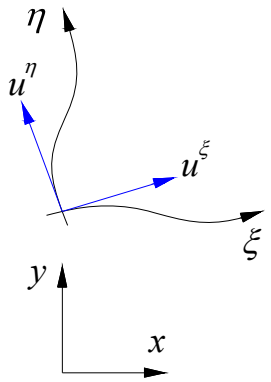

Fig. 3.1 Moving boundary-fitted coordinate system with contravariant components of velocity

$$\begin{pmatrix} u \\ v \end{pmatrix} = \frac{1}{J}\begin{pmatrix} \eta_y & -\xi_y \\ -\eta_x & \xi_x \end{pmatrix}\begin{pmatrix} u^\xi \\ v^\eta \end{pmatrix} \tag{15}$$

Therefore, 2D flow equations are:

$$\frac{\partial}{\partial t}\left(\frac{h}{J}\right)+\frac{\partial}{\partial \xi}\left(\frac{hu^\xi}{J}\right)+\frac{\partial}{\partial \eta}\left(\frac{hu^\eta}{J}\right)=0 \tag{16}$$

$$\frac{\partial u^\xi}{\partial t}+u^\xi\frac{\partial u^\xi}{\partial \xi}+u^\eta\frac{\partial u^\xi}{\partial \eta}+\alpha_1 u^\xi u^\xi+\alpha_2 u^\xi u^\eta+\alpha_3 u^\eta u^\eta=-g\left[\left(\xi_x^2+\xi_y^2\right)\frac{\partial H}{\partial \xi}+\left(\xi_x\eta_x+\xi_y\eta_y\right)\frac{\partial H}{\partial \eta}\right]$$

$$-\frac{C_d u^\xi}{hJ}\sqrt{\left(\eta_y u^\xi-\xi_y u^\eta\right)^2+\left(-\eta_x u^\xi+\xi_x u^\eta\right)^2}+D^\xi \tag{17}$$

$$\frac{\partial u^\eta}{\partial t}+u^\xi\frac{\partial u^\eta}{\partial \xi}+u^\eta\frac{\partial u^\eta}{\partial \eta}+\alpha_4 u^\xi u^\xi+\alpha_5 u^\xi u^\eta+\alpha_6 u^\eta u^\eta=-g\left[\left(\eta_x\xi_x+\eta_y\xi_y\right)\frac{\partial H}{\partial \xi}+\left(\eta_x^2+\eta_y^2\right)\frac{\partial H}{\partial \eta}\right]$$

$$-\frac{C_d u^\eta}{hJ}\sqrt{\left(\eta_y u^\xi-\xi_y u^\eta\right)^2+\left(-\eta_x u^\xi+\xi_x u^\eta\right)^2}+D^\eta \tag{18}$$

in which,

$$\alpha_1=\xi_x\frac{\partial^2 x}{\partial \xi^2}+\xi_y\frac{\partial^2 y}{\partial \xi^2},\ \alpha_2=2\left(\xi_x\frac{\partial^2 x}{\partial \xi\partial \eta}+\xi_y\frac{\partial^2 y}{\partial \xi\partial \eta}\right),\ \alpha_3=\xi_x\frac{\partial^2 x}{\partial \eta^2}+\xi_y\frac{\partial^2 y}{\partial \eta^2} \tag{19}$$

$$\alpha_4=\eta_x\frac{\partial^2 x}{\partial \xi^2}+\eta_y\frac{\partial^2 y}{\partial \xi^2},\ \alpha_5=2\left(\eta_x\frac{\partial^2 x}{\partial \xi\partial \eta}+\eta_y\frac{\partial^2 y}{\partial \xi\partial \eta}\right),\ \alpha_6=\eta_x\frac{\partial^2 x}{\partial \eta^2}+\eta_y\frac{\partial^2 y}{\partial \eta^2} \tag{20}$$

$$D^{\xi} = \left(\xi_x \frac{\partial}{\partial \xi} + \eta_x \frac{\partial}{\partial \eta}\right)\left[\nu_t\left(\xi_x \frac{\partial u^{\xi}}{\partial \xi} + \eta_x \frac{\partial u^{\xi}}{\partial \eta}\right)\right] + \left(\xi_y \frac{\partial}{\partial \xi} + \eta_y \frac{\partial}{\partial \eta}\right)\left[\nu_t\left(\xi_y \frac{\partial u^{\xi}}{\partial \xi} + \eta_y \frac{\partial u^{\xi}}{\partial \eta}\right)\right] \tag{21}$$

$$D^{\eta} = \left(\xi_x \frac{\partial}{\partial \xi} + \eta_x \frac{\partial}{\partial \eta}\right)\left[\nu_t\left(\xi_x \frac{\partial u^{\eta}}{\partial \xi} + \eta_x \frac{\partial u^{\eta}}{\partial \eta}\right)\right] + \left(\xi_y \frac{\partial}{\partial \xi} + \eta_y \frac{\partial}{\partial \eta}\right)\left[\nu_t\left(\xi_y \frac{\partial u^{\eta}}{\partial \xi} + \eta_y \frac{\partial u^{\eta}}{\partial \eta}\right)\right] \tag{22}$$

Generally, ξ and η are non-dimensional values and can be expressed in the computational domain as,

$$0 \le \xi \le 1,\ \ 0 \le \eta \le 1 \tag{23}$$

Therefore, the dimensions of ξ_x, ξ_y, η_x, and η_y are [1/Length], and the dimensions of u^{ξ} and u^{η} are [1/Time]. The directions of u^{ξ} and u^{η} are ξ and η, respectively; but their magnitudes are not in velocity-unit. In order to describe them in velocity dimensions, transformation is needed using local computational grid sizes. Defining the actual local grid-sizes as $\Delta\tilde{\xi}$ and $\Delta\tilde{\eta}$, the ratio with the computational grid-sizes, $\Delta\xi$ and $\Delta\eta$ are as follows:

$$\frac{\Delta\xi}{\Delta\tilde{\xi}} = \xi_r,\ \ \frac{\Delta\eta}{\Delta\tilde{\eta}} = \eta_r \tag{24}$$

Using these relationships, ξ_x, ξ_y, η_x, and η_y can be described as follows:

$$\xi_x = \frac{\partial\xi}{\partial x} = \xi_r \frac{\partial\tilde{\xi}}{\partial x} = \xi_r \tilde{\xi}_x,\ \ \xi_y = \frac{\partial\xi}{\partial y} = \xi_r \frac{\partial\tilde{\xi}}{\partial y} = \xi_r \tilde{\xi}_y \tag{25}$$

$$\eta_x = \frac{\partial\eta}{\partial x} = \eta_r \frac{\partial\tilde{\eta}}{\partial x} = \eta_r \tilde{\eta}_x,\ \ \eta_y = \frac{\partial\eta}{\partial y} = \eta_r \frac{\partial\tilde{\eta}}{\partial y} = \eta_r \tilde{\eta}_y \tag{26}$$

The physical contravariant velocity components in velocity-unit, $\tilde{u}^{\xi}$ and $\tilde{u}^{\eta}$ can be written as follows.

$$\tilde{u}^{\xi} = \tilde{\xi}_x u + \tilde{\xi}_y v = \frac{u^{\xi}}{\xi_r},\ \ \tilde{u}^{\eta} = \tilde{\eta}_x u + \tilde{\eta}_y v = \frac{u^{\eta}}{\eta_r} \tag{27}$$

The assumptions made to simplify the momentum diffusion terms are (i) second order derivatives with metric coefficients are negligible, and (ii) grids are treated quasi co-orthogonal locally. Thus, the diffusion terms are described as follows:

$$D^{\xi} \cong \frac{\partial}{\partial \xi}\left(\nu_t \xi_r^2 \frac{\partial u^{\xi}}{\partial \xi}\right) + \frac{\partial}{\partial \eta}\left(\nu_t \eta_r^2 \frac{\partial u^{\xi}}{\partial \eta}\right) \tag{28}$$

$$D^{\eta} \cong \frac{\partial}{\partial \xi}\left(\nu_t \xi_r^2 \frac{\partial u^{\eta}}{\partial \xi}\right) + \frac{\partial}{\partial \eta}\left(\nu_t \eta_r^2 \frac{\partial u^{\eta}}{\partial \eta}\right) \tag{29}$$

in which the following relationships were used:

$$\xi_x^2 + \xi_y^2 = \xi_r^2\left(\tilde{\xi}_x^2 + \tilde{\xi}_y^2\right) = \xi_r^2\left(\sin^2\theta + \cos^2\theta\right) = \xi_r^2$$

$$\xi_x \eta_x + \xi_y \eta_y = \xi_r \eta_r\left(\tilde{\xi}_x \tilde{\eta}_x + \tilde{\xi}_y \tilde{\eta}_y\right) = \xi_r \eta_r\left(-\cos\theta \sin\theta + \cos\theta \sin\theta\right) = 0$$

$$\eta_x^2 + \eta_y^2 = \eta_r^2\left(\tilde{\eta}_x^2 + \tilde{\eta}_y^2\right) = \eta_r^2\left(\sin^2\theta + \cos^2\theta\right) = \eta_r^2$$

$$J = \xi_x \eta_y - \xi_y \eta_x = \xi_r \eta_r\left(\tilde{\xi}_x \tilde{\eta}_y - \tilde{\xi}_y \tilde{\eta}_x\right) = \xi_r \eta_r\left(\sin^2\theta + \cos^2\theta\right) = \xi_r \eta_r$$

here, θ is an angle between x- and ξ- or , y- and η- axes.

3.2.2 Sediment Transport Equations

Morphological computation involves a combination of flow fields, sediment transports, and bed evolution associated with bank migration. After resolving the flow fields, the sediment transport fields are computed from the expressions of both bed load and suspended load separately. Finally, the changes in the bed topography due to total load are determined.

The bedload in the depth-averaged velocity direction q_b can be calculated by the following Ashida and Michiue (1972) formula,

$$q_b = 17\tau_*^{3/2}\left(1 - \frac{\tau_{*c}}{\tau_*}\right)\left[1 - \sqrt{\frac{\tau_{*c}}{\tau_*}}\right]\sqrt{(s_g - 1)gd^3} \tag{30}$$

in which τ_{*_c} is dimensionless critical shear stress; τ_* is dimensionless total bed shear stress acts on the channel bed $= \dfrac{hI_e}{(s_g - 1)d}$, with I_e is energy slope, s_g is specific gravity; d is sediment diameter. When Manning's formula is applied for I_e, τ_* becomes as follows,

$$\tau_* = \frac{C_d V^2}{(s_g - 1)gd} = \frac{n_m^2 V^2}{(s_g - 1)dh^{1/3}} \tag{31}$$

in which n_m is Manning's roughness coefficient; g is acceleration due to gravity; V is total velocity, which can be defined as, $V = \sqrt{u^2 + v^2}$.

One of the important factors for the computation of bedload transport fields is the effect of gravity on the sand particles in the transverse slope of the bed surface (**Fig. 3.2**).

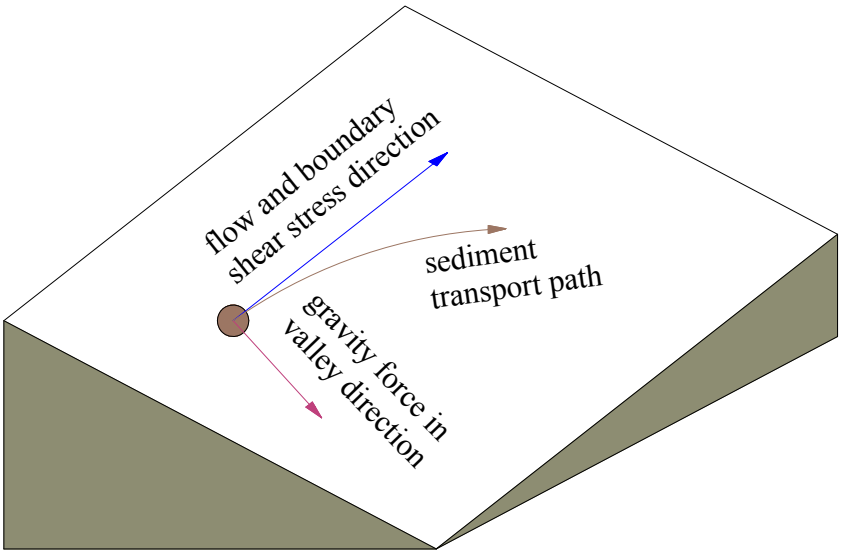

Fig. 3.2 Gravity effect on sediment particles

Watanabe *et al.* (1990) proposed the following equation considering the gravitational effect in streamline and transverse directions,

$$\tilde{q}^{\xi} = q_b \left[\frac{\tilde{u}_b^{\xi}}{V_b} - \gamma_g \left(\frac{\partial z_b}{\partial \tilde{\xi}} + \cos\theta \frac{\partial z_b}{\partial \tilde{\eta}} \right) \right] \tag{32}$$

$$\tilde{q}^{\eta} = q_b \left[\frac{\tilde{u}_b^{\eta}}{V_b} - \gamma_g \left(\frac{\partial z_b}{\partial \tilde{\eta}} + \cos\theta \frac{\partial z_b}{\partial \tilde{\xi}} \right) \right] \tag{33}$$

in which $\tilde{u}_b^{\xi}$ and $\tilde{u}_b^{\eta}$ are velocity components at the bottom in ξ and η directions; V_b is total velocity at the bottom; z_b is bed elevation; and γ_g is an adjustment coefficient for slope gravitational effect. Hasegawa (1983) proposed the following formula for this coefficient,

$$\gamma_g = \sqrt{\frac{\tau_{*c}}{\mu_s \mu_k \tau_*}} \tag{34}$$

Thus, he derived a simple equation for the angle between the sediment movement direction and streamline as follows,

$$\tan\phi = \frac{V_n}{V_s} = \frac{u_{bn}}{u_{bs}} - \sqrt{\frac{\tau_{*c}}{\mu_s \mu_k \tau_*}} \frac{\partial z_b}{\partial n} \tag{35}$$

where V_s and V_n are sediment movement velocity components in *s* and *n* directions (*s*, streamline direction of the depth-averaged flow; *n*, transverse direction perpendicular to streamline), respectively; μ_s and μ_k are static and kinetic friction coefficients of bed materials, respectively with μ_s μ_k = 0.5; u_{bs} and u_{bn} are near-bed velocities in *s*- and *n*- directions, respectively. The first term of the right-hand side of **Eq. 35** is the direction of flow velocity near the bed, and the second term expresses the effect of gravity on sand particles on the transverse slope of the bed surface. If the bed cross-section is transversely flat, the second term disappears, and the directions of the sediment movement and flow near the bed coincide with each other.

Now, the near-bed streamwise velocity can be estimated as,

$$u_{bs} = \beta_v V \tag{36}$$

where u_{bs} is simply related to the depth-averaged flow velocity, β_v is assumed as a parabolic function by Engelund (1974) for velocity profile in depth direction and

proposed as, $\beta_v = 3(1-\sigma_v)(3-\sigma_v)$, where $\sigma_v = \dfrac{3}{\phi_0 \kappa + 1}$, with ϕ_0 = velocity coefficient (=V/u_*). However, in curved flow, secondary flow (spiral flow in transverse direction) induced by the centrifugal force acting on the curved streamline is developed, and q_n driven by the secondary flow is produced (**Fig. 3.3**), which is very important factor to predict river bed topography in curved flow.

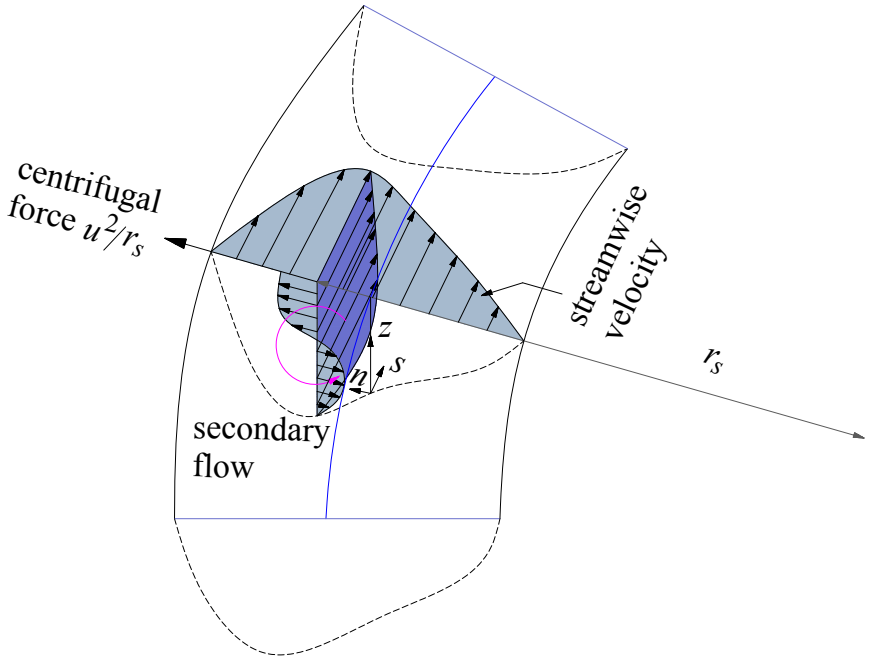

Fig. 3.3 Secondary flow

Accordingly, it has been taken into account as,

$$u_{bn} = -u_{bs} N_* \frac{h}{r_s} \tag{37}$$

where, N_* is a co-efficient to describe the intensity of secondary flow in a curved streamline; and r_s is a radius of curvature of the streamline. Investigations of the value of N_* have been performed by many researchers, e.g., Ikeda (1974), Engelund (1974), Rozovskii (1961), and Zimmerman (1977). N^* = 7.0 is adopted in the calculation as proposed by Engelund (1974). Angle between near-bed velocity vector and s-axis, δ

can be defined as, $\tan\delta = \dfrac{u_{bn}}{u_{bs}} = -N_* \dfrac{h}{r_s}$, and angle between *x*- and *s*-axis, θ_s can be written as, $\tan\theta_s = \dfrac{v}{u}$. Finally, the angle between sediment movement direction and the *x*-axis, β can be known from, $\beta = \phi + \theta_s$ (**Fig. 3.4**).

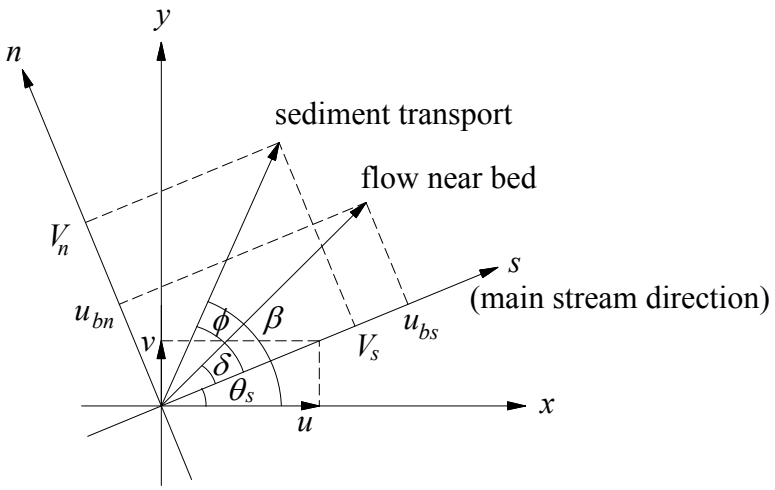

Fig. 3.4 Angles of flow and sediment transport direction

From Eqs. (36) and (37), V_b in Eqs. (32) and (33) can be expressed as,

$$V_b = \sqrt{u_{bs}^2 + u_{bn}^2} \approx u_{bs} \tag{38}$$

It is because the order of u_{bn} is one order smaller than that of u_{bs}. $\tilde{u}_b^{\xi}$ and $\tilde{u}_b^{\eta}$ can be obtained from the following equations:

$$\tilde{u}_b^{\xi} = \frac{\partial \tilde{\xi}}{\partial s} u_{bs} + \frac{\partial \tilde{\xi}}{\partial n} u_{bn} = \left(\frac{\partial x}{\partial s}\frac{\partial \tilde{\xi}}{\partial x} + \frac{\partial y}{\partial s}\frac{\partial \tilde{\xi}}{\partial y} \right) u_{bs} + \left(\frac{\partial x}{\partial n}\frac{\partial \tilde{\xi}}{\partial x} + \frac{\partial y}{\partial n}\frac{\partial \tilde{\xi}}{\partial y} \right) u_{bn}$$

$$= \left(\cos\theta_s \, \tilde{\xi}_x + \sin\theta_s \, \tilde{\xi}_y \right) u_{bs} + \left(-\sin\theta_s \, \tilde{\xi}_x + \cos\theta_s \, \tilde{\xi}_y \right) u_{bn}$$

$$= \frac{1}{\xi_r} \left\{ \left(\cos\theta_s \xi_x + \sin\theta_s \xi_y \right) u_{bs} + \left(-\sin\theta_s \xi_x + \cos\theta_s \xi_y \right) u_{bn} \right. \tag{39}$$

$$u_b^{\tilde{\eta}} = \frac{\partial \tilde{\eta}}{\partial s} u_{bs} + \frac{\partial \tilde{\eta}}{\partial n} u_{bn} = \left(\frac{\partial x}{\partial s} \frac{\partial \tilde{\eta}}{\partial x} + \frac{\partial y}{\partial s} \frac{\partial \tilde{\eta}}{\partial y} \right) u_{bs} + \left(\frac{\partial x}{\partial n} \frac{\partial \tilde{\eta}}{\partial x} + \frac{\partial y}{\partial n} \frac{\partial \tilde{\eta}}{\partial y} \right) u_{bn}$$

$$= \left(\cos\theta_s \tilde{\eta}_x + \sin\theta_s \tilde{\eta}_y \right) u_{bs} + \left(-\sin\theta_s \tilde{\eta}_x + \cos\theta_s \tilde{\eta}_y \right) u_{bn}$$

$$= \frac{1}{\eta_r} \left\{ \left(\cos\theta_s \eta_x + \sin\theta_s \eta_y \right) u_{bs} + \left(-\sin\theta_s \eta_x + \cos\theta_s \eta_y \right) u_{bn} \right\} \tag{40}$$

in which the following relations are used:

$$\frac{\partial x}{\partial n} = -\frac{v}{V} = -\sin\theta_s, \quad \frac{\partial y}{\partial n} = -\frac{u}{V} = \cos\theta_s \tag{41}$$

$$\frac{\partial x}{\partial s} = \frac{u}{V} = \cos\theta_s, \quad \frac{\partial y}{\partial s} = \frac{v}{V} = \sin\theta_s \tag{42}$$

The curvature of the streamline, $1/r_s$ is determined by the angle θ_s between the streamline in the mainstream direction and x-axis in Cartesian coordinates, as shown in **Fig. 3.5** below.

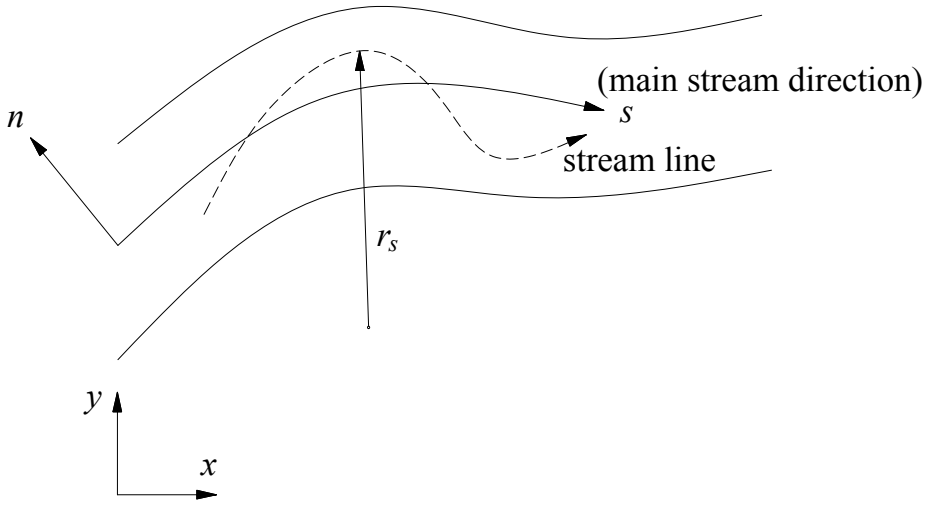

Fig. 3.5 Definition sketch of streamline and radius of curvature (r_s)

$$\frac{1}{r_s} = \frac{\partial \theta_s}{\partial s} \tag{43}$$

$$\theta_s = \tan^{-1}\left(\frac{v}{u}\right) \tag{44}$$

$$\frac{1}{r_s} = \frac{\partial}{\partial s}\left[\tan^{-1}(T)\right] = \frac{\partial}{\partial T}\left[\tan^{-1}(T)\right]\frac{\partial T}{\partial s} = \frac{1}{1+T^2}\frac{\partial T}{\partial s} \tag{45}$$

in which, $T = \frac{v}{u}$, and $\frac{1}{1+T^2} = \frac{1}{1+\left(v/u\right)^2} = \frac{u^2}{u^2+v^2} = \frac{u^2}{V^2}$

$$\frac{\partial T}{\partial s} = \frac{\partial}{\partial s}\left(\frac{v}{u}\right) = \frac{u\dfrac{\partial v}{\partial s} - v\dfrac{\partial u}{\partial s}}{u^2} \tag{46}$$

$$\frac{\partial}{\partial s} = \frac{\partial x}{\partial s}\frac{\partial}{\partial x} + \frac{\partial y}{\partial s}\frac{\partial}{\partial y} = \frac{u}{V}\frac{\partial}{\partial x} + \frac{v}{V}\frac{\partial}{\partial y} = \frac{u}{V}\left(\xi_x\frac{\partial}{\partial \xi} + \eta_x\frac{\partial}{\partial \eta}\right) + \frac{v}{V}\left(\xi_y\frac{\partial}{\partial \xi} + \eta_y\frac{\partial}{\partial \eta}\right) \tag{47}$$

According to **Eq. 47**, the curvature of streamline, $1/r_s$, in the moving boundary-fitted coordinate system is given by

$$\frac{1}{r_s} = \frac{1}{V^3}\left[u^2\left(\xi_x\frac{\partial v}{\partial \xi} + \eta_x\frac{\partial v}{\partial \eta}\right) + uv\left(\xi_y\frac{\partial v}{\partial \xi} + \eta_y\frac{\partial v}{\partial \eta}\right) - uv\left(\xi_x\frac{\partial u}{\partial \xi} + \eta_x\frac{\partial u}{\partial \eta}\right) - v^2\left(\xi_y\frac{\partial u}{\partial \xi} + \eta_y\frac{\partial u}{\partial \eta}\right)\right] \tag{48}$$

In considering suspended load transport, an exponential distribution of concentration is assumed in the vertical direction, and sediment transport expression is used to derive the local equilibrium concentration fields, which is employed to find the spatial distribution of sediment concentration utilizing the depth-averaged advection-diffusion equation. The two-dimensional equation for suspended load transports can be expressed as,

$$\frac{\partial}{\partial t}\left(\frac{Ch}{J}\right) + \frac{\partial}{\partial \xi}\left(\frac{Cu^{\xi}h}{J}\right) + \frac{\partial}{\partial \eta}\left(\frac{Cu^{\eta}h}{J}\right) = \frac{q_{su}}{J} - \frac{w_f c_b}{J} \tag{49}$$

For steady, uniform flow condition, this equation can be rewritten as,

$$\frac{\partial C}{\partial t} + u^{\xi}\frac{\partial C}{\partial \xi} + u^{\eta}\frac{\partial C}{\partial \eta} = \left(q_{su} - w_f c_b\right)/h \tag{50}$$

with

$$\frac{\partial C}{\partial t} + u^{\xi}\frac{\partial C}{\partial \xi} + v^{\eta}\frac{\partial C}{\partial \eta} = 0 \qquad \text{: advection phase} \tag{51}$$

and

$$\frac{\partial C}{\partial t} = \left(q_{su} - w_f c_b\right)/h \qquad \text{: non-advection phase} \tag{52}$$

in which C is the depth-averaged volumetric concentration of suspended sediment, c_b is the reference concentration (here reference level is at $b = 0.05h$ from the bed), q_{su} is the rate of entrainment of suspended sediment from unit area of bed surface, w_f = the fall velocity of sediment. Exponential distribution of suspended sediment is assumed in the model, which can be written as,

$$c = c_b \exp\left(-\beta_s \varsigma\right) \tag{53}$$

with $\beta_s = w_f h/\varepsilon_s$, $\varsigma = z/h$, where ε_s = the depth-averaged diffusion coefficient of sediment = $\kappa u_* h/6$. Integrating **Eq. 53**, the depth-averaged concentration then can be derived as,

$$C = \frac{1}{h}\int_0^1 c\,d\varsigma = \frac{c_b}{\beta_s}\left(1 - \exp\left(-\beta_s\right)\right) \tag{54}$$

According to Itakura and Kishi (1980), the pick-up rate q_{su} can be estimated from the following expression:

$$q_{su} = K_c\left(\alpha_* \frac{\rho_s - \rho}{\rho_s}\frac{gd}{u_*}\Omega - w_f\right) \tag{55}$$

$$\text{with } \Omega = \frac{\tau_*}{B_*}\frac{\int_{a'}^{\infty}\zeta\frac{1}{\sqrt{\pi}}\exp\left(-\zeta^2\right)d\zeta}{\int_{a'}^{\infty}\frac{1}{\sqrt{\pi}}\exp\left(-\zeta^2\right)d\zeta} + \frac{\tau_*}{B_*\eta_0} - 1 \tag{56}$$

where $a' = B^*/\tau_* - 1/\eta_0$; in which $B_* = 0.143$ and $\eta_0 = \sqrt{2}\sigma = 0.5$ could be adopted in the model. A value of $\alpha_* = 0.14$ was determined by an examination of the data reported by Kishi *et al.* (1966), and a value of K_c = 0.008 is determined so as to fit many data for c_b. Also $\zeta = r'/\sqrt{2}\sigma$ = a dummy variable in the equation, where r' is fluctuating component of r and r is normalized hydrodynamic force, and σ^2 is

variance of hydrodynamic force. For the fall velocity of suspended load, the following Rubey's (1933) equation is used:

$$\frac{w_f}{\sqrt{\Delta_g g d}} = \sqrt{\frac{2}{3} + \frac{36\nu^2}{\Delta_g g d^3}} - \sqrt{\frac{36\nu^2}{\Delta_g g d^3}} \tag{57}$$

where ν is kinematic viscosity = 0.01 cm^2/s, Δ_g = submerged specific gravity of sediment = 1.65, d = sediment size (cm).

Two-dimensional sediment continuity equation, when only bedload contributes the change in bed level, can be expressed as,

$$\frac{\partial z_b}{\partial t} + \frac{1}{1-\lambda}\left[\frac{\partial q_x}{\partial x} + \frac{\partial q_y}{\partial y}\right] = 0 \tag{58}$$

where q_x and q_y are bedload transport rates per unit width in x and y directions, respectively; and λ is porosity of bed materials. It has been depicted in the following figure (**Fig. 3.6**),

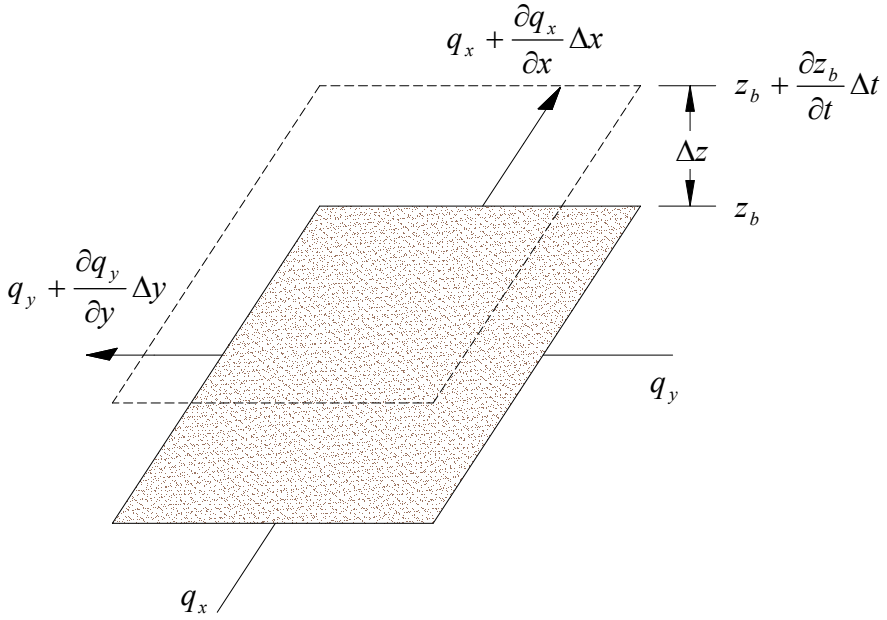

Fig. 3.6 Description of bedload transport and bed evolution

As both bedload and suspended load transports occur in alluvial rivers with fine sand, the continuity equation including suspended sediment, can be written in the general coordinate system as,

$$\frac{\partial}{\partial t}\left(\frac{z_b}{J}\right)+\frac{1}{1-\lambda}\left[\frac{\partial}{\partial \xi}\left(\frac{q^{\xi}}{J}\right)+\frac{\partial}{\partial \eta}\left(\frac{q^{\eta}}{J}\right)+\left(\frac{q_{su}}{J}-\frac{w_f c_b}{J}\right)\right]=0 \tag{59}$$

in which q^{ξ} and q^{η} are contravariant components of bedload transport rate in ξ and η directions. They are also needed to be transformed to describe in actual sediment transport rate in [Length^2/Time],

$$\tilde{q}^{\xi}=\frac{q^{\xi}}{\xi_r},\ \tilde{q}^{\eta}=\frac{q^{\eta}}{\eta_r} \tag{60}$$

3.2.3 Bank Erosion and Channel Migration

The changes in bed topography and the erosion of banks occurred together. In designing a model for such events, particularly for natural rivers where banks are not protected, a model is required that can deal with riverbed evolution and bank erosion simultaneously. As bank erosion highly relates the bed-forms, a submodel to account for bankline migration is incorporated in the numerical scheme, and this is considered for non-cohesive bank materials only. The computations for the flow and the bed evolution are made using the equations as described in the preceding sections. The deformation in the plan shape of the channel with a special attention to the bed evolutions near the banks has been determined according to the following procedure.

Due to currents and scour, when computations show that the cross-sectional slope angle of the riverbank exceeds the angle of repose (θ_c) under the water, the sediment beyond the submerged repose angle is assumed to be momentarily eroded up to the point of this angle (Hasegawa, 1983) and bank erosion will progress. Furthermore, it is assumed that the sediment load equal to the amount of sediment beyond the submerged critical angle of slope, is deposited at the foot of the bank slope [**Fig. 3.7(a)**], and it is included in the computation of the channel bed evolution as a supply

of sediment from the banks. Thus the bank retreats intermittently through the repeated cycles of bank scour, collapse, deposition of the collapsed bank materials, and transportation of the deposited materials.

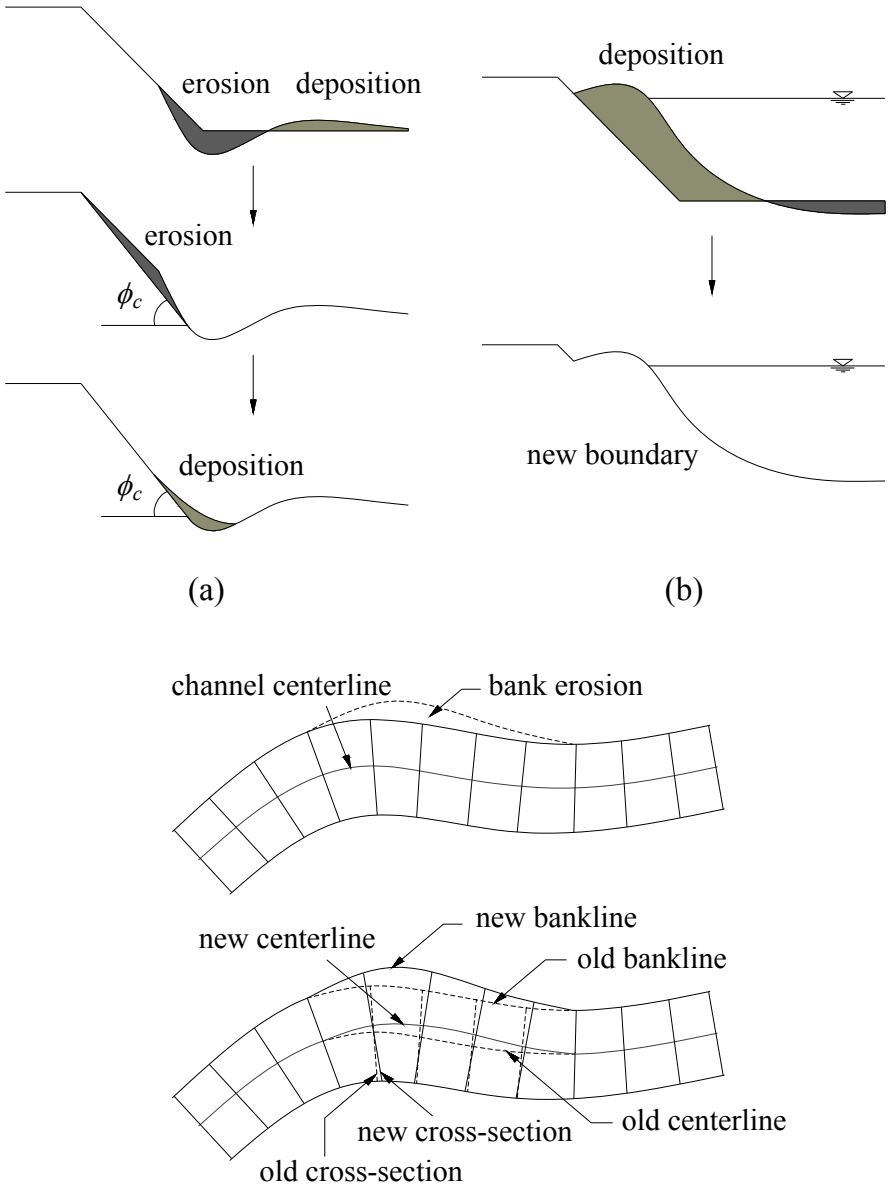

Fig. 3.7 Bankline migration process and the renewal of channel geometry: (a) bank erosion and enlargement of channel width; (b) deposition and narrowing the channel; and (c) renewal of the computational grid by bank degradation

As the banklines shift toward the transverse direction due to the bank erosion processes, the numerical grids are reproduced with the moving boundaries. If the erosion of the bank slope face advances toward the top of the slope, the computational range is enlarged in the cross-sectional direction of the channel. Conversely, if a part of the bed near the banks is transformed into dry land narrowing the water channel, the computational range is successively moved inside to the new waterline [**Fig. 3.7(b)**]. For these changes of water line due to erosion or deposition in the bank, (i) a new central line of the channel is set in each step, and (ii) along this new central line of the channel, new cross-sections perpendicular to this line [**Fig. 3.7(c)**] are set as the initial condition for the next step of the computation. Thus, new computational meshes are formed; the computational data are all transformed from old to new computational grids. While transforming all the computational data between new and old grids, a linear transformation based on geometric locations is carried out. The grid points are rearranged at equal intervals between the right and left banklines in the lateral direction.

Boundary conditions

Two types of boundaries should be prescribed along the boundary of the computational domain in the hydrodynamic as well as sediment transport modules: open and closed boundaries. At closed or solid wall boundary like sidewalls of emerged bars and banks, no velocity is considered in the transverse direction ($v = 0$), but a slip velocity (u) is adopted in the streamwise direction as,

$$\frac{\tau_w}{\rho} = \varepsilon_s \frac{du}{dn} = C_d u_w^2 \tag{61}$$

in which $\tau_w =$ shear stress at the wall, and $C_d =$ friction factor at the wall. The introduction of the diffusion coefficient ε_s enables the calculation of the slip velocity. In considering sediment transport, the bedload transport rate and the suspended load concentration gradient are set to zero: $q_b = 0$, $\partial c/\partial n = 0$, where n is the coordinate in the direction normal to the boundary. For open boundaries, a time series of flow discharge and thus lateral distribution of velocity at the upstream inlet, and a time series of the measured water surface elevation at the downstream outlet section are to

be specified. In the sediment transport simulation, the sediment discharge must be given at each point of the inflow boundary. The lateral distribution of suspended sediment concentration can also be provided from the transport capacity equation utilizing velocity distribution. The bedload transport rate per unit width is also specified in the inflow boundary by the equilibrium formula. In the outlet boundary, the suspended load concentration gradient in the flow direction is set to zero, i.e., $\partial c/\partial s = 0$, where s is the coordinate in the flow direction.

Moreover, some nodes can switch from dry to weight or vice versa, when the water level varies. So it is important to simulate the inundation of flood plains and wetlands, shallow flows over and near islands or emerged bars in rivers, and wave run-up in a coastal line (Bradford and Sanders 2002; Zhao *et al.* 1994). The boundary in the shallow regions around emerged bars and near side banks is dealt with a moving boundary for rearrangements of the computation grid. For a very small value of flow depth, there is flow and flow velocity in the streamwise and/or transverse directions, the momentum equations are not solved and the flow velocity is set to zero in these situations. Here a false water depth is assumed to perform that function.

Computational procedure

The channel is considered here whose width changes by erosion and sediment deposition. For this reason, computation was made by using general coordinates applicable to arbitrary shapes of the channel. The model applies the following processes to calculate the changes in flow fields and channel morphology with time at infinitesimal intervals up to the designated time.

- Computing the depth-averaged flow fields in the given plan shape of a water channel utilizing initial and boundary conditions, which include initial bed topography, initial flow, and sediment conditions,
- Computing the secondary flow perpendicular to the streamline of the depth-averaged flow,
- Computing the sediment transport rate and riverbed evolution,
- Computing bank erosion, sediment deposition, and shape alteration of a channel,

- Setting a coordinate system along a new boundary and updating the computational data,
- Updating time ($t = t + \Delta t$) to repeat the steps mentioned above.

The equations described in the preceding sections are solved on the boundary fitted structured grids. The equations for flow are computed implicitly, while the continuity equation for sediment transport is computed explicitly. Upwind difference scheme and CIP method both are available in the calculation scheme to employ for advective terms of the equations, while SOR method is used to calculate the non-advection phase of momentum equations coupled with continuity equation. CIP method is originally proposed by Yabe and Ishikawa (1990), and modified for the calculation of open channel flow by Nakayama *et al.* (1998). Time depended change of bed elevation is computed using central finite differences. A finite number of equations at a finite number of mesh or grid points in space and time are found through discretization of the equations by finite-difference method. A steady-state solution of these equations is obtained for the unknown nodal values by an iterative process.

3.3 Model Verification

The model was tested first in a laboratory experiment case (Rajaratnam and Nwachukwu, 1983), where flow fields were measured in the recirculation zone behind a groyne-like structure. In the experiment, a straight rectangular flume, which is 37 m long, 0.92 m wide, and 0.76 m deep with smooth bed and sides, was used to quantify the groyne induced flow-fields. The groyne used was an aluminum plate of thickness of 3 mm, 0.15 m long (b), and was projected perpendicular to the vertical side wall into the channel and above the water surface. The flow discharge of 0.045 m^3/s, flow depth of 0.189 m, and Froude number of 0.19 were set as the hydraulic condition of the experiment. Velocity measurements made at four different sections with distances of x/b = 2, 4, 6, 8 downstream of the groyne (x, downstream distance from the groyne section) are chosen to compare with the simulated results, in which the depth-averaged parabolic eddy viscosity model is adopted. The comparison has been shown in **Fig. 3.8**, where it can be seen that the flow fields from the physical model study are

well reproduced by the numerical model outside of the groyne field, but some discrepancies are present downstream of the groyne, where the flow is highly skewed.

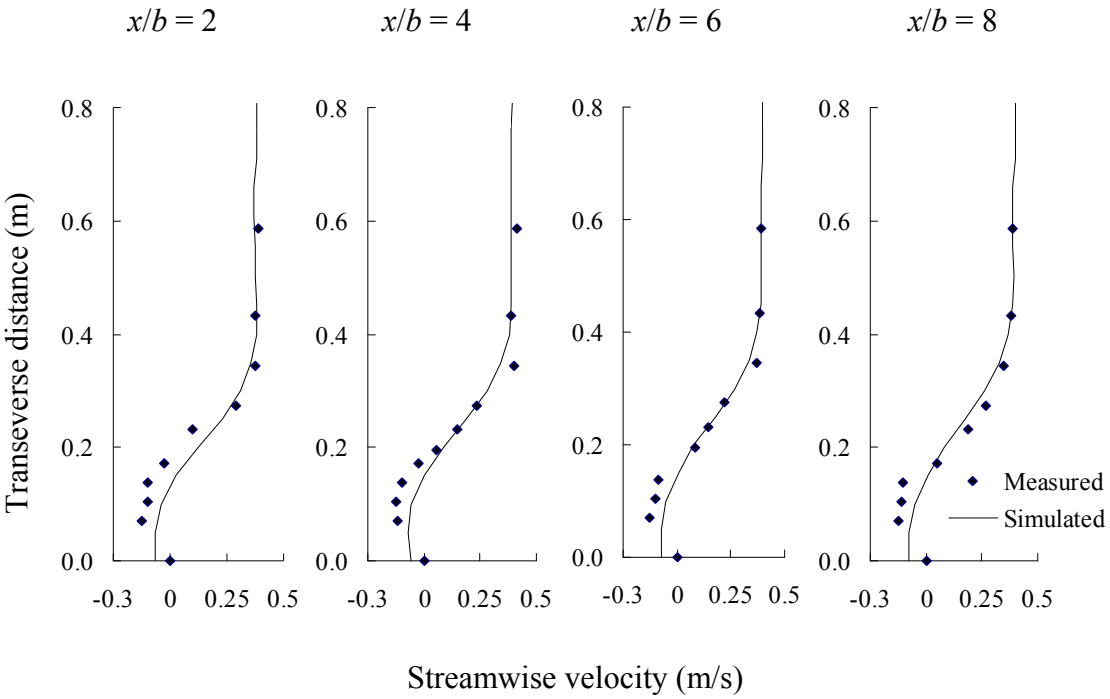

here, b = length of groyne model (0.15m), and x = downstream distance from groyne section

Fig. 3.8 Comparison of the simulated results with the experimental data (Rajaratnam and Nwachukwu, 1983)

Although, the flow phenomena near a single groyne, especially for a submerged one, are three-dimensional (3D), the physics of the present problem, the responses from the series of groynes with shallower embayments to influence deposition in groyne field and erosion in main channel, however, is almost two-dimensional. Moreover, a depth-averaged, 2D model is advantageous for its cost-effectiveness and easiness to calibrate, and it requires less input data for practical engineering applications.

3.4 Model Setup and Procedure

3.4.1 Model Setup

A schematized straight channel reach is considered in the numerical investigations to compare the functions of groynes of various orientations, where length (L) and width (B) of the modeled area are taken 400.0 m and 280.0 m, respectively, with a longitudinal bed slope of 7.5 cm/km. These dimensions are fixed by considering one of the subchannels of the aforementioned river near bank. However, the large scale application of groyne structures in Jamuna shows some local effects near groynes for variable discharges, which can endanger the stability of the structures, too. This may cause by the solitary behavior of the groynes in respect of corresponding waterline (bankline), i.e, the groyne behavior changes due to the change in water stages and hence bankline. Four groyne structures of same orientation are placed on one side of the channel to investigate the channel responses against each type of groynes. Projected length (L_g) of a groyne structure is 40.0 m, and a certain interval (S_g) 100.0 m (i.e., aspect ratio, S_g/L_g = 2.5) is maintained in applying them in the channel, based on the studies and practices, in consideration of both bank protection and maintenance of navigation channel (section 2.4.2). **Figs. 3.9(a and b)** depict the model layout with a typical orientation of groynes and grids, and channel cross-section, respectively. The flow is in the x-direction with x = 0 at upstream end, and y-axis is pointing to the left bank in the transverse direction.

Since at high water stages, discharge is distributed over a much wider area, the bank regions are provided with a mild slope 1:9 on either side, i.e., a shallow area near bank, to avoid the deviation of channel geometry from the natural situation; whereas it is much larger from the consideration of submerged repose angle. This is important to consider, reflecting the effect of low flow, as only a part of a groyne length (around 50%) is effective to function that time. Four different orientations of groynes such as 100^o, 90^o, 80^o, and 70^o to the direction of flow as designated by **100d** through **70d** (**Fig. 3.10**), respectively, are considered to find the optimum one. An angle of a groyne structure is defined as the angle between the longitudinal axis of the groyne and bankline at downstream side. Two types of groynes in terms of permeability are considered to understand the effect of a groyne angle rightly: (i) non-permeable (**100d**, **90d**, **80d**, **70d**) and (ii) permeable (**90d**, **80d**, **70d**). For the former ones, the cells in

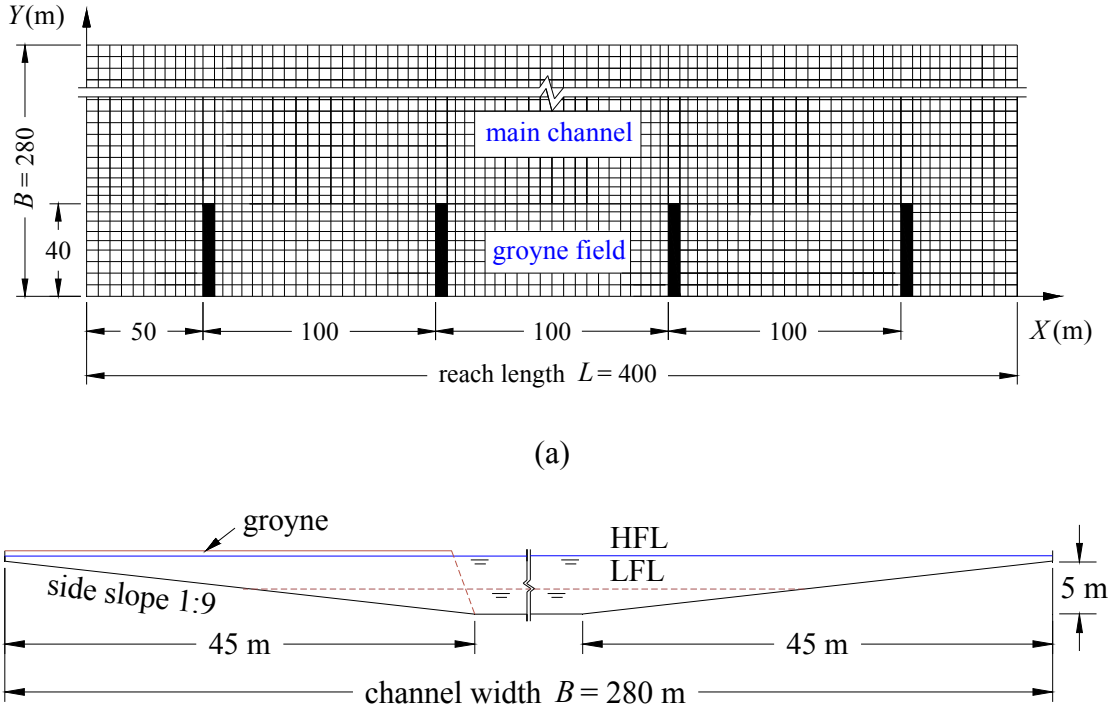

Fig. 3.9 (a) Planview of the reach of interest; (b) Channel cross-section

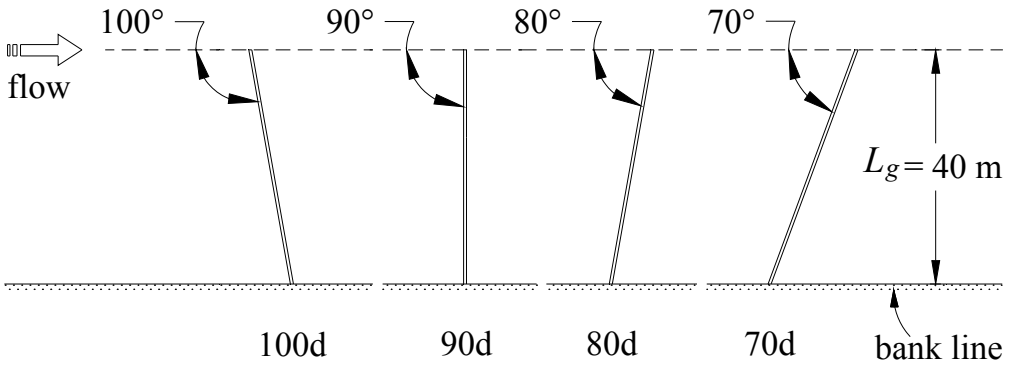

Fig. 3.10 Orientations of straight groynes

computation domain are made solid; while for the later ones, the area of a groyne is occupied by a group of non-submerged cylinders which have form drag against flow, and the parameters related to this drag, such as diameter (d_v), density (N_a) and drag co-efficient (C_{dv}) are combined into the factor K_v which becomes 14.16 in the

computation. The groyne angle 100^{oo} is not considered in permeable case because there may have a tendency of flow to concentrate towards the bank, thus to cause some adverse effects.

3.4.2 Procedure

As the target of the present study is to find an appropriate orientation of groynes for lowland rivers, the functions of the structures are to be well-understood; these can involve both hydrodynamics and morphodynamics influenced by them. We, however, concentrate mainly on the alterations in the bed morphology resulted from groyne interactions in defining the groyne functions, not details on the dynamics of flow. To compare the functions of various groynes, it is important to select some suitable features which will describe rightly the performance of a groyne structure. In this study three key features have been considered as the design criteria of a groyne, through which its performance be confirmed: (i) erosion in main channel (thalweg) (ΔZ_{ch}, Y_{ch}), (ii) deposition in groyne field (ΔZ_{gf}), and (iii) scour near groynes (ΔZ_g) (**Fig. 3.11**).

The first one specifies the availability of flow depth in the main channel for navigation at low flow time, the second one the protection of channel bank from recession at high flood, and the third one indicates the stability of the groyne structures against scour near groyne-tip at high flood time, respectively. Here the values of the indices are averaged over the middle area of the computation domain, except that ΔZ_g means the average of maximum scour depths near 2^{nd} and 3^{rd} groyne-tips. In getting the above key-parameters, the channel responses caused by the interaction of the series of various groynes are examined by numerical investigations. The numerical model which is utilized in this study has been described in the preceding section (Section 3.2), and it has been verified with experimental data before using in the present problem.

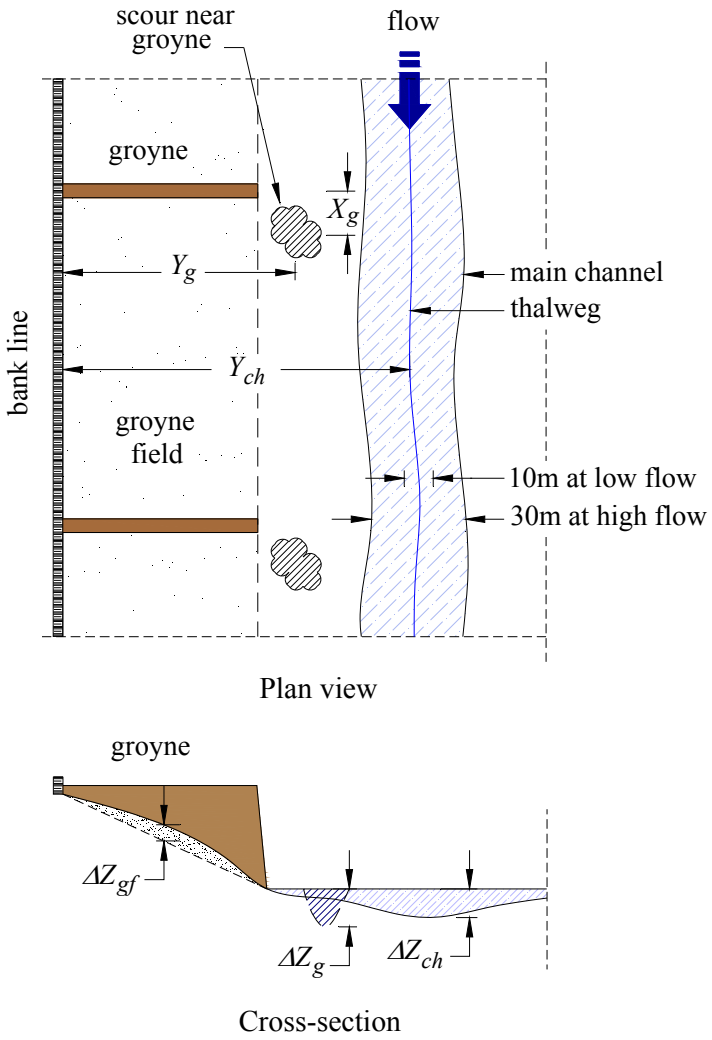

Fig. 3.11 Definition sketch of the key features

Idealized flow and sediment parameters are considered in these analyses. Two different discharges, one higher and another lower, are considered to replicate the channel responses from groynes for both high flow and low flow conditions. So a constant discharge (Q_h) of 2600.0 m^3/s as high flow and another smaller value (Q_l) 650.0 m^3/s as low flow are taken, considering the variation of flow in the river over the hydrological year. In the simulation, these discharges in the upstream inflow section are considered as the boundary condition for the hydrodynamic modeling. Initial water surface and downstream water surface elevations are set by uniform flow condition. Although, the sediment sizes vary along the river from upstream to downstream, especially for long distances, we assume a uniform sediment distribution

for a relatively short domain length, and the median size of sediment (*d*) is chosen 0.16 mm for the whole computation area. A dynamic equilibrium state of sediment transport is assumed at the upstream end, where the bed load transport rates per unit width are specified using the Ashida and Michiue (1972) formula, and entrainment rate for suspended sediment is calculated according to Itakura and Kishi (1980) and near bed concentration is given as $c_b = q_{su} / w_f$. The computations are made for flow and bed topography both past an infinite series of emerged groynes (periodic conditions in the streamwise direction). The advective terms are calculated by upwind difference scheme. In these computations we use a time step of 0.1 sec., and all of the runs are made for the duration of 7 days, when the temporal variations of variables are considerably reduced. Relatively smaller grid sizes are used near groynes, increasing gradually as distance increases away from the groynes.

3.5 Results and Analyses

Some selected results including both flow fields and bed deformations have been presented in this section to understand the channel morphodynamics resulted from the interaction of groynes with various orientations, and to identify the effective one. Three main features such as erosion in channel bed (thalweg), deposition near bank, and scour depth near groynes, where the first one represents the maintenance of navigation, the second the anti-erosion of bank, and the third the stability of groyne structures, respectively, are considered to evaluate the performance of groynes. These parameters have been explored here for various groynes from the results described below.

3.5.1 Flow Patterns

The computations show that flow contracted due to intrusion of groynes into the channel and thus cause the flow to accelerate in the main channel. These can be observed from **Figs. 3.12(a-d)**, where the existence of a skewness of streamwise components of velocities (*u*) is recognized with higher intensity at high flow condition

and vice versa. Among the groynes a little variation of this intensity can be marked; like, a little higher value is found for smaller angles at smaller distances at high flow; similar results can also be recognized at low flow condition except that distances vary in opposite way for impermeable groynes. These could be due to some bed-forms near the groyne areas (more about this will be explained in the next).

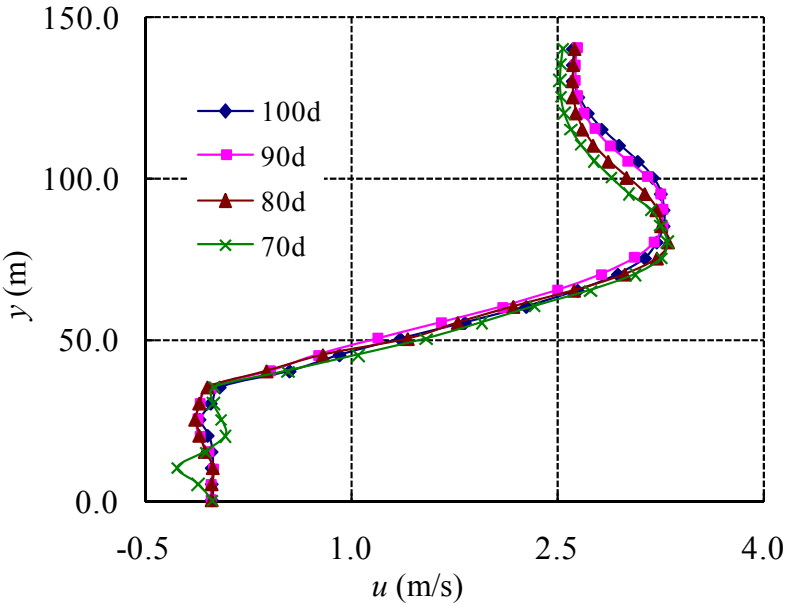

(a)

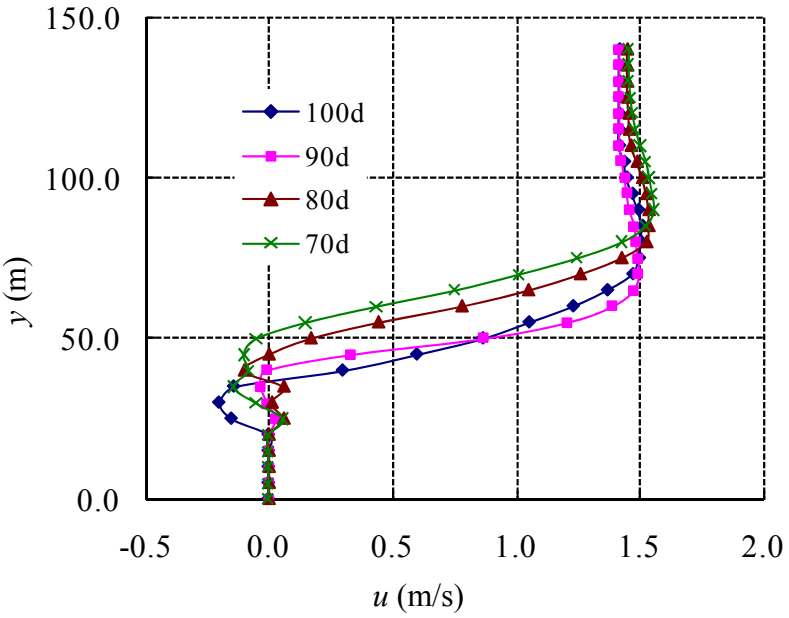

(b)

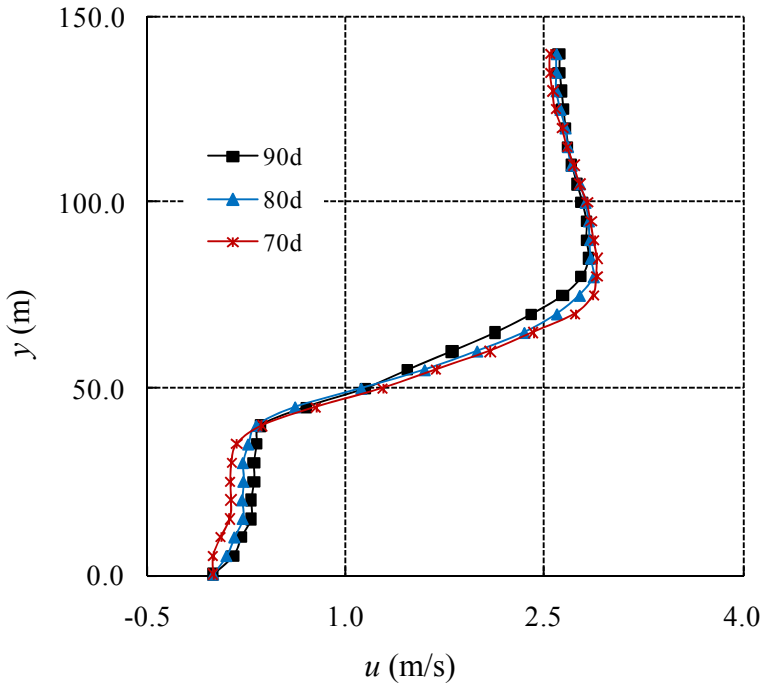

(c)

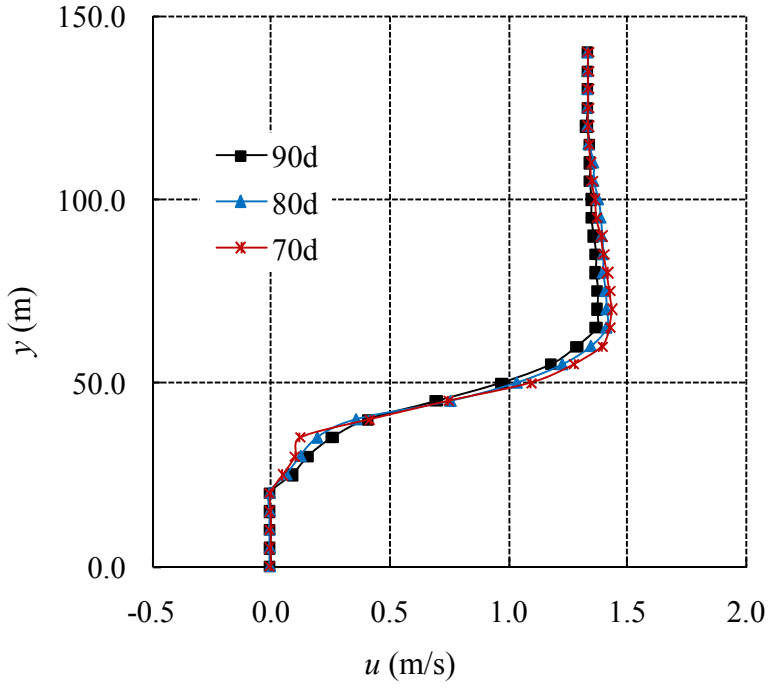

(d)

Fig. 3.12 Streamwise velocity profiles at 20.0 m downstream of second groyne: impermeable (a) high and (b) low flow, and permeable (c) high and (d) low flow

Figs. 3.13(a-d) show depth-averaged flow fields along with bed topographies in both groyne field and main channel portions for various orientations and types of groynes. In the case of high flow, mostly one gyre (large-scale secondary flow eddy inside the embayment) system occupies the whole area of the impermeable groynes [**Fig. 3.13(a)**]. Whereas, two-gyre velocity fields are observed in the groyne field at low flow condition with higher aspect ratio [**Fig. 3.13(b)**], except that it is not so clear for the case of **100d** at high flow and low flow both. The upstream part of an embayment contains the secondary gyre in the direction opposed to the primary one which is formed at downstream part. The mean velocity of recirculating flow is much less than

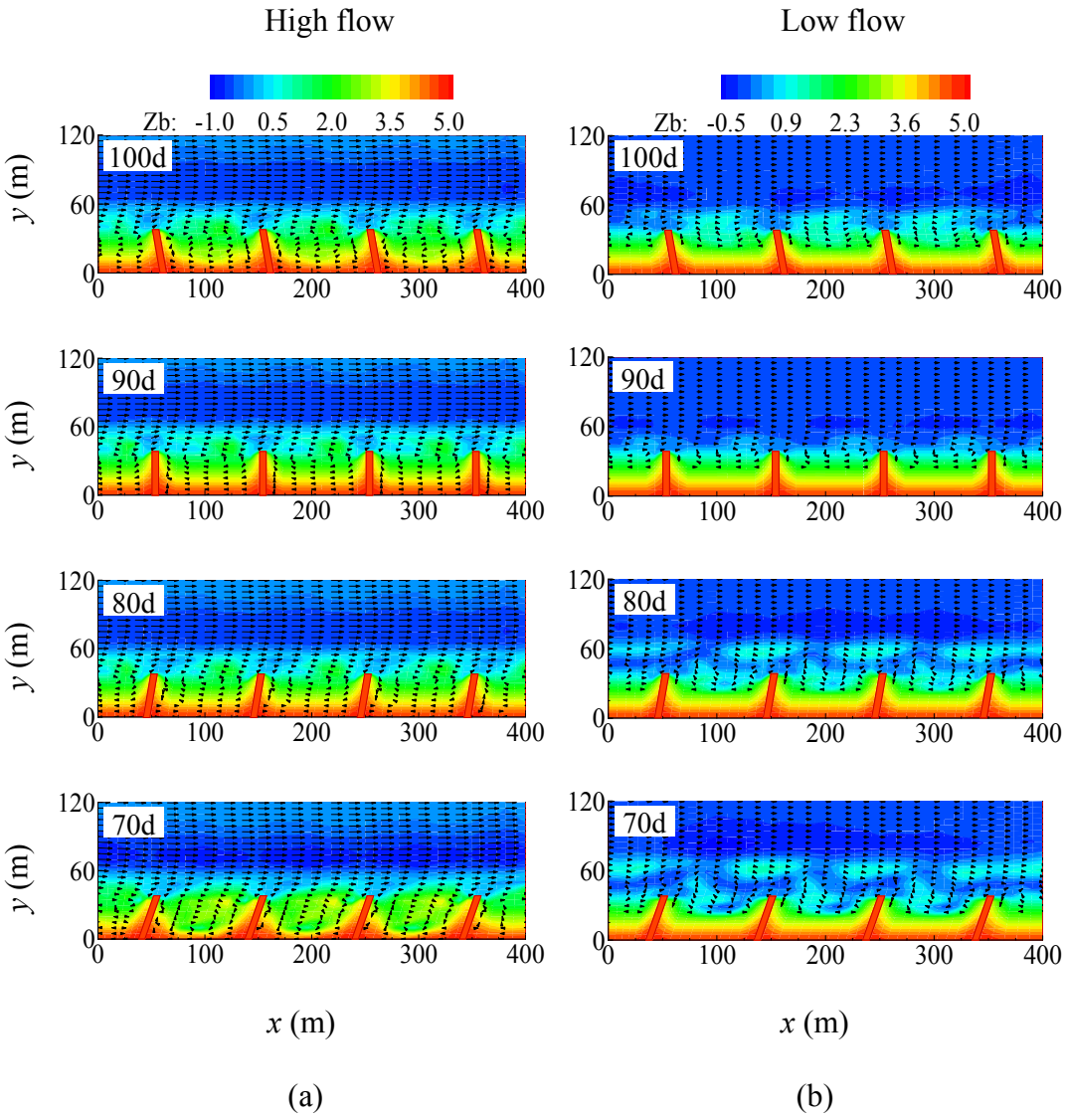

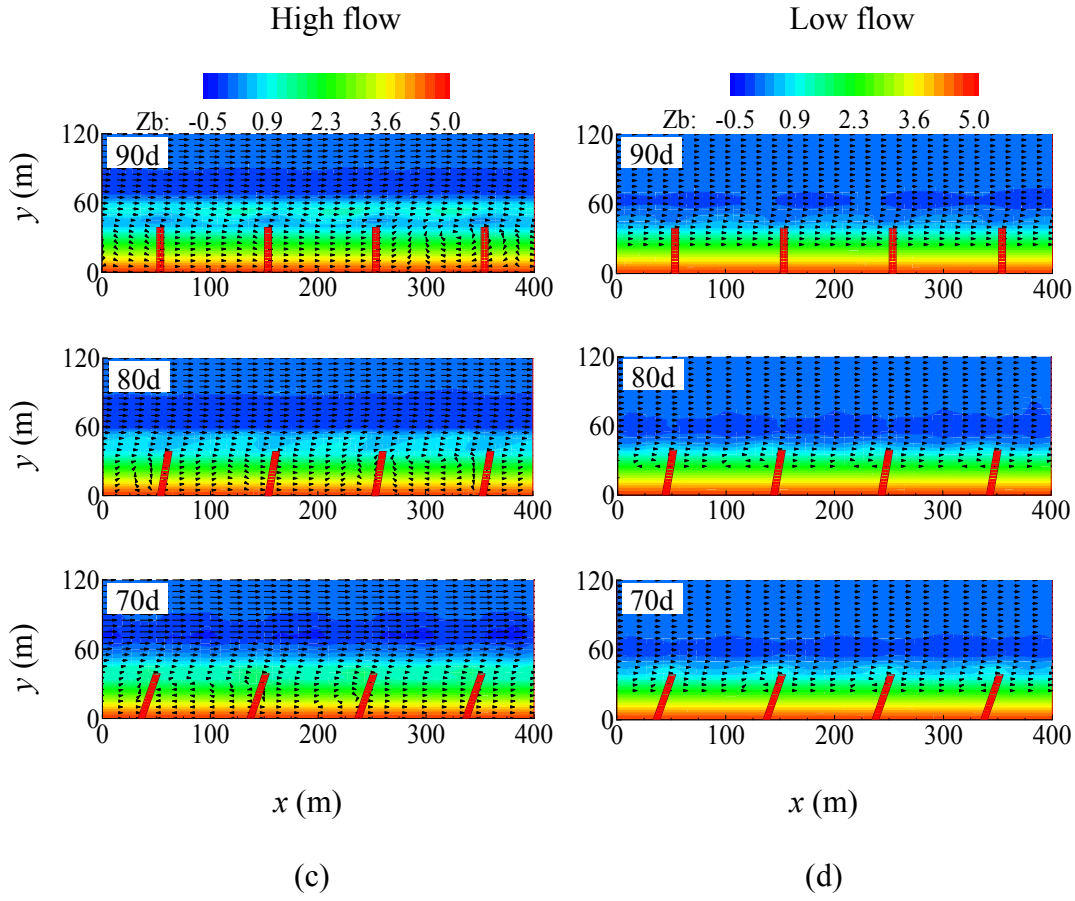

Fig. 3.13 Velocity vectors and bed contours against various orientations of impermeable (a) high flow and (b) low flow, and permeable (c) high flow and (d) low flow, groynes

the approaching flow velocity (=2.15 m/s for high flow), so that sediment concentrations exceed the transportation capacity and they settle in the recirculation zone. But, recirculation of flow is observed stronger at high flow for the groyne, **70d** in the groyne field, and hence, near bank erosion occurred. In contrast with the impermeable groynes, the momentum transfer by the water flowing through the permeable ones prevents the formation of a recirculating flow, and mostly results in a unidirectional flow in the groyne field [**Figs. 3.13(c and d)**] with some irregularity at high flow condition. The amount of flow diversion and flow reduction towards the main channel and the bank side, respectively, depend mainly on permeability of the structure. So, permeability in the structures should be optimized considering these factors.

3.5.2 Bed Topographies

In the case of impermeable groynes at high flow, bed-changes can be seen almost identical [**Fig. 3.13(a)**], except that impact from larger-angled groynes is higher at larger distances and vice versa, correspond to the velocity profiles [**Fig. 3.12(a)**]. Also local scour, though less in magnitude, can be recognized near groyne structures, which could due to strong eddies present near groyne head. At low flow condition, channel erosion is observed higher for smaller-angled groynes [**Fig. 3.13(b)**]. However, some irregular patterns in channel bed are formed near groyne region; may be, this is the reason of getting thalweg at larger distances. This is also advantageous in sense of wave-effect from water-vehicles, which creates an additional outflow velocity and transports sediment out from the groyne field (Yossef, 2005). Similar results are also observed in the case of permeable groynes, where smaller-angled groynes favor deeper channels [**Figs. 3.13(c and d)**], and some scour can also be marked near these structures at high flow.

All sets of the simulated and averaged data in the middle region of computation domain (between second and third groynes) for the parameters such as erosion in channel bed (ΔZ_{ch}), distance of thalweg (Y_{ch}), deposition in the groyne field (ΔZ_{gf}), and scour depth near groynes (ΔZ_g) and its location (X_g, Y_g) are summarized in **Table 3.1**, to compare the performances of the groynes of various orientations. As the channel responses from a series of groynes should be similar throughout the length (for cyclic boundary condition), the middle region of the domain is considered for analyses, and the values of the indices are averaged there, except that ΔZ_g means the average of maximum scour depths near second and third groyne-tips.

As mentioned earlier, groyne orientation 100^o is not considered in the case of permeable groynes as there may have some adverse effects to attract flow towards the bank. It can also be noted here that depth of scour near groynes is not significantly high; this might due to three-dimensionality of the flow phenomena there, which can not rightly be replicated by 2D numerical model; however, influence of the neighboring groynes also minimizes the local scour when they are applied in a series.

So the data for local scour are only noted for the case of high flow and for impermeable groynes. For better understanding the relative functions of the groynes, these data (**Table 3.1**) are also presented with **Figs. 3.14(a-f)**, where the variation of the variables against various groynes is rightly visible. Erosion in channel bed is observed higher for impermeable groynes compared with that for permeable ones, and also significant difference in erosion can be recognized for different orientations, even

Table 3.1 Average values of the key features defining groyne performance

Groyne orientation	Features		High flow (Q_h = 2600 m^3/s)		Low flow (Q_l = 650 m^3/s)	
			Imper.	Per.	Imp.	Per.
100°	main channel erosion	$\Delta Z_{ch}/h_l$	-0.293		-0.093	
		Y_{ch}/L_g	2.025		1.750	
	groyne field deposition	$\Delta Z_{gf}/h_l$	0.164		0.058	
	near groyne scour	$\Delta Z_g/h_l$	-0.124		-	
		$X_g/L_g, Y_g/L_g$	0.00, 1.25		-	
90°	main channel erosion	$\Delta Z_{ch}/h_{low}$	-0.284	-0.133	-0.089	-0.022
		Y_{ch}/L_g	2.000	1.950	1.575	1.675
	groyne field deposition	$\Delta Z_{gf}/h_{low}$	0.151	0.067	0.062	0.031
	near groyne scour	ΔZ_g	-0.111	-	-	-
		$X_g/L_g, Y_g/L_g$	0.08, 1.25	-	-	-
80°	main channel erosion	$\Delta Z_{ch}/h_{low}$	-0.298	-0.151	-0.133	-0.036
		Y_{ch}/L_g	1.950	1.850	2.000	1.550
	groyne field deposition	$\Delta Z_{gf}/h_{low}$	0.124	0.071	0.053	0.031
	near groyne scour	ΔZ_g	-0.071	-	-	-
		$X_g/L_g, Y_g/L_g$	0.38, 1.20	-	-	-
70°	main channel erosion	$\Delta Z_{ch}/h_{low}$	-0.324	-0.173	-0.142	-0.053
		Y_{ch}/L_g	1.900	1.800	2.125	1.550
	groyne field deposition	$\Delta Z_{gf}/h_{low}$	0.067	0.058	0.036	0.022
	near groyne scour	ΔZ_g	-0.044	-	-	-
		$X_g/L_g, Y_g/L_g$	0.75, 1.20	-	-	-

at low flow time [**Figs. 3.14(a and d)**]. At high flow condition, deeper channel is formed at larger distance by larger-angled groynes, but it is differing at low flow time due to formation of some bed-irregularities near groynes [**Figs. 3.14(b and e)**].

High flow

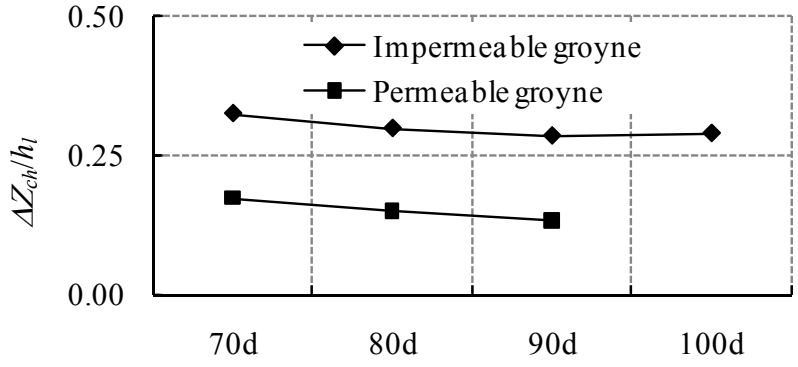

(a)

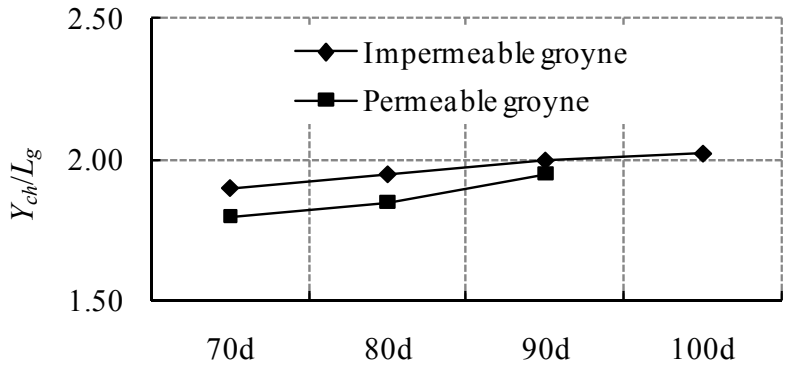

(b)

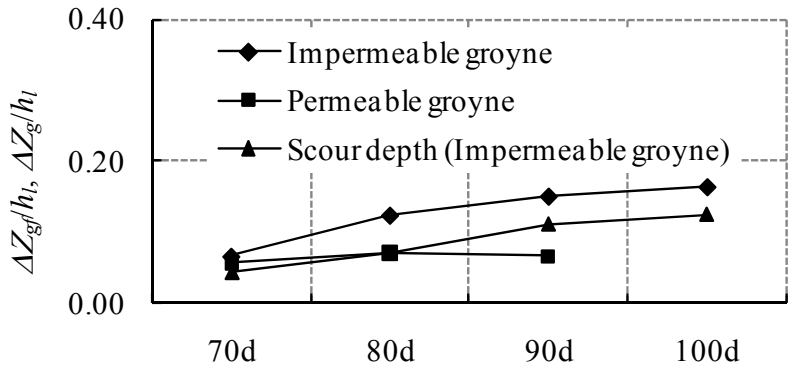

(c)

Straight groynes with various orientations

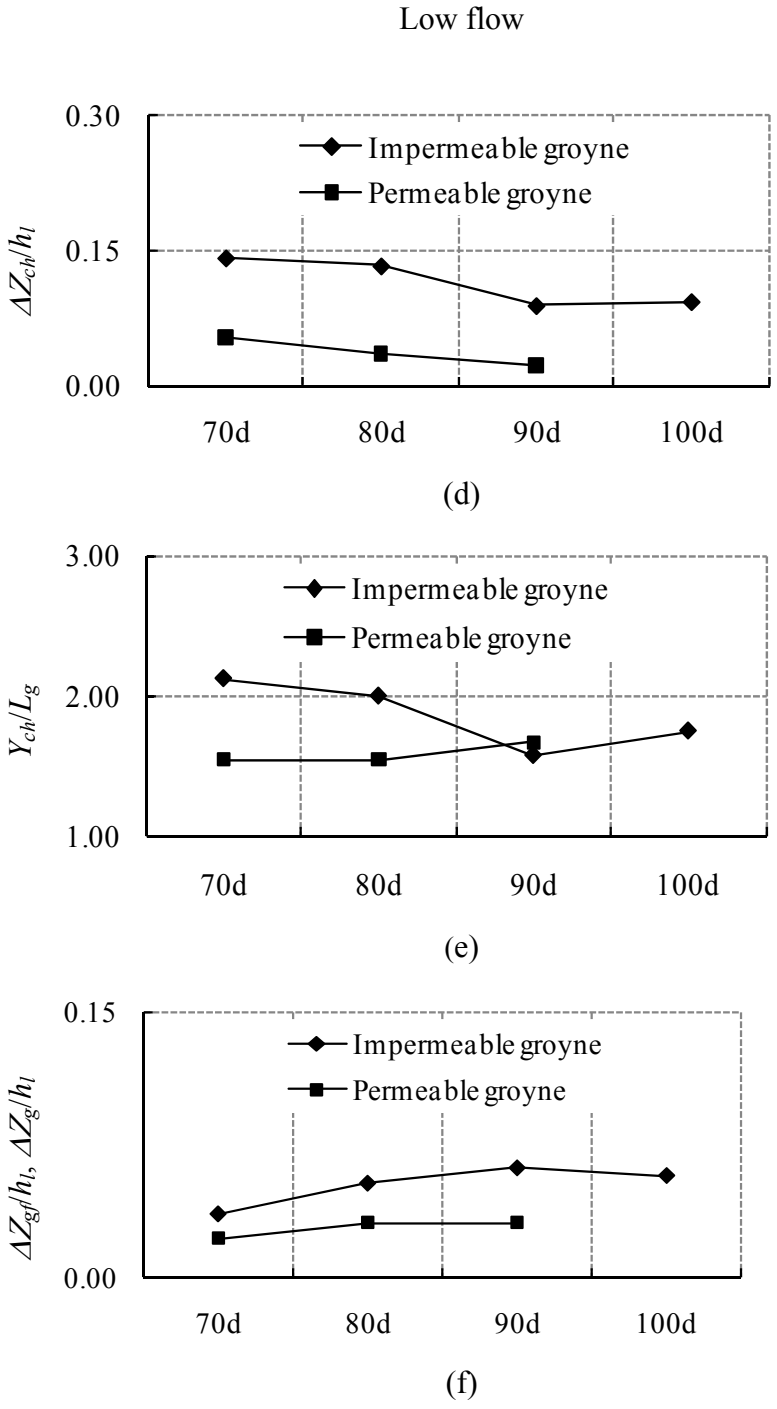

Fig. 3.14 Key features for various groynes at both high flow and low flow conditions: (a,d) erosion in channel bed ($\Delta Z_{ch}/h_l$); (b,e) location of thalweg (Y_{ch}/L_g); (c,f) deposition in groyne field ($\Delta Z_{gf}/h_l$) and scour near groynes ($\Delta Z_g/h_l$) (high flow, impermeable case)

Aggradations in the embayment regions with impermeable groynes are observed higher for larger angles, but this trend is not apparent with permeable groynes [**Figs. 3.14(c and f)**]. **Fig. 3.14(c)** also shows the variation of scour depth near impermeable groynes at high flow condition, where lower values are evident for smaller angles.

3.6 Conclusions

This study is conducted to test the performance of groynes installed in a series with various orientations to find the one which will function more efficiently at high flow and low flow both. The conclusions drawn from the simulated results are summarized in the following points:

- Erosion in channel bed is found higher with smaller-angled groynes for both impermeable and permeable ones, even this is apparent at low flow condition. However, the location of thalweg is closer to the groynes of smaller angles; except low flow (impermeable) case, due to the formation of some sand-bars near groynes.
- Depth of scour near groynes which represents the structural stability is considerably reduced in the case of smaller-angled groynes.
- For the groynes of larger angles, higher deposition is observed in the groyne field with impermeable groynes, however it is not obvious for permeable ones.

Therefore, the smaller angled groynes are functioning better in respect of deepening the channel bed, except that deposition near bank is reduced; even near bank erosion is present at high flow for 70^o impermeable groyne. Thus the 80^o aligned groyne can be the suitable one in consideration of both navigation and bank erosion problems in sand-bed alluvial rivers.

CHAPTER 4

MODIFIED ALIGNMENTS OF GROYNES

Summary

The lowland river channels suffer from both bank erosion at high flow and navigation problem at low flow. Groynes are constantly practiced to overcome the problems, which are usually straight aligned. As the angle of the groyne has significant role in the morphological changes, the combination of various orientations in a structure is an important consideration to improve the groyne functions, in respect of both high flow and low flow problems. This study investigates the optimum alignment of a groyne for its effective functioning at variable flow stages. RIC-Nays, a two-dimensional model for flow and morphology, is utilized in this study upon confirmation through the detailed experimental data. The channel and flow parameters are based on conformity to a typical river channel of Bangladesh. Three different alignments modified over straight ones are considered here to obtain the optimum one. The performance of a groyne is evaluated through three key features – erosion in channel bed (thalweg), deposition in groyne field, and scour near groynes. Computations reveal that modified groynes function better over the conventional straight ones in respect of bank protection at high flood and maintenance of navigation channel at low flow as well.

4.1 General

The channel responses from the groynes of various orientations have been discussed in the preceding chapter (Chapter 3), where some significant effects can be known due to the change in groyne angles. There are some merits and demerits for each of the groyne angles in respect of better management of lowland rivers: the groynes of larger angles divert the flow highly and provide safety to the bank through sediment deposition in the groyne field; however, high separation of flow and hence huge scour

near groyne-head are expected; also big diversion of flow can either affect other important land on opposite side like islands, or reflect the flow back to the bank the groynes installed to be protected. Whereas, the groynes of smaller angles minimize local scour at high flow and favor higher erosion in the channel bed at low flow, but deposition near bank reduces, even erosion is recognized there by return currents at downstream area. Thus, the 80^o aligned groyne is identified as the straight optimum one (Alauddin and Tsujimoto, 2010a).

As the present research aims at finding an optimum solution for lowland rivers, both high flow and low flow problems should be addressed rightly, i.e., river banks should be protected from erosion together with structural safety at high flood, and sufficient depth of flow should be ensured for navigation at low flow as well. Although the groynes have been documented to be the most durable solution (Shields, *et al.*, 1995) compared with other restoration structures like bank covers, and so on, and they have very long history and widespread use, a little effort has been put in optimization in their designs. A way of overcoming the problems is thought in the form of some modified alignments of groynes that would act to guide flow efficiently, thus to optimize the deflection of flow from the bank so as to minimize the impact to other regions, and to train the flow gently in the desired direction for the development of deeper channel to favor navigation in dry season. In view of that a combination of groyne orientations in a structure can be considered that could serve better functions.

Therefore, the channel responses from the groynes of various alignments (combining different angles in one structure) are investigated to evaluate their functions. Thus their performances are compared to identify the suitable one for field uses, and presented in this chapter. Thus, as done for finding the optimum orientation of groynes, the following functions of groynes are set to examine:

- Flow dynamics caused by various alignments of groynes in sand-bed alluvial river channels.
- Changes in bed topographies in the far and near-bank regions against the groynes.

Finally, the performance of the groynes are evaluated through some typical features and compared to suggest the best one for field uses.

4.2 Solution Appproach

4.2.1 Groyne Alignments

Various configurations of groynes designated by **m1**, **m2** and **m3**, as depicted in **Fig. 4.1**, are considered in this study to find the most suitable one. As has been discussed the role of groyne angles (Chapter 3), it is known that 100^o aligned groyne diverts the flow rightly providing safety to the bank from erosion at high flow, but the navigation channel is not influenced at low flow. Therefore, first-half portion of **m1** is oriented towards upstream with an angle 100^o, then towards downstream with an angle 80^o, to minimize big diversion of flow to avoid some possible adverse effects on/from opposite side, to minimize local scour from strong eddies due to flow separation at the sharp edge of the groyne to the flow, and to improve deepening the channel bed at low flow.

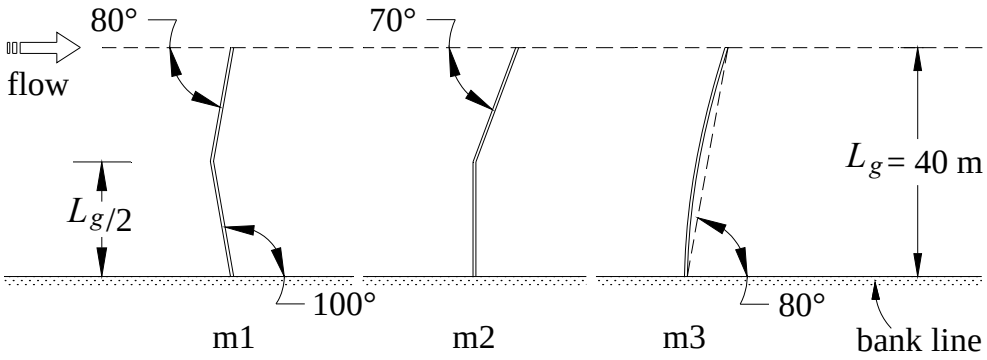

Fig. 4.1 Modified alignments of groynes

Similar to the modified groyne **m1**, **m2** is comprised of two straight parts: first-half part is perpendicular to the bank and then aligned towards downstream with an angle 70^o to the flow at upstream. Although 70^o aligned groyne is found to be the most effective one for higher erosion at low flow, but the flow is turned back as return

currents toward the bank to attack at high flood. So, this combined arrangement in the groyne structure is expected to modify the back-flow effect by the provision of first perpendicular portion so that this would divert the flow more better way at high flow and serve the maintainance of the thalweg for navigation at low flow.

In contrast to other two groynes, the alignment of groyne **m3** is gradually varied towards downstream, and it maintains an average angle 80^o to the direction of flow. It is parabolic in shape as $x = cy^n$, where, c = 0.01, exponent n = 1.78, and x and y are the along-stream and transverse distances, respectively. It is considered so as to guide the flow smoothly at high flow and low flow both for minimization of flow separation at high flow and for formation of navigation channel concentrating the flow at low flow as well.

4.2.2 Model Setup

The modeled area is a schematized straight river reach with four emerged groynes of same alignment, which is 400.0 m long (L) and 280.0 m wide (B) with a bed slope of 7.5 cm/km, as considered for the straight groyne case (Chapter 3). Groynes are located on one side of the reach with projected length, L_g = 40.0 m and spacing, S_g = 100.0 m (i.e., aspect ratio, S_g/L_g = 2.5). **Figs. 4.2(a and b)** depict the model layout with one of the alignments of groynes and grids, and channel cross-section, respectively. The flow is in the x-direction with x = 0 at upstream end and y-axis is pointed to the left bank in the transverse direction. Since at high water stages, discharge is distributed over a much wider area, the shallower embayments are provided with a mild slope, 1:9 on either side to avoid the deviation from the natural situation. Moreover, at low flow time, only a part of the groyne length (around 50%) is effective to function, therefore it is important to consider replicating the effect of groynes that time.

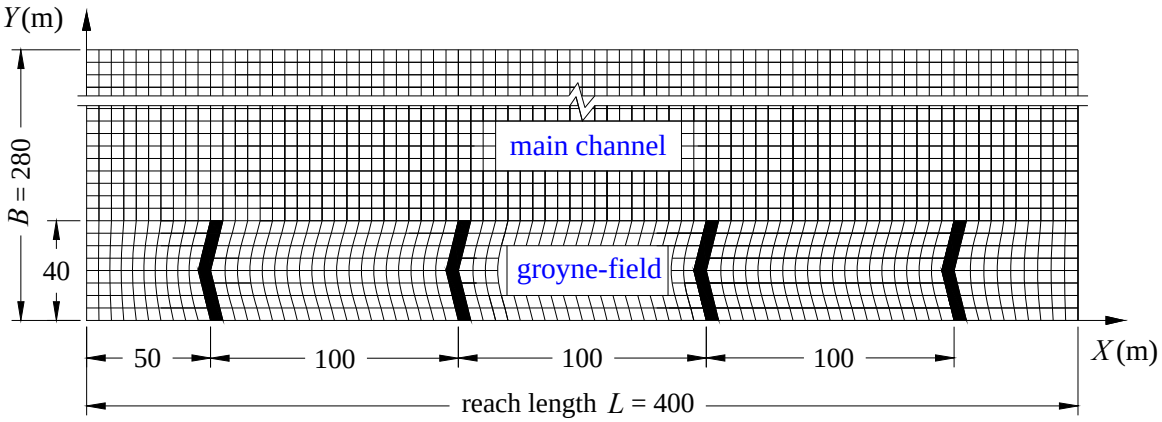

(a)

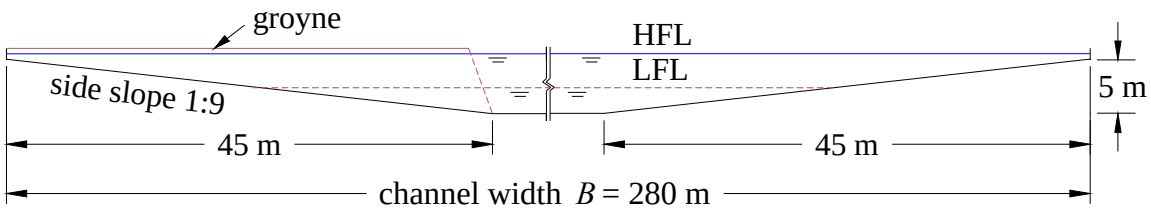

(b)

Fig. 4.2 (a) Planview of the reach of interest; (b) Channel cross-section

4.2.3 Procedure

As the main goal of the present study is exploring a suitable alignment of a groyne structure for lowland rivers, the effect of groynes in the river channels is to be investigated. As described in the previous section, several alignments of groynes are considered to identify the most suitable one in consideration of both bank protection from erosion at high flow and establishment of thalweg for navigation at low flow. Thus, there are many aspects to reach the targeted goal, like various alignments of groynes, different flow conditions, series of groynes necessary for better effect in the channels, and shallower embayments to maintain natural situation. Therefore, a numerical investigation is planned to be conducted. The two-dimensional model for flow and morphology is utilized in this study, in which the shallow-water equations for two-dimensional unsteady flow expressed in a general coordinate system are

calculated on the boundary-fitted structured grids using the finite-difference method. Depth-averaged parabolic model is employed for considering turbulence. The model is verified with the detailed experimental data investigated by Rajaratnam and Nwachukwu (1983). This is not included herein (Chapter 3).

Flow and sediment parameters of Jamuna River are simplified and are considered in the numerical computation as the initial and boundary conditions. For the hydrodynamic model, constant discharge is set in the upstream inflow section, and water surface elevation in the downstream outflow section is set by uniform flow condition. Also the initial water surface elevation is set by uniform flow. Two different discharges, one higher and another lower, are considered to replicate the channel responses from groynes at both high flow and low flow conditions. So a constant discharge (Q_h) of 2600.0 m^3/s as high flow and another smaller value (Q_l) 650.0 m^3/s as low flow are taken, considering the variation of flow in the river over the hydrological year. Although, the sediment sizes vary along the river from upstream to downstream, especially for long distances, we assume a uniform sediment distribution for a relatively short domain length, and the median size of sediment (d) is chosen 0.16 mm for the whole computation area. A dynamic equilibrium state of sediment transport is assumed at the upstream end, where the bed load transport rates per unit width are specified by Ashida and Michiue (1972) formula, and entrainment rate for suspended sediment is calculated according to Itakura and Kishi (1980) and near bed concentration is given as $c_b = q_{su} / w_f$. The computations are made for flow and bed topography both past an infinite series of emerged groynes (periodic conditions in the streamwise direction). The advective terms are calculated by upwind difference scheme. In these computations we use a time step of 0.1 sec., and all of the runs are made for the duration of 7 days, when the temporal variations of variables are considerably reduced. Relatively smaller grid sizes are used near groynes, increasing gradually as distance increases away from the groynes.

In this study three key features are considered as the design criteria of groynes through which the performance of groynes is confirmed (described in Chapter 3); these are (i) erosion in main channel to establish thalweg, (ii) deposition in groyne-

field, and (iii) scour near groynes. The first one specifies the availability of flow depth in the main channel for navigation at low flow time, the second one the protection of channel bank from recession at high flood, and the third one indicates the stability of groyne structures against scour near groyne-tip at high flood time.

4.3 Results and Analyses

To understand the modifications in both flow patterns and bed topographies due to the influence of various groynes, some selected results have been presented and discussed in this section. As mentioned earlier, some typical features have been defined to evaluate the performance of groynes, such as erosion in channel bed (thalweg), deposition near bank, and scour near groynes, these parameters are explored for various groynes from the morphological changes in the alluvial channel and presented in this section as described below.

4.3.1 Flow Fields

Due to the blockage of flow by the groyne structures into the channel, flow contracted in the main channel and thus causes the flow to accelerate there. These can be recognized from **Figs. 4.3(a and b)**, where the existence of a skewness of streamwise components of velocities (u) is depicted with higher intensity at high flow condition and vice versa. Among the groynes a little variation of this intensity can be marked, like **m1** shows relatively lower intensity with peak value at higher distance at high flow condition [**Fig. 4.3(a)**]; reversely, **m2** is with higher intensity at lower distance, and **m3** is in between these two. Similar results are also observed for low flow condition, except differing the distances [**Fig. 4.3(b)**].

Figs. 4.4(a and b) show depth-averaged velocity fields along with bed topographies in groyne field as well as in main channel portions for various configurations of groynes. For almost all cases, two-gyre system occupies the whole area of the groyne-embayments at high flow and low flow both, except in the case of **m2** at high flow condition [**Fig. 4.4(a)**], where one-gyre velocity-fields can be observed with some

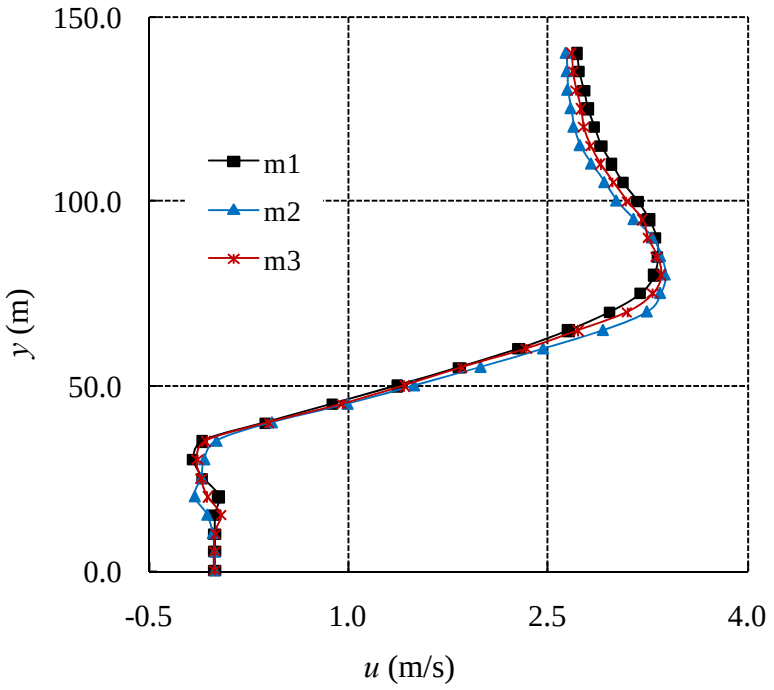

(a)

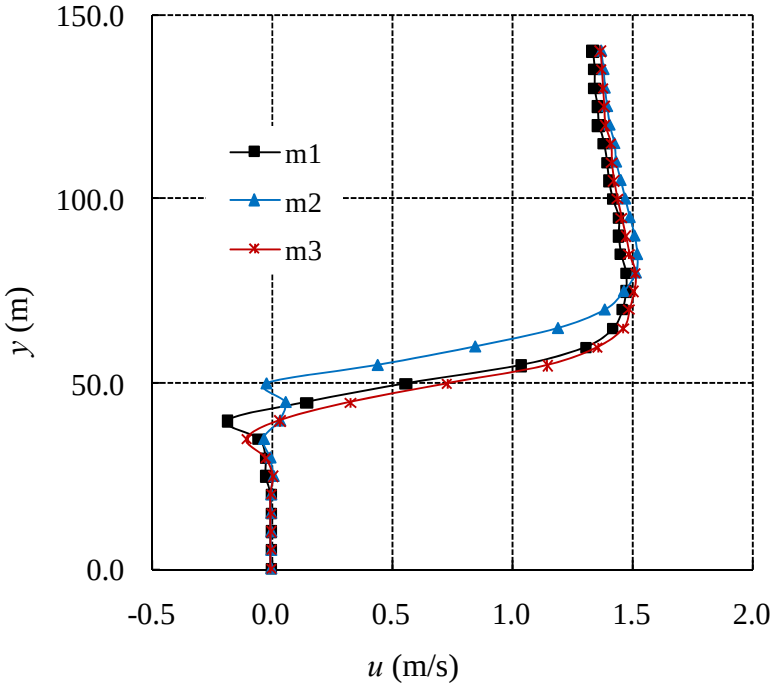

(b)

Fig. 4.3 Streamwise velocity (u) profiles at 10.0 m downstream of second groyne for various alignments: (a) high flow condition; and (b) low flow condition

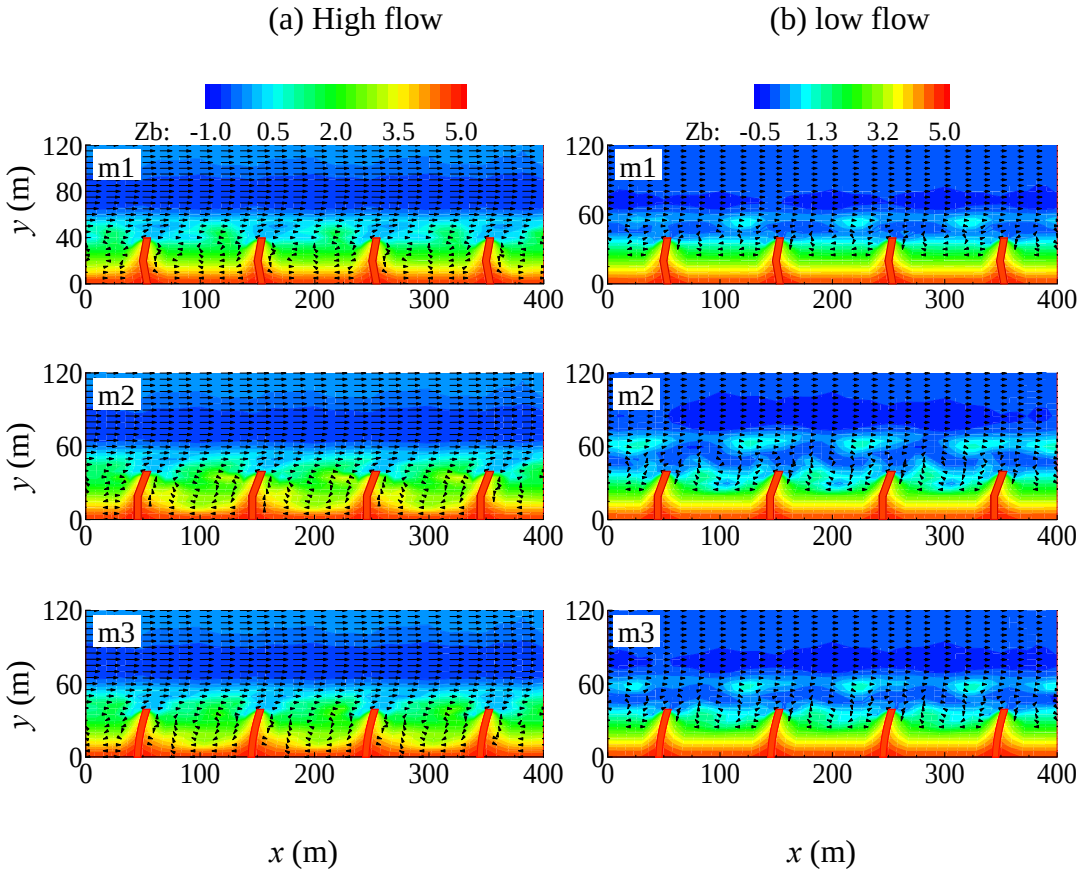

Fig. 4.4 Velocity vectors and bed topographies for various alignments of groynes: (a) high flow condition; and (b) low flow condition

irregularity. The upstream part of a groyne-field contains the secondary gyre in the direction opposed to the primary one. The mean velocity of recirculating flow is much less than the approaching flow velocity (=2.15 m/s for high flow), so that sediment concentrations exceed the transportation capacity, and they settle in the recirculation zone. Here the recirculation is not so stronger in the groyne field and hence, no near bank erosion occurred, as found in the previous study for 70^{o} aligned groynes (Alauddin and Tsujimoto, 2010a). May be, 90^{o} first-half portion of the groyne favors in doing so.

4.3.2 Bed Topographies

At high flow condition, bed-changes for various groynes are almost identical [**Fig.**

4.4(a)], except that a little variation in channel-erosion and thalweg-location can be marked, which correspond to the velocity profiles [**Fig. 4.3(a)**]. It can be noted that no near bank erosion is observed for any of the groynes. At low flow, channel erosion is observed higher for model **m2** [**Fig. 4.4(b)**], and some irregular patterns of channel bed are formed near groyne-regions for all of the groynes only differing their scale and location; this may be the reason of getting thalweg at larger distances at low flow case. This is also advantageous in sense of wave-effect from waterway vehicles, which creates an additional outflow velocity and may transport sediment out from the groyne fields (Yossef, 2005). A little scour can be recognized at some distances around the groynes at high flow condition; whereas, a channel-like formation is observed near the normal line at low flow condition, followed by formation of some sandbars beside this.

All sets of the computed and averaged data in the middle groyne area (between second and third ones) for the parameters defining the performance of various groynes, such as erosion in channel bed (ΔZ_{ch}), distance of thalweg (Y_{ch}), deposition in the groyne field (ΔZ_{gf}), and scour depth near groynes (ΔZ_{g}) are summarized in **Table 4.1**, to compare their performances. Here, the vertical distances are non-dimensioned by low-flow depth (h_l) and horizontal distances by groyne length (L_g). It can be mentioned that the scour near groynes is not recognized much; this may due to the influence of neighboring groynes, as a series of groynes are applied with cyclic boundary condition, and the modification in their configurations. That is why these data are noted only for high flow condition for comparison. These data (**Table 4.1**) are also presented with **Figs. 4.5(a-d)**, where the variations of the parameters among the various groynes are visible rightly. Erosion in channel bed is observed higher in the case of model **m2** at high flow and low flow both [**Fig. 4.5(a)**], provided that thalweg is formed at a little closer distance compared with other groynes at high flow, but it is differing at low flow time due to formation of some bed-irregularities near groyne-structures [**Fig. 4.5(b)**]. Whereas, the erosion is found lower in the case of **m1**, and the response from **m3** is within the range of these two values. Aggradation in the embayment regions with the groyne **m1** is observed higher, and this is found lower and almost similar values with the groynes **m2** and **m3** [**Fig. 4.5(c)**]. **Fig. 4.5(d)**

Table 4.1 Average values of the key features defining groyne performance

Groyne alignment	Parameters		High flow (Q_h = 2600 m^3/s)	Low flow (Q_l = 650 m^3/s)
m1	erosion in main channel	$\Delta Z_{ch}/h_l$	-0.29	-0.13
		Y_{ch}/L_g	2.00	1.88
	deposition in groyne field	$\Delta Z_{gf}/h_l$	0.16	0.06
	scour near groyne	$\Delta Z_g/h_l$	-0.06	-
		$X_g/L_g, Y_g/L_g$	0.30, 1.25	-
m2	erosion in main channel	$\Delta Z_{ch}/h_l$	-0.31	-0.14
		Y_{ch}/L_g	1.93	2.10
	deposition in groyne field	$\Delta Z_{gf}/h_l$	0.11	0.04
	scour near groyne	$\Delta Z_g/h_l$	-0.04	-
		$X_g/L_g, Y_g/L_g$	0.63, 1.18	-
m3	erosion in main channel	$\Delta Z_{ch}/h_l$	-0.30	-0.13
		Y_{ch}/L_g	1.94	1.95
	deposition in groyne field	$\Delta Z_{gf}/h_l$	0.12	0.04
	scour near groyne	$\Delta Z_g/h_l$	-0.05	-
		$X_g/L_g, Y_g/L_g$	0.38, 1.20	-

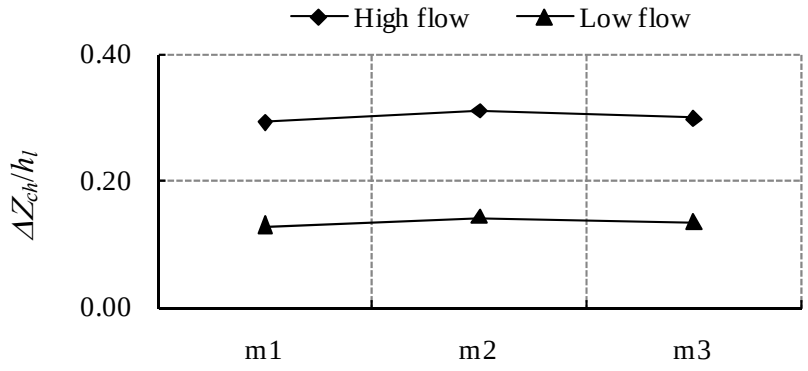

(a)

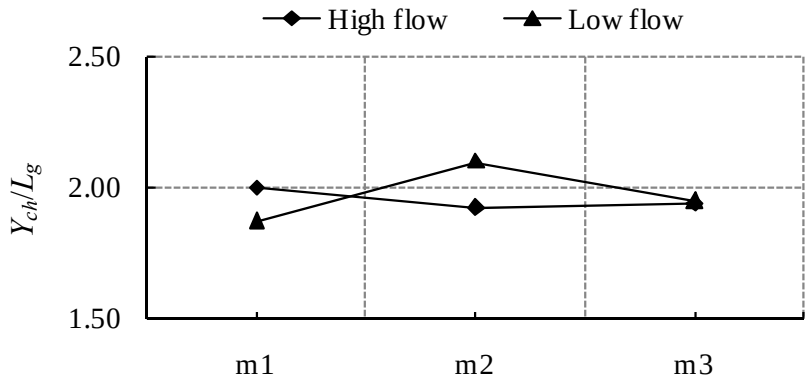

(b)

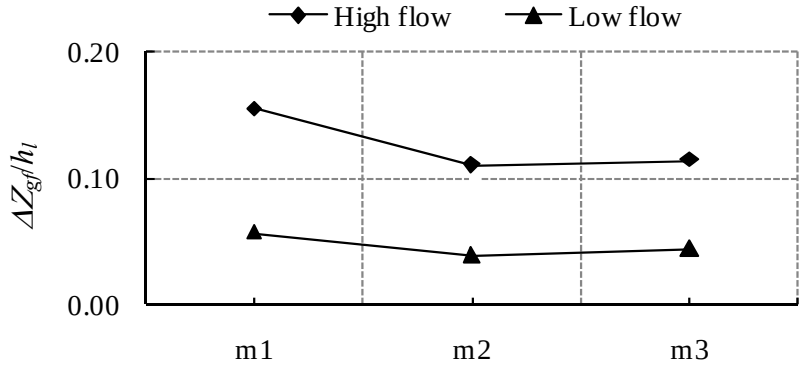

(c)

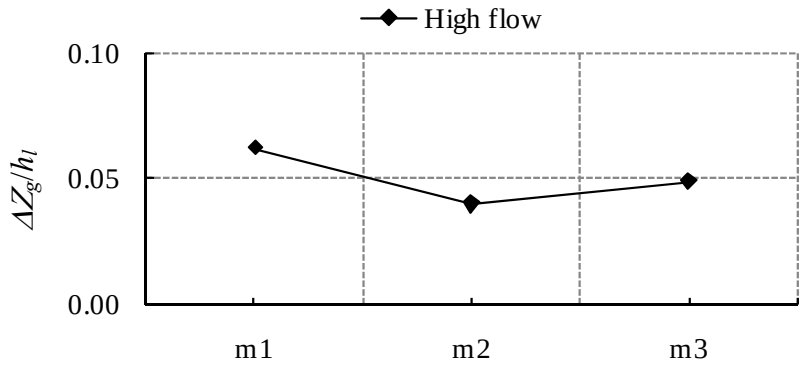

(d)

Groynes with modified alignments

Fig. 4.5 Changes of the features at both high flow and low flow conditions: (a) erosion in channel bed ($\Delta Z_{ch}/h_l$); (b) location of thalweg (Y_{ch}/L_g); (c) deposition in groyne field ($\Delta Z_{gf}/h_l$); and (d) scour near groynes ($\Delta Z_g/h_l$) (high flow only)

shows the variation of scour depth near the groynes at high flow condition, where lower values are evident for **m2** and then **m3**.

4.4 Conclusions

The channel responses due to the interaction of groynes with various alignments installed in a series have been investigated in this study. Thus, their functions are evaluated through some typical features, and their performances are compared to choose the optimum one that would function effectively at both high flow and low flow conditions. The following conclusions have been drawn from the analyses of the computation results:

- Erosion in channel bed is found higher with groyne **m2** (first-half part is perpendicular to the bank, then 20^o towards downstream), even this is apparent at low flow time.
- The location of thalweg at high flow is relatively closer for groyne **m2**, but it differs at low flow time due to formation of some sandbars near groynes.
- Higher deposition in the groyne field is observed in the case of groyne **m1**, and these are relatively lower for **m2** and **m3** both. No near-bank erosion is present for any of the modified groynes.
- Depth of scour near groynes was negligibly small in the case of groyne **m2** and then **m3**, and it is relatively higher for **m1**.

Here the numerical results demonstrate that the groyne model **m2** functions better in respect of deepening the channel bed at low flow and protecting the channel bank from erosion at high flow as well, and it improves the channel responses compared with the conventional straight ones. Thus, this alignment of groynes can be recommended to optimize the problem of navigation and bank erosion both in sand-bed alluvial rivers. However, more experimental data with different aspect ratios as well as field observations for the proposed configuration are required to test their general applicability.

CHAPTER 5

MODIFIED CONFIGURATIONS OF GROYNES – Laboratory Experiments

Summary

A groyne is an important river restoration structure. Although its history is for long and widespread use, the optimized design of new groynes is not attempted much, which is very important to treat the highly unstable lowland rivers. A completely blocked impermeable groyne suffers from instability of the structure itself; whereas, fully permeable structure can not divert the flow rightly. Recently, the concern about river environment is added with groyne functions. Considering the present demands, five different groyne structures including modified combined and bandal-structures are examined in the laboratory to recognize modifications of the fluvial processes by them. The performance of a groyne is confirmed through three key features: scour near groynes (structure stability), deposition in groyne field (bank stability), and erosion in main channel (navigability). Analyses of data show that the combined groynes cause gradual deceleration of flow towards the land, and minimize local scour compared with the straight conventional one. Also two other important features: deposition near bank and channel erosion are better responded from modified bandal-structure and modified combined groyne; thus, they favor a quality river landscape.

5.1 General

The rivers through flat delta lands of Bangladesh, especially Jamuna, one of the largest rivers in the world, with fine-grained non-cohesive sediments on banks cause severe erosion with high frequency at high flood time, and the river persistently widens rather than deepens the bed. This destroys huge farmlands, homestead lands,

and so on; on the other hand, inland waterways frequently lose navigability due to rapid sedimentation at low flow time and disrupt very important inland waterway transports there. So far, numbers of studies have been conducted to understand the dynamism of the river, and to develop and improve the techniques in stabilizing the channels (Coleman, 1969; Klassen and Vermeer, 1988; Elahi, *et al.*, 1991; Thorne, *et al.*, 1993; Bristow, 1993; Halcrow, *et al.*, 1994; Zhou and Chen, 1998; and CEGIS, 2004, 2005, 2006 and 2007). The groynes are constantly practiced including other methods like bank covers (revetments) and repeated dredging, to overcome the aforementioned problems. Besides, though the social needs for river environment were not taken care much yet, recently these have drawn much attention to improve the ecological values of the river landscapes. However, these issues are being addressed in advanced world like Japan, Europe, and so on, for a long time. The river environment which is severely affected by human activities can get relief by a series of groynes through ecosystem restoration (Tsujimoto *et al.* 2009). Thus the significance of groynes as a bank protection technique with the consideration of quality landscape has been increased, and the performances of the present measures have been criticized by many researchers such as Klaassen *et al.* (2002), Rahman *et al.* (2004), Mosselman (2005), and many others.

In the cases of fully blocked impermeable groynes, there are many chances of strong recirculation of flow downstream of the structures (Klingeman *et al.* 1984, Ishii *et al.* 1983, Chen & Ikeda 1997) depending on the groyne intervals, or reflected flow from some large-scale sandbars, which can attack the bank back again where the structures are installed; this may spoil one of the major targets, where deposited riverine landscape could serve improved environments through vegetation, and so on, in addition to the protection of floodplain area. Moreover, instability of the structures (Halcrow and Haskoning, 1999; Klassen *et al.*, 2002) due to local scour is an endemic problem, which can lose the huge investment for them; also there are destructive consequences due to hydraulic actions after their failures at downstream region planned to be protected. Sudden and big responses from these structures, in one way, leave behind strong eddies near the groyne-head causing scour holes responsible for this structural instability; furthermore, these affect other regions such as islands where

numbers of people are living or other bank, and so on, and make them unstable. Also, there is a presence of huge scour due to strong parallel flow at upstream side of longer groynes as known from field observations in Bangladesh, such as Betil and Enayetpur spurs, where the velocity is found even much higher than the main channel (Nazim *et al.* 2010). This can make the structure unstable. Besides, the desired channel for navigation at low flow is not influenced rightly, for which waterway transports are greatly interrupted there. Thus, the stable river course is not established yet.

The disadvantages of impermeable groynes can be minimized replacing some length with permeable portion, which decrease flow velocities near bank, hence rapid deposition in that area; particularly, in alluvial rivers with high sediment load. The conventional permeable groynes, however, can not diverse the flow rightly and some local scour can still be present near groyne-tip due to large-scale fluctuation in the mixing layer (Jansen *et al.*, 1979) or near bank depending on the permeability provided in the structures. Also some studies were conducted on the flow from different groyne designs with straight alignment perpendicular to the bankline, and providing the permeable part at top and mild slope at groyne-tip (Uijttewaal, 2005). They improved the functions over the conventional type; however, high velocity fluctuations were still marked in the downstream mixing area over a limited range of water depths.

For an optimal solution of lowland river problems, both high flow and low flow conditions must be considered rightly. To surmount the aforementioned drawbacks, permeability of the structure can be varied from higher to lower value so as to prevent flow separation and to achieve a gradual deceleration of flow velocities towards the bank. Thus, after gradual reduction of flow intensity, more stagnant region of flow can be developed providing impermeable portion in a groyne adjacent to the bank, without influencing strong recirculation there; so that fluvial processes will be responded more natural way to allow for the improved quality of landscape as well as improvement of ecology. Here, it is worth mentioning that the deposition of sediment in the groyne field will occur due to reduction of flow velocity due to form-drag against flow through them, not by transferring mass flux through mixing layer by

return currents (Uijtewaal *et al.*, 2001). Therefore, a combination of permeable and impermeable components in a groyne structure, inclining far-bank permeable portion towards downstream, can be an effective alternative for significant modification of fluvial processes such as strong recirculation (bank attack) and local scour (structural instability), also to concentrate the flow in the main channel to favor maintenance of thalweg for navigation. The alignment could be the same as the optimum alignment of a groyne as found from the consideration of bank protection and navigation channel both (Alauddin and Tsujimoto, 2011a).

The groynes used in the sand-bed braided river, Jamuna are very large because of vulnerability of bank attack and large dimension of the river; namely the Betil spur consists of 150 m long RCC (Reinforced Cement Concrete) part along with 651 m earthen shank adjacent to the bank, and its RCC part got open during the flood in 2004 removing the protection materials from the bottom due to seepage and some other hydraulic actions. As the flow is blocked by the upper impermeable part, this allows flowing in-between the piles near bottom, working as a so-called bandal-structure. Interestingly, field observations confirm that the strong return current is counterbalanced by the flow passing beneath the RCC part. Although many studies have been conducted with bandal-structures, as practiced at low flow or in sub-channels for both bank protection and maintenance of navigation depth (Rahman *et al.*, 2004; Mosselman, 2005; and Sharmin *et al.*, 2007), their large-scale use at varying flow conditions are not evident yet. In the present study these structures are modified with both alignment and configuration: straight impermeable part is provided at adjacent to the bank to develop more stagnant region of flow there without influencing strong return currents at high flood (as motivated from the abovementioned example), and the alignment is maintained as in the optimum one. So that near bank flood plain area can be provided with impermeable part, and other combined portion lies on the channel inside where bed level is expected to be almost uniform. Thus it is attempted for its extensive use in lowland rivers. There is still lack of consideration for influencing the flow for navigation at low flow time, if design is based on the bank-full discharge condition from the consideration of bank erosion (Mosselman, 2005). More discussion is made on this at the end of this chapter.

All complex flow phenomena persistent to alluvial river channels like turbulent flow, secondary flow, sediment transport, and so on, must be treated rightly prior to applying any engineering interventions in the river course to get some defined benefits. In order to design a suitable engineering structure for addressing the aforementioned problems, channel responses from the interventions could be analyzed by computational or experimental tools. Unfortunately, experimental data concerning the bed variation around a series of groynes is still very few in the state-of-the-art of the literatures; available researches include, e.g. Ohmoto *et al.*, 1998; Bahar and Fukuoka, 1999; Muto *et al.*, 2003; Kitamura, 2003. In view of that, a set of experiments using a series of impermeable and combined groynes are conducted in this study. In the present study, thorough investigations of the channel responses in the laboratory for various combinations of both permeability and alignment in the groyne structures including conventional straight impermeable one are attempted to recognize the modifications of fluvial processes by them to compare their performances, all aiming at improving the understanding in stabilization of lowland river channels, and the development of quality river landscapes as well.

Thus this chapter discusses the channel responses against five different groyne-structures: straight impermeable, straight combined, optimum aligned impermeable, optimum aligned combined and bandal-like structure modified with straight impermeable (near bank) portion and alignment as that of modified combined one. Emphasis is given to the morphological consequences from a series of groynes; also first groyne area has been discussed to understand the fluvial responses from the individual structure with various geometries of the groynes.

5.2 Methodology

This section describes the laboratory preparations for the experimental runs with experiment conditions to be maintained for different types of structures, and working procedures to fulfill the aforementioned objectives.

5.2.1 Experimental Setup

The experimental setup includes the details of model channel where the tests are conducted, various groyne models designed to modify the fluvial processes, and the experiment conditions; these have been described in the following sub-sections:

Model channel and structures

The experiments are performed in a tiltable open-channel flume located in the Hydraulic Engineering Laboratory of Nagoya University. The flume is straight and of rectangular cross-section, 20.0 m long, 0.5 m wide, 0.3 m deep, and is capable of a discharge not exceeding 50.0 m^3/hr. The side walls of the flume are made of a transparent weather-resistant acrylic sheet, thereby allowing visualization of the flow and the scour process during an experimental run. Its bed at both upstream and downstream areas is made rigid with wooden planks, and extended by 5.5 m and 4.5 m from the inlet tank and discharge tank, respectively. Relatively fine uniform sands with a median size d_{50} = 0.13 mm covered the remaining area of the channel with a thickness of around 16 cm. The projected length of all groyne models (L_g) is 18.0 cm. A set of six numbers of same model-structure are placed on right side of the channel perpendicular to the side, as the groynes should preferably be installed in a series to protect a certain reach of a river bank and also to maintain thalweg for navigation. The center of the first structure is at 10.0 m downstream from the inlet boundary, which is theoretically sufficient to achieve a fully developed turbulent flow in the control area. The model structures are installed with an interval of S_g = 0.55 m, i.e., aspect ratio $S_g/L_g \approx 3.0$, and cover the total distance 2.75 m by five embayments. A schematic representation of experiment setup (side view and top view) has been shown in the following figure (**Fig. 5.1**).

The x-axis is the downstream direction with $x = 0$ at center of the first groyne; y-axis is pointing towards the left side in the transverse direction with $y = 0$ at the right-side where the groynes are placed; and z starts from the initial bed level with upward positive. The velocity components u and v are corresponding to their directions x and y, respectively.

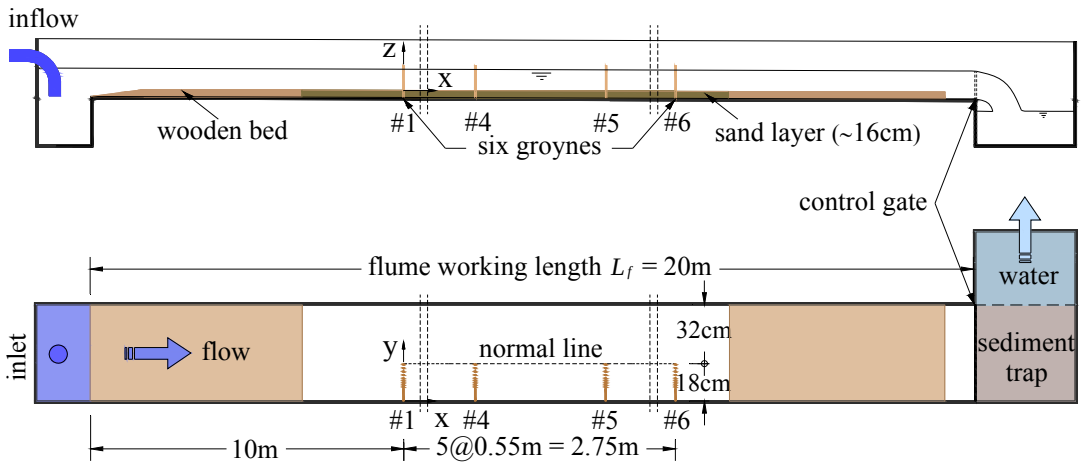

Fig. 5.1 Experimental setup: side view (top) and top view (bottom) of model channel

Five different model-structures are considered in this study varying alignment and permeability, two of which are impermeable and other three are combined. First model (St_Imp) is straight impermeable; this is the conventional design of groynes (**Fig. 5.2**). Although it is reported with some disadvantages, as mentioned in Section 5.1, it is considered here to compare its functions with other groynes.

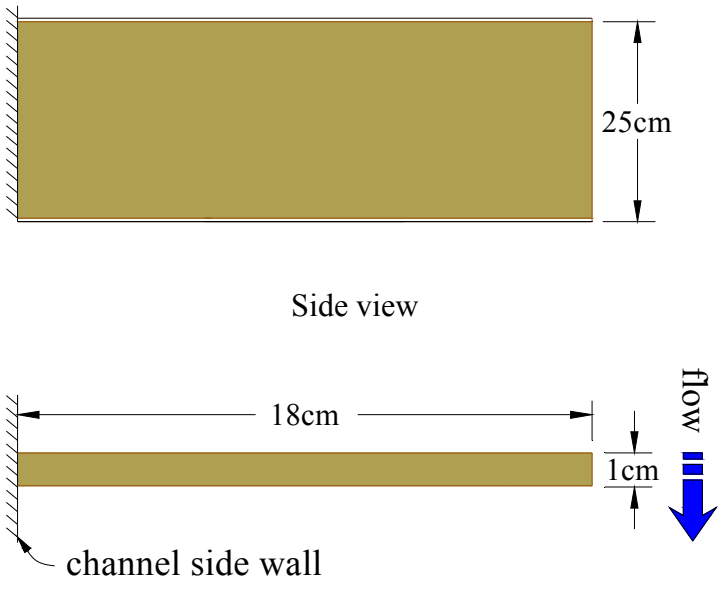

Fig. 5.2 Straight impermeable groyne (St_Imp)

Second groyne model (St_Com) is straight combined one. It is also straight, but first one-third portion adjacent to the channel side is impermeable, and rest part is made permeable with round sticks. However, permeability of the structure is varied along the longitudinal axis of the groyne changing blockage area; blockage is 67% near impermeable part; whereas, it is 50% at far-end, i.e., first-half of permeable portion is of 67% blockage and rest portion is of 50% (**Fig. 5.3**). As has been discussed earlier, these arrangements of permeability are provided in the structure to offer gradual obstruction to the flow, hence to minimize higher disturbances as impermeable groynes do, and to favor adjustment of flow more natural way.

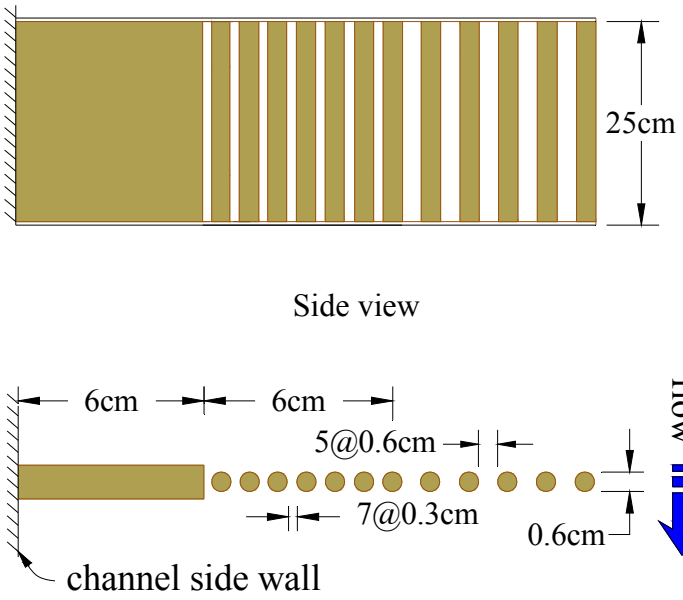

Fig. 5.3 Straight combined groyne (St_Com)

One-third part of optimum aligned impermeable groyne (OA_Imp) is perpendicular to the channel side and then aligned 20^0 downstream (**Fig. 5.4**). It is named so, because of its alignment and better performance at both high flow and low flow conditions over other alternatives (Alauddin Tsujimoto, 2011a). First perpendicular portion functions for diversion of flood flow and minimizes scour near groyne with the

combination of downstream aligned portion, and in addition, later part is effective to influence navigation channel at low flow.

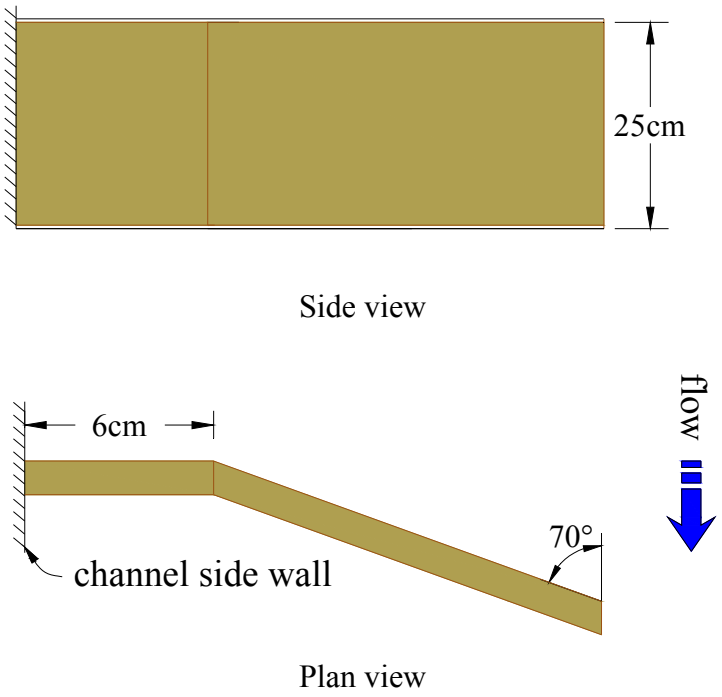

Fig. 5.4 Optimum aligned Impermeable groyne (OA_Imp)

Alignment of OA_com (optimum aligned combined groyne) is similar to OA_Imp; it is further modified with the provision of permeability into the downstream aligned two-third portion (**Fig. 5.5**), and its permeability is similar to St_Com with the same intention of decelerating the flow gradually. Here inclined portion is considered for favoring navigation channel at low flow.

Last one (OA_MBS) is optimum aligned modified bandal-structure. It is of same alignment as in OA_com, except that permeability of downstream-aligned portion is varied vertically: upper portion is blocked and lower portion is kept open or highly permeable, i.e., bandal-structure; here it is further modified with straight impermeable portion adjacent to the bankline (**Fig. 5.6**), in consideration of providing more calm area there keeping the currents far from the bank at high flow, and to make the structure useful for both high flow and low flow providing the downstream aligned portion in almost flat-bed part of alluvial river channels. In designing the model

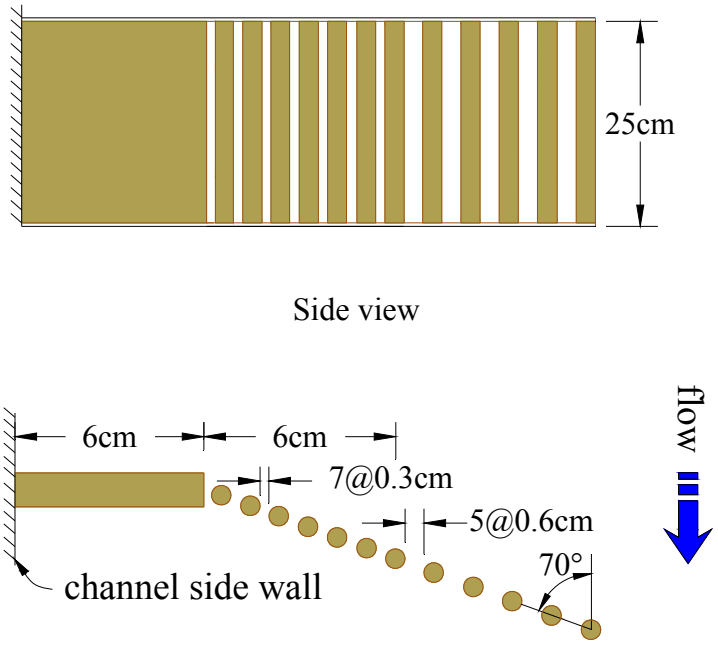

Fig. 5.5 Optimum aligned combined groyne (OA_Com)

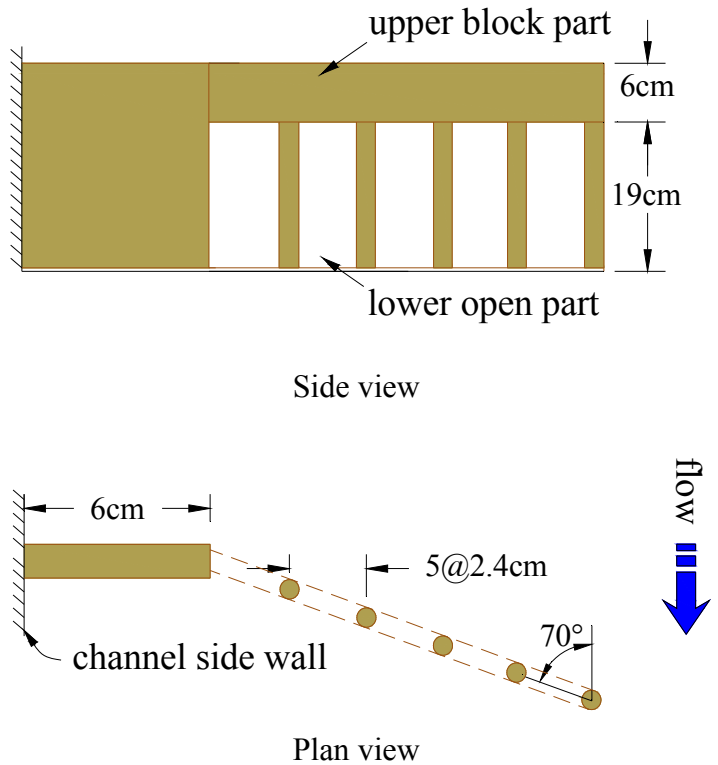

Fig. 5.6 Optimum aligned modified bandal-structure (OA_MBS)

dimensions, similar projection area is maintained as that of other combined groyne structures (St_Com and OA_com).

This can be mentioned here that, in the modified alignment, first one-third portion of the groyne length is made perpendicular to the bankline; which differs to the groyne-structure identified to be the optimum one from numerical investigations. There, half of the groyne length is made perpendicular to the bank, and then the rest part aligned 20^0 towards downstream. It is done here to provide the permeable part of significant length with different permeability, in the limited length of a groyne for better understanding of their corresponding responses. The figure, **Fig. 5.7** illustrates the channel cross-section with the placement of a model structure and sand bed.

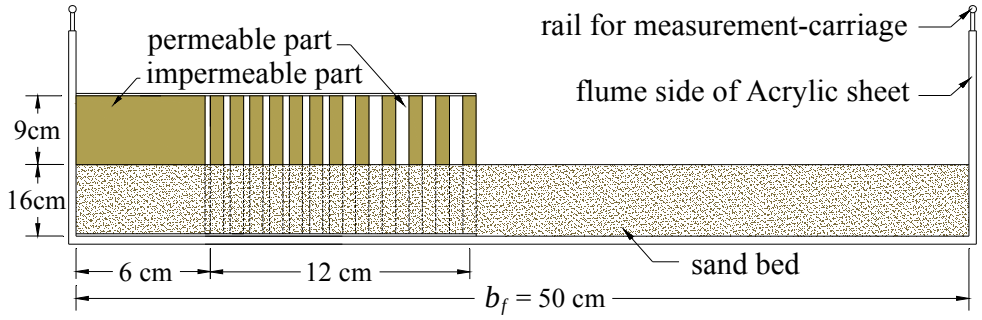

Fig. 5.7 Flume cross-section with a combined groyne and sand bed

5.2.2 Experimental Conditions

The experiments in the channel are conducted under clear-water scour condition. It is done by adjusting a control valve and a tail gate so that a bed shear velocity (u_*) does not exceed the critical shear velocity for initiation of motion of the bed sediment (u_{*c}) for the approach flow to avoid bed-forms at upstream of the control reach. This has been decided after some trials such that except control section, the channel bed has been remained unchanged, i.e., the condition of clear- water scour. Flow uniformity is verified by comparing the free-surface slope and the flume's bed slope. Two different flow discharges and approach depths are maintained for two types of groynes: impermeable and combined, considering the establishment of similar mean velocity in

the control area. It is decided based on the blockage area of the structures. In all tests, the groynes are emerged and the Froude number ($Fr = U/\sqrt{gh}$) is small enough to ensure sub-critical flow, as the flow in Jamuna river is generally characterized by lower *Fr*. Also the Reynolds number ($\mathrm{Re} = Uh/\nu$) is maintained high enough to ensure fully developed turbulent flow in the control section. The details of the tests undertaken, including the hydraulic and sediment transport conditions are presented in **Table 5.1.** The figure, **Fig. 5.8** shows size distribution of sands used in the experiments.

Table 5.1 Hydraulic conditions of the entire tests

Parameters	**Groyne type**	
	Impermeable	**Combined**
Flow Q (m^3/hr)	12.5	16.5
Flow depth h (cm)	5.0	5.5
Mean velocity U (cm/s)	13.9	16.7
Sediment size d_{50} (mm)	0.13	0.13
u_*/u_{*c}	0.88	0.92
Froude number *Fr*	0.20	0.23
Reynolds number *Re*	6944	9167

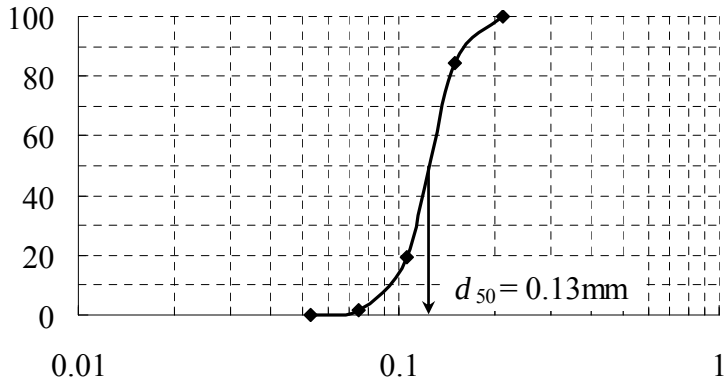

Fig. 5.8 Gradation curve of sands used in the experimental channel

5.2.3 Procedure

Before starting the flow into the flume, after placing one set of model structures on one side, the loose bed surface of fine sediment placed in the channel is leveled with a scraper wooden plate mounted on a moving carriage which can ride over the steel frames on both sides of the channel. After that, the flow is allowed to enter gently in the flume; when the bed is completely wetted, then it is drained and a profile of this bed surface is collected as an initial bed. The flume is then filled slowly with water and the specific flow in consideration of clear-water scour as defined in the preceding section is allowed to run. A control gate at the end of the flume is adjusted along with bed slope while allowing final flow to run, to ensure uniform subcritical flow and clear-water scour condition. Then, the change in bed topography, especially the depth of local scour near the first groyne-structure is monitored by a CMOS (complementary metal-oxide semiconductor) laser sensor (a sensor head IL-300 with an amplifier unit IL-1000, KEYENCE Corp.) to identify the equilibrium condition when the rate of change decreases considerably. Then all the measurements, such as flow depth, velocity fields, and final bed topographies are taken along some selected sections.

Measured data are then analyzed to extract some typical features to recognize the modification of fluvial responses by various groyne structures. As done before, in evaluating the performance of groyne structures, three typical features are investigated rightly: depth of scour near groyne (ΔZ_g), deposition of sediment in the groyne field (ΔZ_{gf}), and erosion in the main channel (ΔZ_{ch}), where the first one signifies the stability of the groyne-structures, the second one the protection of bank from erosion, and the third one the maintenance of navigation channel, respectively. Here, the values of the parameters for erosion in main channel and deposition in groyne field are averaged over the area between second and fifth groynes for combined groyne case, and second and fourth groynes for impermeable case, to avoid the effect of reflected flow. However, local scour is considered the maximum scour depth near the first groyne. For the analyses of data, the groyne field is considered from channel side to the normal line of the groynes (the line joining the groyne tips), and the main

channel is considered from 25 to 45 cm from the side wall, where the groynes are installed. The following figure (**Fig. 5.9**) illustrates the definition of the features considered:

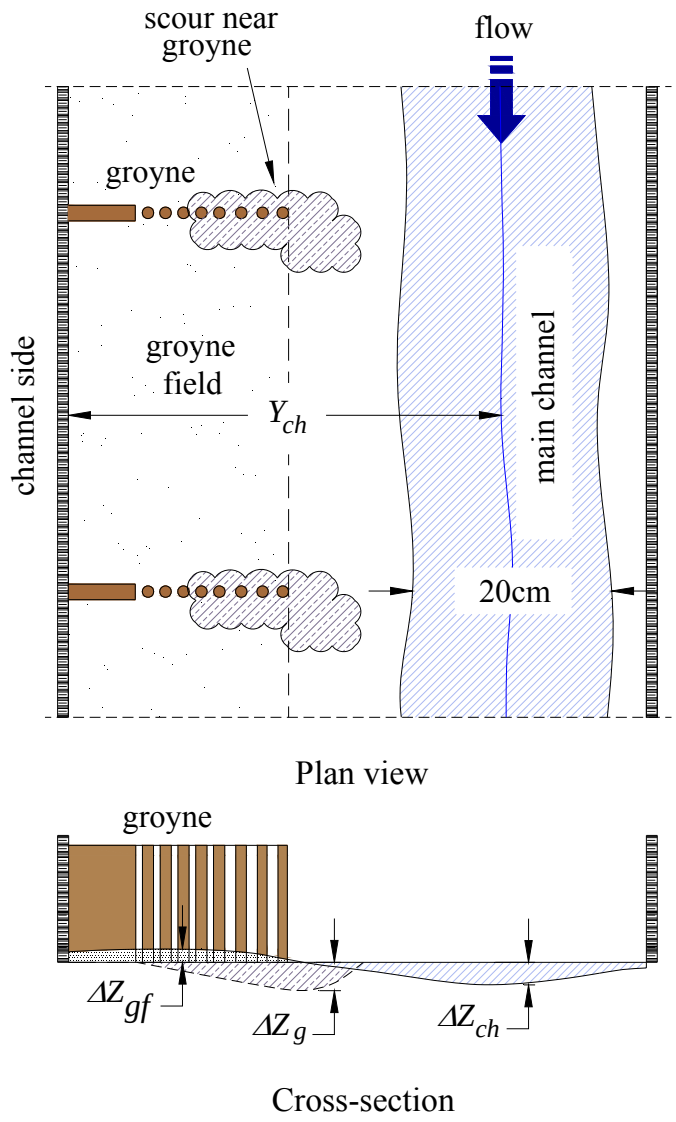

Fig. 5.9 Definition sketch of key features to evaluate groyne performance

5.3 Measurements

With the available setup for measurements, the flow depths, velocity fields, and bed topographies are measured for analyzing. Velocity measurements are taken once in

every test case at equilibrium state of flow. After continuous running the flow, when the channel bed seemed to be unchanged, then that state can be assumed to be reached equilibrium state, and it is considered 9.0 hrs in the tests. One test case is, however, conducted first for 18.0 hrs to recognize this time length, after which the change in bed level is observed insignificant. Bed levels are measured in the test area before the start of each test for reference and after the end of the tests, respectively.

5.3.1 Velocity Fields

Two-dimensional velocity components are collected with an electromagnetic velocimeter (VM-602HT, KENEK Co., LTD.) under dynamic flow conditions utilizing I-shape sensor, which is attached to a moveable platform. The measuring devices recorded a signal in *x*- and *y*-directions simultaneously, which later converted into velocities in cm/s. Three measurements are taken at each point to get the average value, and the area between first and second groynes is chosen for the velocity measurements to inspect the modification of flow patterns influenced by the individual structure after coming in the flow from uninterrupted area. To grasp the velocity fields rightly, these measurements are taken along 16 longitudinal transects with 3.0 cm intervals starting at 2.5 cm from the channel wall and 9 transverse transects, from 2.5 cm upstream of the first groyne to 2.5 cm upstream of the subsequent groyne. The measurements are made at approximately 60% of the water depth, measured from the water surface. It is assumed that the magnitude of the velocity at this depth equals the magnitude of the depth-averaged velocity. The locations of the measuring sections and points are delineated with the figure, **Fig. 5.10**.

5.3.2 Bed Levels

After the velocity measurements, the flow is gradually decreased in such a way as to cause minimal disturbances to the bed. The channel is drained and after the bed is dry, typically after one day of the run, the elevation of the bed is measured in the control area using a computer aided laser sensor. Bed levels are measured in the entire groyne

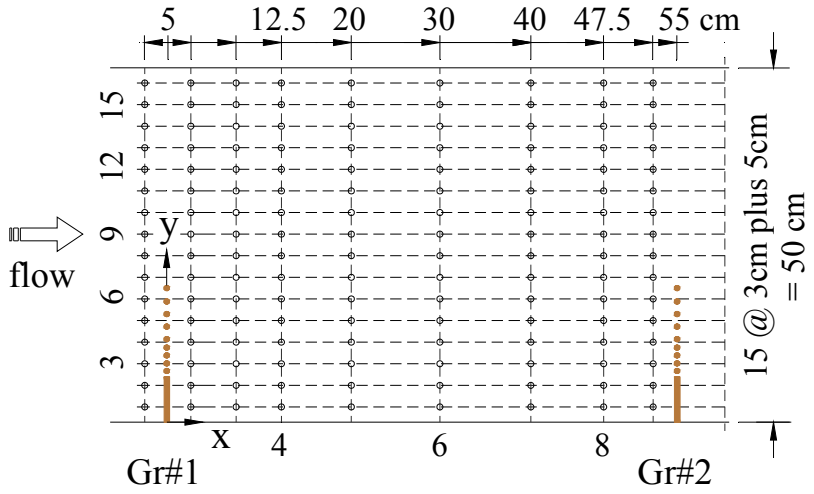

Fig. 5.10 Measuring points and sections for velocity measurements

area along 18 longitudinal transects with 2.5 cm intervals. Three sensors are attached to a moving carriage to cover three transects at each sweep that travels over a steel frame on both sides of the channel. The equipments used for measuring velocity fields and bed topographies have been shown in **Fig. 5.11**. Also two photographs have been given in **Fig. 12**: one of which with initial bed condition and model OA_MBS before starting the flow into the channel, and the other one with final bed after finishing the run.

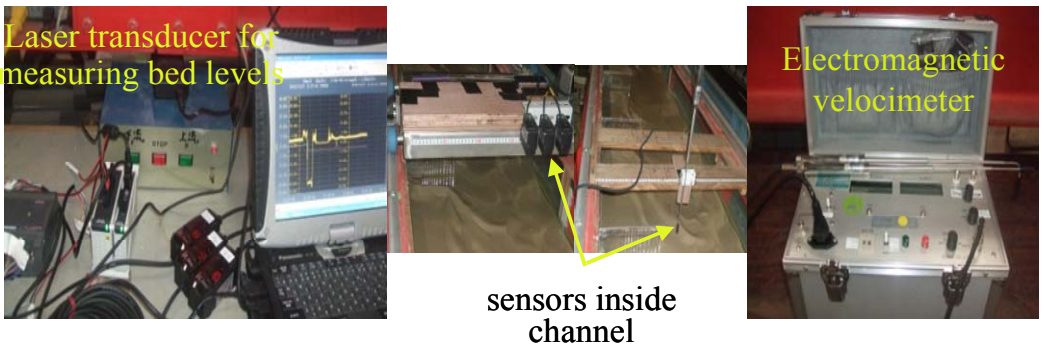

Fig. 5.11 Equipments used for measuring bed topographies and velocity fields

(a) Initial bed (b) Final bed

Fig. 5.12 Experiment channel with model OA_MBS: (a) initial bed; and (b) final bed

5.4 Results and Analyses

As the main two purposes of installing groynes are bank protection through deposition of fine sediment near the bank and maintenance of thalweg for navigation channel accompanied with structural safety, three typical features such as scour depth near groynes, height of deposition of sediment in the groyne field, and depth of erosion in the main channel, are considered to confirm the performance of groynes. Velocity distributions and bed topographies measured with available setup in the selected sections are presented in this section to understand the modification in flow patterns and to explore all the features influenced by the structures.

5.4.1 Flow Fields

Depth-averaged flow fields in the first groyne area influenced by the model structures are presented in **Fig. 5.13**. It can be seen here that the magnitude of velocity vectors in the groyne field near bank for combined groynes (St_Com, OA_com, OA_MBS) are appreciably reduced and no strong recirculation of flow can be marked there, except a smaller one from OA_MBS behind the impermeable portion [**Figs. 5.13(b, d and e)**]; whereas in the case of impermeable groynes (St_Imp, OA_Imp), high separation of flow can be marked near groyne head with flow circulation [**Figs. 5.13(a and c)**]. The return currents from the groyne head, if groynes are not closely spaced, are sometimes threatening at high flood time to cause scour near bank and hence bank recession, rather than forming sustainable riverine landscape. Moreover, this inherently causes strong eddies and hence huge scour near groyne-tip to hamper stability of the structure itself, as evident in Jamuna: several failures of RCC spurs due to separation of flow are reported (Uddin, 2007) including many others.

Fig. 5.14 depicts the transverse distributions of streamwise velocities from all of the models non-dimensioned by mean flow velocity in impermeable case (U_{imp} = 13.9 cm/s) at 7.5 cm downstream of first structure to compare the flow patterns affected by various groynes. From the average trend of transverse distributions of streamwise velocity for combined groynes, it can be recognized that velocity reduces gradually towards the channel boundary where the groynes are installed, not sudden reduction at the end of the structure, or at the end of the impermeable part, what impermeable structures do, leaving strong eddies there. This modification of flow-patterns can be attributed to the permeable components of the structures and gradual reduction of permeability along the longitudinal axis of groynes towards the side wall. From the figure, it can also be seen that variation of velocity is very rapid for impermeable groynes, and it is steepest for the straight conventional one.

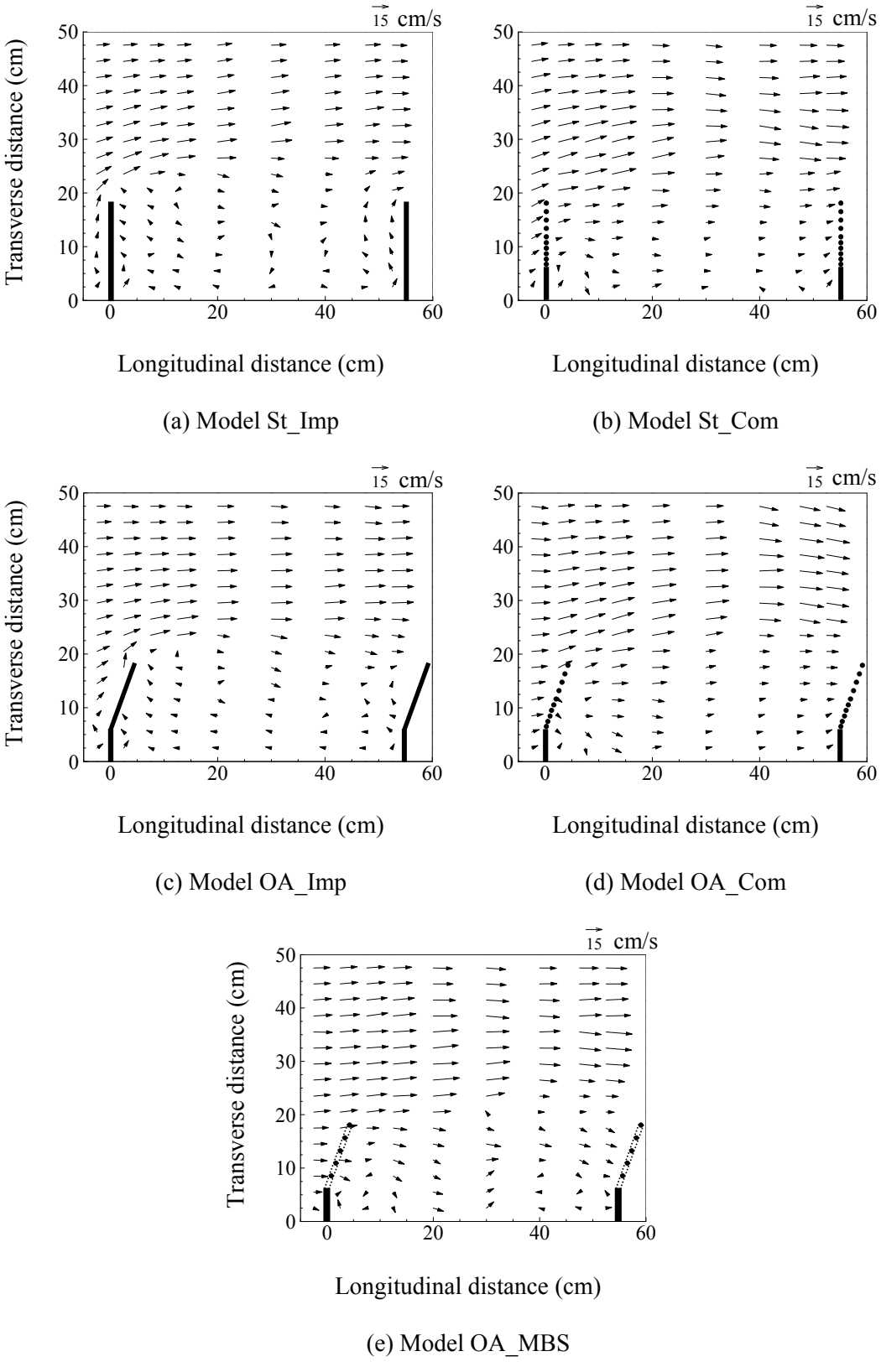

(a) Model St_Imp

(b) Model St_Com

(c) Model OA_Imp

(d) Model OA_Com

(e) Model OA_MBS

Fig. 5.13 Flow fields in the first groyne area induced by various groynes

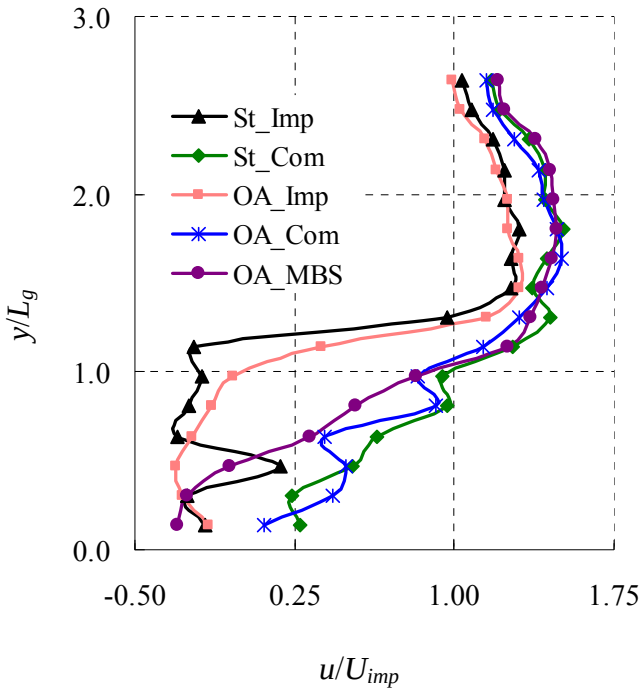

Fig. 5.14 Depth-averaged streamwise velocity (dimensionless) distributions across the channel at 7.5 cm downstream of first structure

5.4.2 Bed Topographies

The bed topographies resulted from the interactions of various groynes have been presented in **Fig. 5.15**, where (relatively) higher impact near the first structure causing deeper scour as well as higher erosion in the channel bed can be marked (downstream embayments are not discussed here, which are seriously affected by the reflected flow from the opposite wall). Channel ripples of various dimensions are observed in the control area with larger dimension in the main channel and smaller extent in the groyne field, not in the upstream part of the area. Here, variation in channel responses can be marked for various groynes due to the variety of obstruction to the flow by the structures. As local scour around the first groyne was significantly more pronounced, so this can be explained from the fact that the first groyne is exposed to the strongest current, which results in an increased erosion rate. However, in the case of

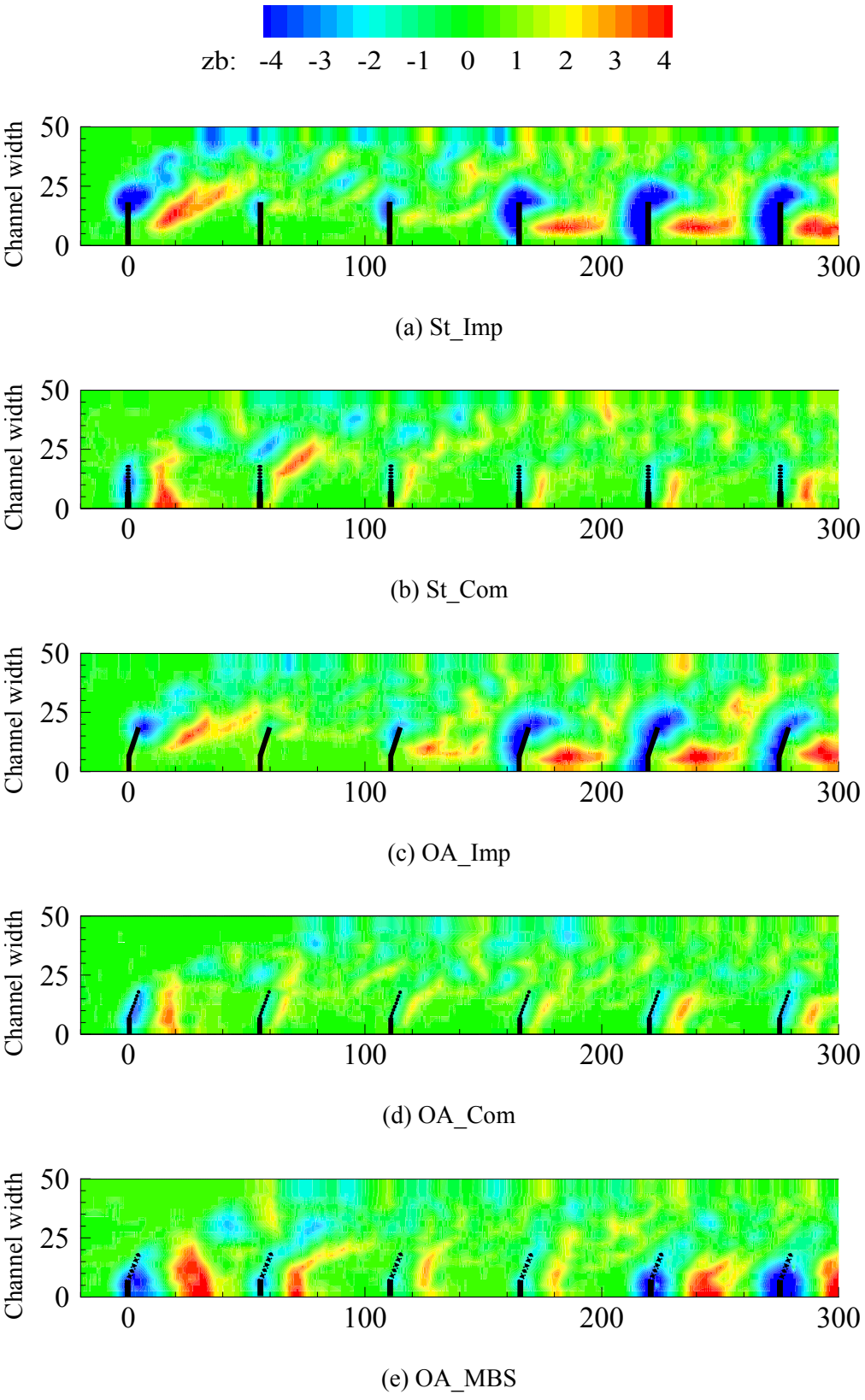

Fig. 5.15 Bed topographies against various model structures (all units are in cm)

impermeable groynes, the flow is highly diverted, so that it is reflected from the opposite wall of the channel and turned back to attack the downstream embayments causing much scour near groynes there. It is surprising to notice here that the impact by the back flow can even be severe to destroy the downstream structures, depending on the intensity of oblique flow from the islands, large sandbars, or other bank on opposite side in the case of the natural river. In the region behind the last groyne, as the channel becomes wider, consequently, deposition has taken place due to the decreased velocity.

From the data of bed topographies, dimensionless transverse distributions of erosion and deposition averaged over the area between second and fifth groynes for combined groyne case, and second and fourth groynes for impermeable case, have been presented in **Fig. 5.16**, to recognize the influence of various configurations of groynes in the main channel and groyne field, respectively. Here, depth of flow in impermeable case (h_{imp} = 5.0 cm) is considered to make the parameters dimensionless. In averaging the value of the features, the distances are differed for two types of groynes to avoid the effect of reflected flow by the impermeable groynes. As the flow velocity decreases significantly in the embayments, sediment settles there with

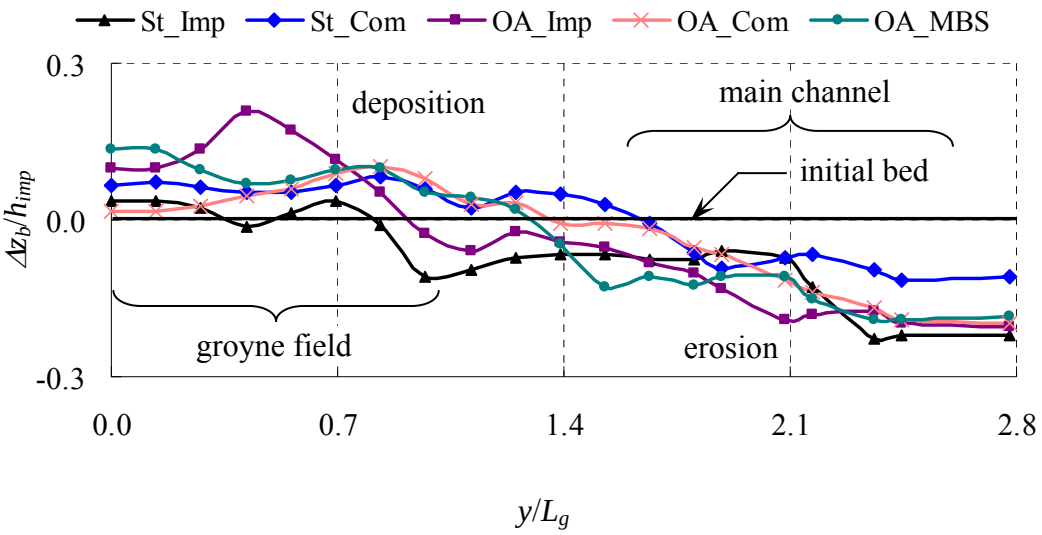

Fig. 5.16 Transverse distributions of erosion and deposition from various model-structures

different mechanisms of material transports for impermeable and combined groynes, respectively. Thus, the important features to evaluate the performance of groynes such as: scour near groynes, deposition in groyne field, and erosion in main channel induced by the structures, can be extracted from these bed topographies (will be discussed in the next section).

5.5 Performance of Model Structures

The performance of a groyne is evaluated through three key features: scour near the groyne, deposition in the groyne field, and erosion in the main channel; where the first one signifies the stability of the structure, the second one the anti-erosion of bank, and the third one the maintenance of navigation depth in the main channel. To compare the groyne functions, the measured maximum scour depth near the first groyne, average deposition in the groyne field, and average erosion in the channel bed (25 cm to 45 cm from the side wall where the groynes are installed), are summarized in **Table 5.2**. The area considered for finding average feature values of erosion and deposition is similar to that considered for their transverse distributions as described in Section 5.4.2, to avoid the effect of back flow from opposite wall in the case of impermeable structures. Also these data have been presented with a figure (**Fig. 5.17**) for clear understanding of the comparative features among various groynes.

Table 5.2 Dimensionless features from all model-structures

Dimensionless features		**Groyne models**				
		St_Imp	**St_Com**	**OA_Imp**	**OA_Com**	**OA_MBS**
Max. scour near groyne	$\Delta Z_g/h_{imp}$	1.150	0.850	0.910	0.700	0.890
Avg. deposition in groyne field	$\Delta Z_{gf}/h_{imp}$	0.010	0.059	0.090	0.056	0.078
Avg. erosion in main channel	$\Delta Z_{ch}/h_{imp}$	0.095	0.033	0.093	0.076	0.085

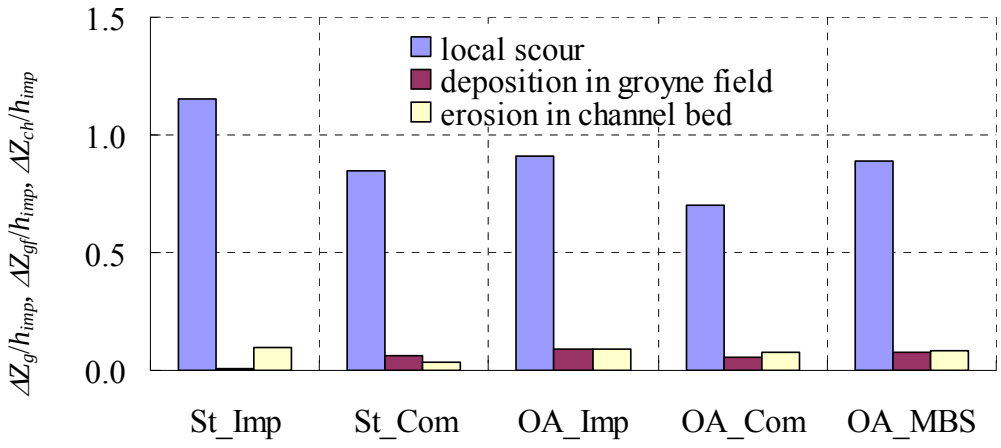

Fig. 5.17 Comparison of dimensionless features among the groyne models: local scour ($\Delta Z_g/h_{imp}$), deposition in groyne field ($\Delta Z_{gf}/h_{imp}$), erosion in channel bed ($\Delta Z_{ch}/h_{imp}$)

Here, better responses in the channel in respect of local scour can be recognized due to both alignment and permeability: local scour reduces from St_Imp to St_Com, and also from St_Imp to OA_Imp; the consistency of the results can be seen from other studies such as Muraoka *et al.* (2009), Mojtaba and Abbas (2009), Kang *et al.* (2011), and others. From the model OA_MBS, local scour is similar to OA_Imp in magnitude, but higher area **(Fig. 5.15)**, and it is minimum for OA_Com. Sediment deposition in the groyne field can be seen higher for the models OA_Imp and OA_MBS, and then St_Com and OA_com, and it is minimum for the case of model St_Imp. Average erosion in the channel bed is found higher for the models St_Imp and OA_Imp, and then OA_MBS, and it is minimum for St_com. However, from **Fig. 5.15**, it can be recognized that erosion is relatively regular for OA_com, but moderate in magnitude. The irregularity of bed profiles are also analyzed by statistical parameters, from which the minimum deviation from the regression line of average erosion-deposition patterns **(Fig. 5.16)** (σ = 0.008) is evident for OA_Com; whereas, these are found σ = 0.019, 0.015, 0.022, and 0.018 for groyne models OA_Imp, St_Com, OA_Imp, and OA_MBS, respectively. However, the details of the statistical analyses are not

included herein. Moreover, as seen in the figure in impermeable case, flow is reflected from the other side of the flume and attacks the downstream embayments, where pronounced scour is observed near groynes. It could be possible by strong return currents from fully blocked impermeable structures depending on groyne intervals, or reflecting the flow from large sandbars or any hard strata on the channel boundary on opposite side, as recognized the failure of Betil and Enayetpur spurs several times in Bangladesh due to obliquely striking flow (Klingeman *et al.*, 1984; Nazim *et al.*, 2010).

It can be seen from **Fig. 5.14** that flow beneath the upper impermeable portion of model OA_MBS counterbalances the recirculation of flow and causes bed formation in the downstream area; this is also evident from the field observation where the concrete dyke part of a large groyne (this is a combination of an earthen shank and a concrete dyke) behaves like this structure (Nazim *et al.*, 2010). Diversion of flow is made by the straight impermeable and inclined upper blocked-portion of the structure which favors deepening the channel bed; whereas, only sediment-laden water near the bed passes beneath the blocked portion and deposited in the groyne field. However, compared to the model OA_com, scour depth and scour area both are found higher in the case of model OA_MBS, this may due to the formation of vortices induced by downward flow to pass through lower open part (Zhang *et al.*, 2010)**;** in contrast, height of deposition in the groyne field as well as erosion in the channel bed both are better responded in this case compared with others. Therefore, from the experimental results, although OA_MBS is advantageous in respect of anti-erosion of bank and maintenance of navigation channel, structural safety may have to be sacrificed or much attention should be paid for that at high flow condition. In addition, it is difficult to maintain certain area-ratio between upper impermeable and lower permeable portions for better functioning (which is maintained around 50%, as a thumb rule), as water level varies highly in the river, especially in Jamuna over the annual hydrologic cycle. Even if bankfull stage, say, is considered in consideration of bank protection from erosion (Mosselman, 2005), this may not function properly to address low flow problem due to less diversion of flow by lower highly permeable portion. As the erosion in channel bed in the case of both OA_com and OA_MBS is significantly

improved than St_Com and relatively uniform due to their modified configurations, so introducing the modification in groyne designs, which minimizes both local scour and big diversion of flow, does not have to compromise the quality of waterway or stability of river bank.

Moreover, as bed fauna in the river system is strongly related to the hydro and morphodynamics in the main channel and groyne field areas, and the design of model OA_Com inclines towards a more natural one, i.e., gradual reduction of flow velocities is made towards the bank by its modified design, thus an increased biodiversity in bed fauna is to be expected. The spectrum of species and density of the bed fauna will become more balanced and natural. Also the less turbulent flow climate in the groyne field further enhances ecological potential (Van Heereveld *et al.*, 2007). As the tendency of attacking the bank is minimized by strong recirculation of flow, deposited bed-forms of fine sediments near bank could support stable growth of vegetation, having a very important contribution to sustainable habitat. Furthermore, as this model minimizes strong return currents, aspect ratio could be increased, also maintenance on these groynes is expected to be significantly lower than that for the conventional one, adding to the sustainability of the concept. Hence, the initial and lifecycle cost both are greatly reduced.

5.6 Conclusions

In this study, the channel responses from various groynes are investigated in the laboratory experiments under clear-water scour condition. It is mainly aimed at scrutinizing the fluvial responses from various configurations of groynes, through which their performances can be known; thus to find a suitable design of a groyne for lowland river problems. From the discussion in the preceding sections, the following conclusions can be drawn:

- St_Imp: In the case of straight impermeable groyne, high separation of flow occurred; consequently, causes high scour near groyne-tip. Also the flow is

highly diverted to hit the other wall and turned back to attack the downstream embayments.

- St_com: Due to permeable nature in the straight combined groyne, velocity is reduced gradually and local scour is minimized, but erosion in the main channel is not significant and not regular.
- OA_Imp: Flow separation is moderate in the case of optimum aligned impermeable groyne and hence, local scour is reduced in area and magnitude both compared with the straight conventional one (St_Imp) due to its modification in alignment. Flow is also turned back in this case after reflection from the other side.
- OA_com: Optimum aligned combined groyne favors much lower local scour to occur than all other models; also deposition in the groyne field as well as erosion in the main channel are relatively regular, but moderate in magnitude.
- OA_MBS: Local scour is found higher in the case of modified bandal structure in area and magnitude both compared with the models St_com and OA_com; however, two other important features: erosion in channel bed and deposition in groyne field are better responded.

As the model OA_com offers more gradual transition from main channel to land, this bears a high importance to improve the quality of river landscape. The ecological connectivity increases through the permeable parts in the groynes. The lower flow velocities allow for better migration of species.

The features explored from the laboratory investigations imply that further modification in the lower permeable portion in OA_MBS can be made with the arrangements for permeability in OA_com, so that the modified structure can serve optimal function both at high flow and low flow conditions at lowland rivers; however, scour condition by downflow at upstream side of the structure needs further investigations. The combined structures (St_com, OA_com and OA_MBS) offer more gradual transition from main channel to bankline compared with the conventional impermeable one, thus these bear a high importance for the quality of landscape.

Besides, as these structures minimize scour near groynes and strong return currents, aspect ratio could be increased, thus a cost-effective design approach can be expected.

CHAPTER 6

FORMATION AND CHARACTERISTICS OF SANDBARS

Summary

The large-scale sandbars resulted from the instability of loose sedimentary materials are very common in lowland rivers. They make the river highly unstable forming anabranches, influencing bank erosion, and so on. Thus the study on their formation processes and their characteristics at natural scale becomes very urgent for better management of river engineering. RIC-Nays, a two-dimensional model for flow and morphology, is utilized in this study. Formation processes of alternate and multiple bars are studied first to verify the simulation results. The effects of initial and boundary conditions on the bar formation processes and the cause of reduction of bar mode observed in experiments are also clarified. The results show reasonably good agreement when compared with theoretical and experimental data. The multiple bar patterns present in the natural rivers are reproduced by the numerical simulation, where the evolution of bars is apparent with a pool-bar complex. However, bar heights and irregularities are not reproduced rightly; variable discharges along with some other hydraulic factors may be responsible in happening so in nature.

6.1 General

The bed and banks of lowland rivers are comprised of loose sedimentary materials transported by the streams. Therefore, these are susceptible to major morphological changes as the alluvium is eroded, transported and deposited throughout the channels. This instability forms the bars that have a diverse range of planform shapes and produce a complex alluvial architecture. These have significant roles in both

engineering and ecological aspects in fluvial processes: pools cause successive side-bank erosion, while sandbars are habitats for various species in rivers. Large sandbars are very common in lowland rivers like Jamuna in Bangladesh, resulted from various causes such as huge sediment flux from upstream, less flow strength due to mild slope or slack water developing in a reverse eddy at the downstream of node points or some similar hydraulic factors (Coleman, 1969), bank erosion, and so on.

A large number of studies, theoretical and experimental, also recently numerical studies have been devoted to understanding the physical mechanisms underlying the formation and development of these bedforms, from which only a few of the related studies have been briefly reviewed herein. Ikeda (1984) proposed empirical formulae to predict the wavelength and wave height of alternate bars. He tested his formulae by a number of experimental data obtained by him and other researchers. Fujita and Muramoto (1985), and Fujita (1989) performed several experiments to investigate the formation processes of alternate bars, multiple bars and braided streams, where they found that in most of the cases, the bar mode is reduced as time progresses.

Theoretical studies started with linear stability analysis (Hansen, 1967; Engelund and Skovgaard, 1973; Parker, 1975; Fredsoe, 1978), which successfully described the regime of bar formation. However, the linear theories can describe only very beginning of the bar formation. When the amplitude grows to be finite, the linear theory is invalid because of the domination of the nonlinear terms. Also Fukuoka and Yamasaka (1985) performed a nonlinear analysis assuming the interaction between two different modes of bars to treat equilibrium states. Colombini *et al.* (1987) proposed a nonlinear stability analysis by the growth rate expansion method to obtain the wave height of alternate bars. Pornprommin and Izumi (2001), and Izumi and Pornprommin (2002) proposed another nonlinear analysis to extend Colombini *et al.* (1987)'s to more general cases. In order to remove the restriction of small growth rates, the amplitude expansion method was used to derive the equilibrium wave height of both alternate and multiple bars.

Among the numerical models developed for bar formation by the rapid development of computers: Takebayashi *et al.* (2001) performed numerical simulations of bar

formation, and succeeded in reproducing the reduction of bar mode as observed in Fujita (1989)'s experiments. Kurabayashi and Shimizu (2002) proposed another simulation model using the Cubic-Interpolated Pseudoparticle (CIP) method (Yabe *et al.* 1990) that minimizes the numerical diffusion. Also Pornprommin *et al.* (2002) simulated and investigated the formation of alternate and multiple bars utilizing the NHSED2D model.

The studies as mentioned above are mostly contributed to the upstream rivers. The discussions on the formation and characteristics of sandbars at lowland rivers are not sufficient yet. Undue and rapid sedimentation resulted as large sandbars in the lowland rivers like Jamuna greatly hampers the navigational routes at low flow time. Also the presence of these bars makes the channels highly unstable forming anabranches, eroding riverbanks, and so on. Although several studies have been conducted on bar formation processes at laboratory scale, discussions on the bar formations and their characteristics at natural scale in alluvial rivers with fine sediments are not sufficient yet. Therefore, this is crucial to study for better management of river engineering. In this study, a two-dimensional (2D) model is employed to examine the formation processes of large-scale bars and their characteristics. First, the formation processes of alternate and multiple bars are investigated in experiment scale; simulation results are then verified with both theoretical (Pornprommin and Izumi, 2001; Izumi and Pornprommin, 2002), and experimental results (Fujita and Muramoto, 1985; Fujita, 1989), and the effects of initial and boundary conditions on the bar formation processes and also the cause of the reduction of bar mode observed in experiments are clarified.

6.2 Solution Approach

So far bar formation processes are explored in numerical simulations various ways, although some are failed to describe the actual phenomena appearing in real rivers (Teramoto and Tsujimoto, 2003). We have applied RIC-Nays, a two-dimensional (2D) model for flow and morphology, where the shallow-water equations for 2D

unsteady flow expressed in a general coordinate system are solved on the boundary-fitted structured grids.

The equations are discretized by finite-difference method, and are solved for the unknown nodal values by an iterative process. The CIP method is utilized for the advective terms in the water flow equations, and a model with a constant eddy viscosity coefficient is used in considering turbulence. Initial water surface and downstream water surface both are set by uniform flow condition. At upstream and downstream ends periodic boundary conditions are applied for assuming a sufficient long channel, and small disturbances are given to the initial flat bed to achieve instability. First, the flow field is computed utilizing initial and boundary conditions; the sediment transport field is then computed utilising two separate expressions for suspended load and bed load, and used to compute erosion and deposition rates, followed by bed topography updating. After bed topography changes, the flow field has to be recomputed.

Also a submodel to account for bank recession due to scour by currents is included in the computation scheme, as this affects highly the bed-forms. This is considered for non-cohesive bank materials only. When the slope angle of the riverbank exceeds the angle of repose under the water, the slope is assumed to collapse, and bank erosion will progress. Thus the bank retreats intermittently through the repeated cycles of bank scour, collapse, deposition of the collapsed bank materials, and transportation of the deposited materials. As the banklines shift toward the outer direction due to the bank erosion processes, the numerical grids are reproduced with the moving boundaries. The grid points are rearranged at equal intervals between the right and left banklines in the lateral direction.

6.3 Simulation of Bars at Laboratory Scale

Hydraulic and sedimentological parameters and geometry of the simulation channel used in the study are similar to those used in the experiments by Fujita and Muramoto

(1985) and Fujita (1989). The simulation results are compared with the corresponding experimental and theoretical results to demonstrate the applicability of the model.

6.3.1 Alternate Bars

The simulation of the formation of alternate bars is included in this section. The model is tested with Fujita's Run C-2 (Fujita and Muramoto, 1985) described in **Table 6.1**, in which the aspect ratio β is the ratio between channel width and flow depth. The aspect ratio is an important parameter, which determines the bar mode n_b, when larger β generally corresponds to larger n_b.

Table 6.1 Experimental data of Fujita's Run C-2 (Fujita and Muramoto, 1985)

Channel width B (m) x length L (m)	0.40 x 18
Water discharge Q (l/s)	1.95
Slope S	0.01
Sediment Diameter d (mm)	0.99
Water Depth h (mm)	12.6
Aspect ratio β	31

Conditions of the numerical simulation

Conditions employed in the simulation are described in **Table 6.2**, in which Z_0 is the initial bed elevation. RD means the random disturbances with a normal distribution,

Table 6.2 Conditions of the simulation for Fujita's Run C-2

Domain B (m) x L (m)	0.40 x 3
Δt (s)	0.01
Z_0 type	RD
Total time (min)	92

which has a mean value of zero and a standard deviation of 0.1. We adopt these disturbances that are considered to reproduce experimental situation appropriately. The length of the calculation domain is taken to be 3.0 m which corresponds to the bar wavelength observed in the experiment.

Results of the simulation

Fig. 6.1 shows the bed variations at different time steps obtained in the simulation. Initially, the small random disturbances evolve into double-row bars on the bed, which are not stable. These bars increase in length and height as they evolve until they

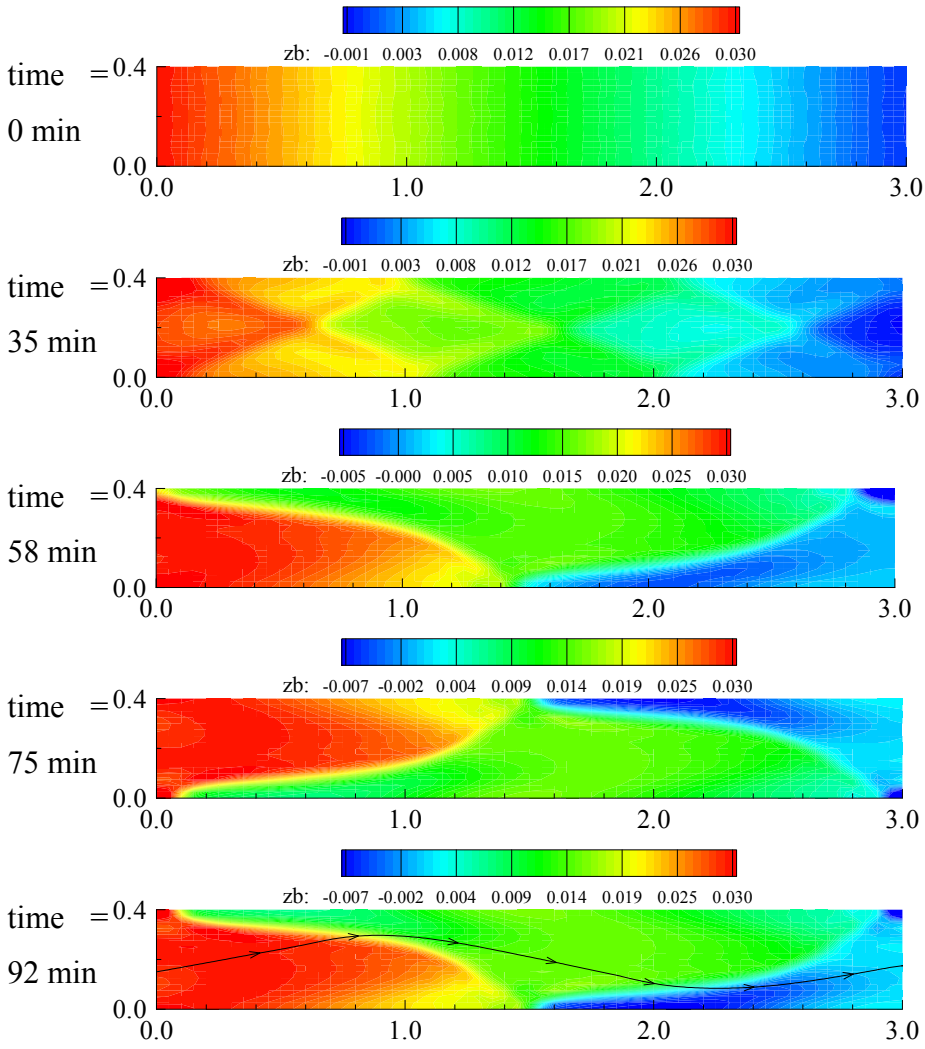

Fig. 6.1 Bed topographies of the simulation for Fujita's Run C-2 (Fujita and Muramoto, 1985)

are in equilibrium with water flow and sediment transport. Gradually they form into alternating sides of the channel with progression downstream. After around one hour, these reach an equilibrium state to become fully developed alternate bars, propagating downstream with a stable regular shape and an almost same celerity (= 5.3 m/hr). The water flow over these bars is sinuous in plan (**Fig. 6.1**, 92 min), with wavelength equivalent to that of the bars in the row.

The bar height H_b, defined as the difference between the elevations of the crest and the trough, observed in the experiment is 25.8 mm and that derived from theory, stability analysis of Pornprommin and Izumi (2001), and Izumi and Pornprommin (2002) is 29.5 mm, while the numerical simulation gives a little smaller value 22.3 mm.

6.3.2 Multiple Bars

In this section, simulation of multiple bars and comparison with the theoretical and experimental results are discussed. Here the aspect ratio β is set to be higher than that in the simulation of alternate bars, implying shallow water channels. Three cases with different initial conditions and domain lengths are considered in order to clarify the influence of the initial and boundary conditions on the bar formation processes, and to discuss the mechanisms of the reduction of bar-modes and the transition to braided channels observed in nature.

The model is verified with the Fujita's Runs B-2 and B-4 (Fujita, 1989), where the multiple bars appeared and developed with bar movement towards downstream; the conditions of which are shown in **Table 6.3**. These experiments are conducted under same hydraulic conditions, except that in the run B-4, the experiment was interrupted six times to measure the bed topography. **Figs. 6.2(a and b)** show the changes of bed topographies observed in the Runs B-2 and B-4, respectively.

Table 6.3 Hydraulic conditions of Fujita's Runs B-2 and B-4 (Fujita, 1989)

Channel width B (m) x length L (m)	3.01 x 43
Water discharge Q (l/s)	30.75
Slope S	0.005
Sediment Diameter d (mm)	0.88
Water Depth h (mm)	25.5
Aspect ratio β	124

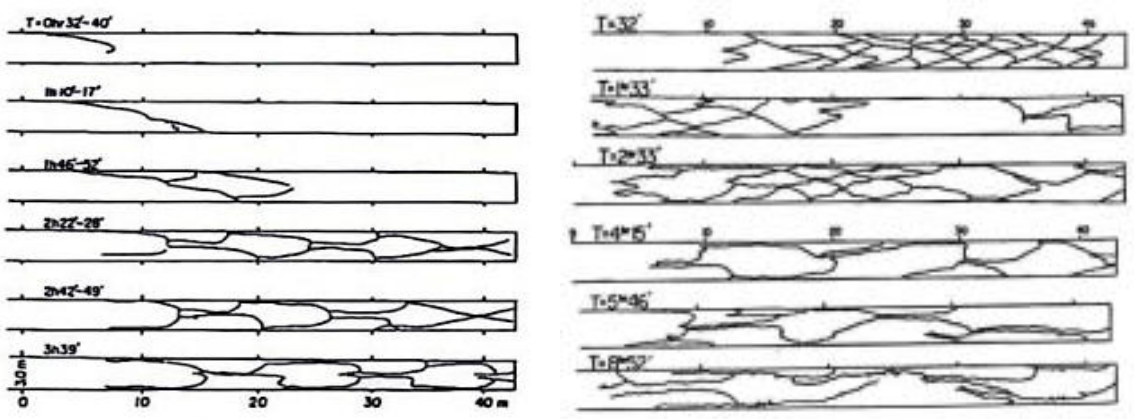

(a) (b)

Fig. 6.2 The changes in bed topographies observed in (a) Run B-2, and (b) Run B-4 (Fujita, 1989)

Conditions of the numerical simulation

The different initial conditions are employed to clarify their influences, and also different domain lengths are used in the simulations as the periodic boundary condition is assumed to have a strong influence on the bar wavelength. The conditions used in the three simulations are described in **Table 6.4**, where 'Sine' in the table means that Z_0 is set to be a sinusoidal shape.

Table 6.4 Conditions of the simulations for Fujita's Runs B-2 and B-4

Simulation No.	**1**	**2**	**3**
Domain B (m) x L (m)	3.01 x 5		3.01 x 15
Δt (s)	0.01		0.02
Z_0 type	Sine	RD	RD
Total time (hr)	3.1	3.1	3.5

Results of the simulations

Simulation No. 1

It is found that, at the beginning, the initial sinusoidal bed topography with the mode n_b = 1 evolves into a stable symmetrical form of multiple bars with the mode n_b = 3, the wavelength of which is equivalent to the domain length. This is shown in **Fig. 6.3(a)**.

Simulation No. 2

Fig. 6.3(b) shows the sequential formation process of the simulation no. 2, where the disturbances with a normal distribution are given on the bed surface as an initial condition. While the mode n_b = 5 with the wavelength around 3 m is observed at the beginning, it is reduced to the mode n_b = 4. The bar height increases with reducing mode. Symmetrical bars with the mode n_b = 4 become dominant in equilibrium state. Although all the conditions other than the initial condition are identical between both simulations, the final bar modes are found different from each other. This implies that there are two different equilibrium solutions.

Simulation No. 3

In this case, the domain length is extended to 15 m. The initial condition is small random disturbances with a normal distribution. The time variations of the bed topography are shown in **Fig. 6.3(c)**. At the beginning, there is appearance of weakly developed multiple bars with mode n_b = 4. Then the bars with the mode n_b = 3 become dominant in the whole region. The bars increase in both magnitude of height

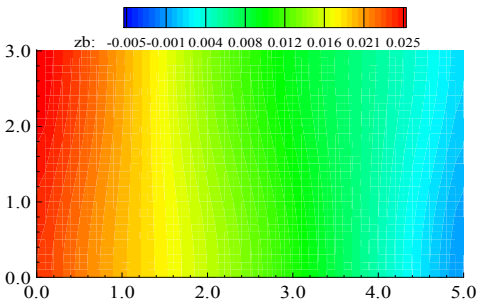

time = 0.0 hr

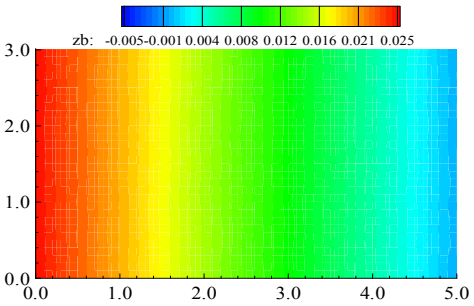

time = 0.0 hr

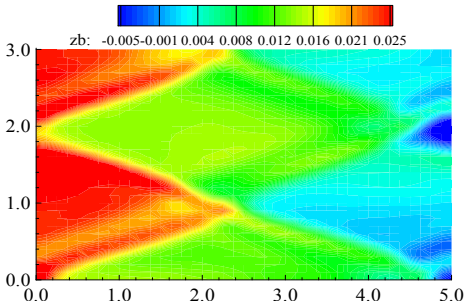

time = 2.25 hrs

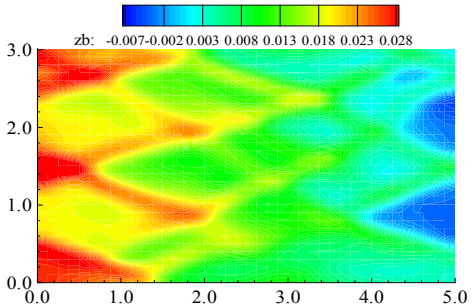

time = 1.6 hrs

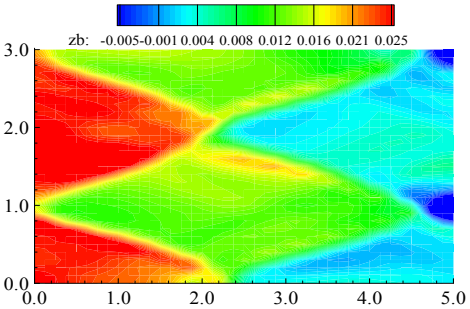

time = 2.6 hrs

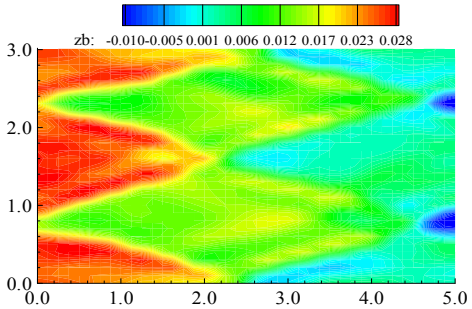

time = 2.6 hrs

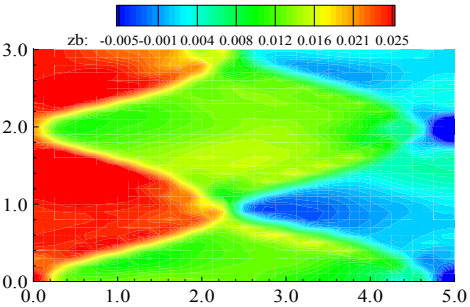

time = 3.1 hrs

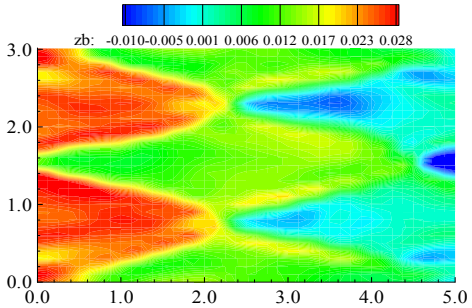

time = 3.1 hrs

(a) (b)

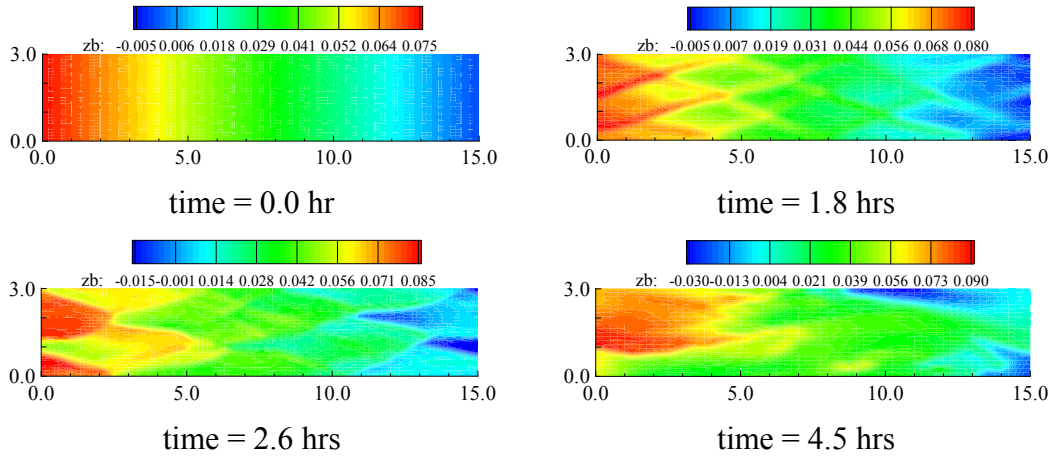

(c)

Fig. 6.3 Bed topographies: (a) Simulation No. 1; (b) Simulation No. 2; and (c) Simulation No. 3

and wavelength with decrease in bar mode with time, even up to mode n_b = 1, and finally they get highly irregular (not included herein).

Discussions on the simulation of multiple bars

In each simulation, the process of bed evolution is found to be rather different. This is caused by the influence of the domain length and the initial conditions. In the simulations no. 1 and 2, the stable patterns of multiple bars appear. The bar wavelength λ_b is forced to be equivalent to the domain length by the periodic boundary conditions because the domain is not long enough. It can be concluded that the large effect of the boundary condition seems to stabilize multiple bars. In addition, these two cases end up with different final patterns, where two different initial conditions result in two different final configurations: mode number three and four [(**Figs. 6.3(a and b)**]. These results suggest that there exist at least two equilibria that are induced by different initial conditions even under a rather strict boundary condition. Whereas, it is found in case of simulation no. 3 [**Figs. 6.3(c)**] that the bars with mode n_b = 4 and wavelength λ_b around 4 m firstly appear; then the variation in bar amplitude, bar wavelength and bar mode over time is continued, that indicates the state of the system non-equilibrium.

From the theory, the relation between the bar height H_b and the wavelength λ_b for several modes reveals that the bar height H_b corresponding to the modes n_b = 3 and 4 are 28 mm and 36 mm, respectively, when the wavelength λ_b is 5 m. In the simulations no. 1 and 2 in which the modes n_b = 3 and 4 appeared, respectively, and the wavelength is constrained to be 5 m by the domain length, the bar heights H_b are 32 and 38 mm, respectively. However, bars with n_b = 4, H_b = 40 mm, and λ_b = 5 m were observed in Fujita's experiment (Run B-4 at t = 2hr 33min). So the quantitative agreement is not perfect, though the qualitative agreement is found to be good among the simulation, experiment, and theory. **Fig. 3(c)** also shows that the lower modes give the larger bar height H_b. This causes the fact that higher modal multiple bars with shorter wavelength tend to merge each other, and evolve into lower modal bars with larger bar height. The irregularity that appeared in the reduction process of the bar mode suggests the nonlinear interaction between multiple modes of bars. The nonlinear interaction may be an essential factor to cause the strong irregularity and instability of braided streams.

6.4 Formation of Bars at Prototype Scale

6.4.1 Conditions of the Numerical Computation

The flow and stream parameters are considered here based on prototype examples, but not intended to precisely reproduce a particular river. Two computation domains of different lengths with same channel properties with bed slope 0.00033 are considered in prototype scale with the dimensions as mentioned in the table (**Table 6.5**) below. A uniform discharge of 1500 m^3/s is considered for two simulations for which the aspect ratio β becomes 323, and the Froude number Fr gets the value 0.49. The median size of bed material is taken 0.3 mm.

Table 6.5 Conditions of the numerical computation for bar-formation at prototype scale

Simulation No.	**1**	**2**
Domain B (m) x L (m)	500 x 1000	500 x 2500
Δt (s)	0.1	0.1
Z_0 type	Sine	Sine
Total time (day)	14	14

Water level at the downstream open boundary is set by the uniform flow condition, as required by the subcritical state of flow. Sediment discharge per unit width is calculated by using the local hydraulic conditions, with the sediment transport formula. Periodic boundary conditions in the streamwise direction is applied for better response in bar formation process getting infinite channel length, and small perturbations (Sine) combined with the bed slope are provided as an initial condition. The computation is made for 14 days in each simulation for the full development of large bars.

6.4.2 Results and Discussions

A well-formed bar train are clearly observed which migrates downstream along the channel increasing their amplitudes; after around 5.0 days, they grow into stable and regular forms with bar mode $n_b = 4$ from both simulations. **Figs. 6.4(a and b)** show a time sequence of plan views of bed topographies in the two simulations. The channel bed progressively gets a characteristic alternate pattern in which deep pools follow deposition fronts. Also this is studied with higher discharge than the present one, the growth rate of bars is observed much smaller than the present case because the development of bars is restricted. These results are not included herein. The wavelength of bed-topography is found almost same though the bars are growing with the increase in their heights. The bars are asymmetrical in along-stream section (**Fig. 6.5**) and have an avalanche face on the downstream side, i.e., the upstream side of the

bar-crest has a mild slope, and the downstream side has a sharp drop-off; and they migrate in the downstream direction.

The height of bars increases with the river bed degradation because little sediment transport exists in the high-elevation parts of the streambed, and the development of bars is promoted. Sufficient bar growth is observed with a pool-bar complex: flow is convergent in the pools and divergent on the bars [**Fig. 6.4(b)**, 14.0 days]. The bed configuration obtained by numerical simulation reproduces well multiple bar patterns present in the natural rivers, but irregularities in their evolutions are not reflected rightly.

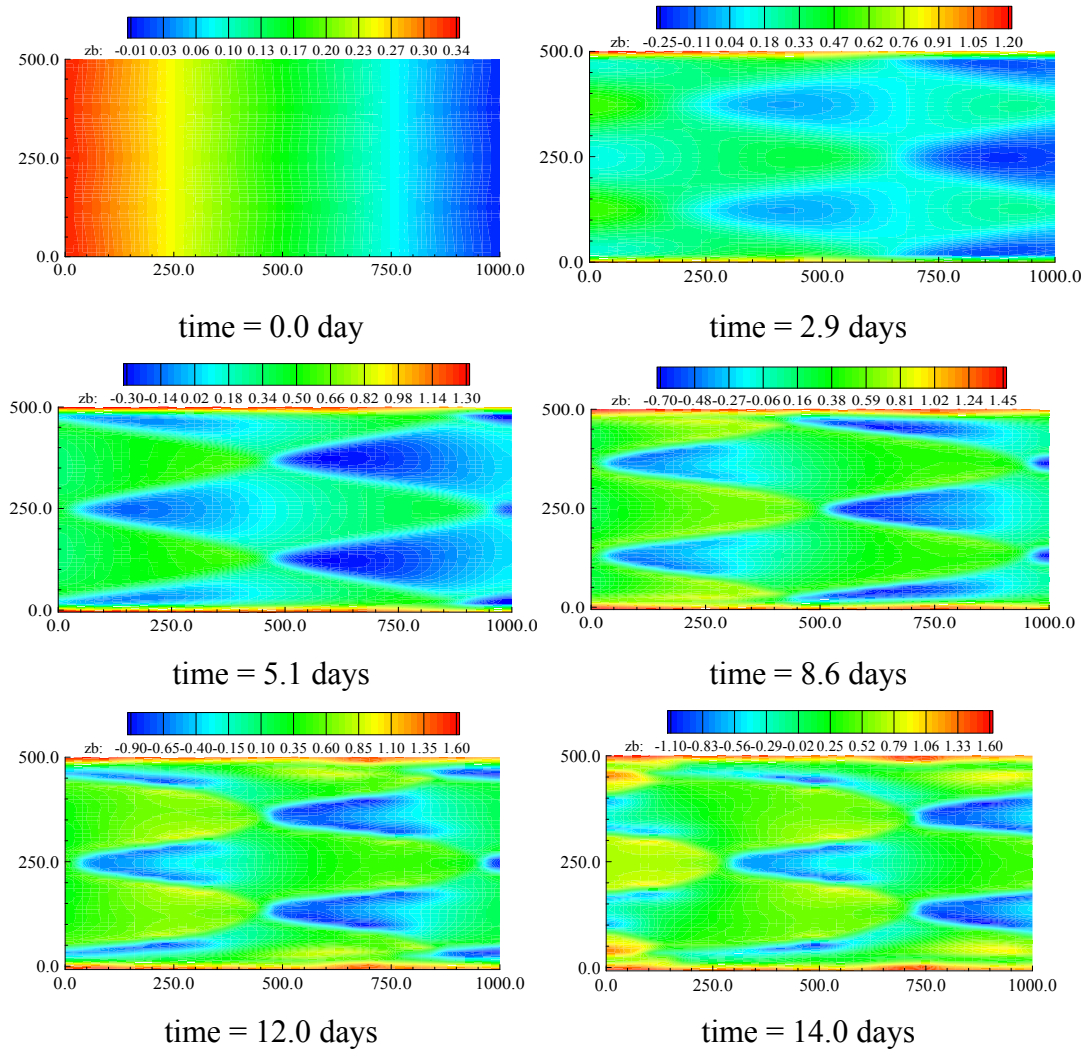

time = 0.0 day

time = 2.9 days

time = 5.1 days

time = 8.6 days

time = 12.0 days

time = 14.0 days

(a)

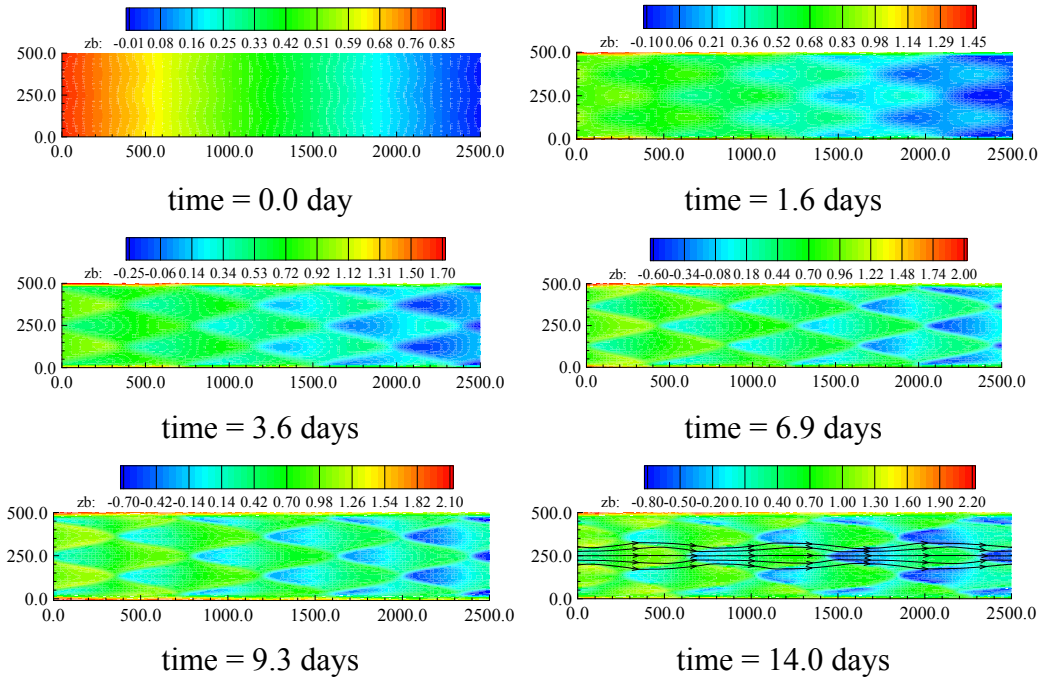

(b)

Fig. 6.4 Bar topographies at natural scale: (a) Simulation No. 1; and (b) Simulation No. 2

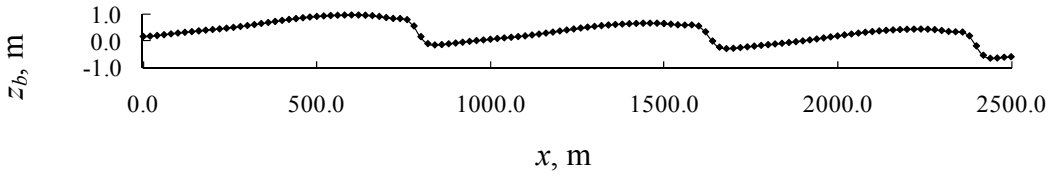

Fig. 6.5 Bed profile (longitudinal) at 247.0 m and time = 9.3 days [**Fig. 6.4(b)**]

Some convenient and representative variables describing important characteristics of bar morphologies are chosen as: height of bar, length of bar, and velocity of bar displacement, i.e., bar celerity.

Bar height

The growth of bar height with respect to time is depicted in **Fig. 6.6**. The general trend followed in the plotted curves from both simulations indicates that the evolution

of the bar heights does not get the equilibrium state yet, i.e., stable patterns are yet to be established; they tend to be equilibrium.

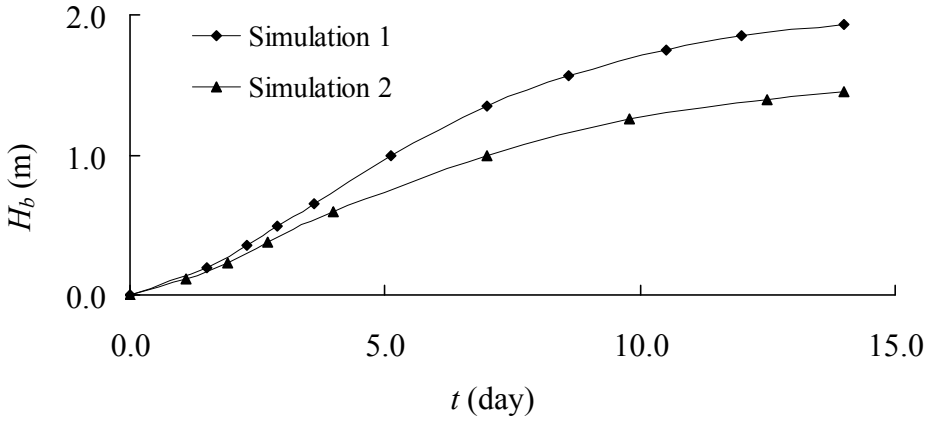

Fig. 6.6 Growth of bar-height (H_b) with respect to time (t)

Bar length

Bar length is calculated as the longitudinal distance between two subsequent zero-downcrossing points, located around the position of the bar crest. This is found around 500.0 m and 415.0 m in the simulations no.1 and 2, respectively.

Bar celerity

The migration velocity of the bars is estimated by tracking a selected bar crest over time. This is found around 5.8 m/hr for simulation no. 1 and 6.0 m/hr for simulation no. 2.

6.5 Conclusions

In this study numerical simulation is employed to examine bar formation in straight channels with the use of 2D model, RIC-Nays and this was capable to reproduce alternate and multiple bars. The method of describing bar formation process by numerical simulation shows reasonably good agreement when compared with theoretical and experimental results. At short domain length, stabilized multiple bars seem due to the periodic boundary conditions. However, the irregularity appeared in

the reduction process of the bar mode at longer domain might due to the nonlinear interaction between multiple modes of bars.

The multiple bar patterns present in nature are reproduced by the numerical computation in this study, where the evolution of bars with a pool-bar complex can be observed; but their heights and irregularities in bar evolutions with different wavelengths are not reproduced rightly; variation in discharges with some other local hydraulic factors may be responsible for these in nature.

There are some dissimilarities in bar formation processes between experiment and prototype scales such as irregularities in bar formations, time required for equilibrium state, and so on. Bar irregularities are observed in experiment scale for longer domain length compared with width of the channel, i.e., for higher length-width ratio, whereas it is not recognized in prototype scale. Also time required for the equilibrium state of flow is several hours in experimental scale; however it is several days in the prototype scale, when it tends to be equilibrium. These discrepancies may due to the differences in bed slope which is much higher in flume experiments and scale in dimension, respectively.

CHAPTER 7

INTERACTIONS OF GROYNES WITH SANDBARS

Summary

Bedforms in various scales are very common features in alluvial rivers with fine sand as in Bangladesh. These, not only, interrupt the inland waterways at low flow, but also make the channels highly unstable forming anabranches, influencing bank erosion, and so on. Destabilization of these alluvial structures from some areas is important to establish a stable water course; at the same time, stability of the bars which are important habitats for many species or the islands in the rivers where numbers of people are living should also be considered. Groynes have key roles to play in such cases. So, this study explores the interaction between sandbars and groynes in a schematized channel of Jamuna, which is crucial for better management of river engineering. 2D model, RIC-Nays is utilized in the study after confirmation through theoretical and experimental results. Simulation results reveal that accelerating flow due to intrusion of groynes triggers the sediment movement in the main channel, moves the bars reducing their scale, and finally disappears.

7.1 General

As has been discussed in the preceding chapter (Chapter 6), the bed-forms in various scales are common features in lowland rivers. The large-scale alluvial structures greatly hamper the navigational routes at low flow time. Also the presence of these bars influences bank erosion, forms anabranches, and thus, makes the channels highly unstable. These are to be destabilized from some regions to minimize the above problems, also to establish thalweg for navigation. Moreover, there are some large sandbars (islands) inside the river, where a large number of people are living; also the sandbars are the important habitats for various species in the river ecology. Stability

of these bars should also be considered to make available the lands for the people or the aquatic lives in the river. Thus, the importance of maintaining the large bars stable, where people are to live; on the other hand, destabilization of the bars from some areas to maintain thalweg for inland water transports at low flow as well as to protect the riverbanks from recession at high flow are to be considered critically, where groynes play the key roles. Therefore, the behavior of sandbars due to intrusion of groynes into the river has become very urgent to investigate, for better management of river engineering.

A number of researchers have contributed to the study of bar formation processes through theoretical studies (Parker, 1975; Colombini *et al.*, 1987; Izumi and Pornpromin, 2002), experimental observations (Ikeda, 1984; Fujita, 1989), and numerical studies (Takebayashi *et al.*, 2001; Pornprommin *et al.*, 2002, Alauddin *et al.*, 2011e). Although numbers of discussions on the bar formation processes have been made as mentioned, but the characteristics of large sandbars due to installing groynes are a very few (Abe, 1982). Therefore, this study deals with the interactions between groynes and large sandbars, and thus, this chapter presents the responses of the large sandbars as observed in lowland rivers against the groynes installed in a series.

The macroscale bedforms in the hierarchical bedform classification of Jackson (1975) and Church & Jones (1982) in Jamuna are considered here as the initial bed condition with the channel dimensions of some of the simplified subchannels of the river. This is attempted here to recognize the effect of groynes on the sandbars to understand better way the stabilization of channel dynamics through minimizing bank erosion, maintaining thalweg for navigation; also to understand the careful applications of groynes in the river so as not to harm the important islands where living people may be affected. The importance of the bars in some areas of the river can also be prioritized from ecological aspects, as they are very important habitats for various species of river environments.

7.2 Procedure

The responses of alluvial channels with large sandbars at natural scale against a series of groynes are considered to study with numerical model. The 2D model, RIC-Nays is utilized in the present study. The CIP method is utilized for the advective terms in the water flow equations, and a depth-averaged parabolic eddy viscosity model is used in considering the turbulence. The model was first validated for the detailed bar-formation processes for both alternate and multiple bar cases at experiment scale, including the effect of initial and boundary conditions, the cause of reduction of bar mode observed in experiments, and so on. The method of describing bar formation processes by numerical simulation showed reasonably good agreement when compared with theoretical (Pornprommin and Izumi, 2001; Izumi and Pornprommin, 2002), and experimental (Fujita and Muramoto, 1985; Fujita, 1989) results, the details of which are not included herein (Chapter 6).

This study is conducted for the channels of two types of bars observed in nature: alternate and multiple bars; so that two schematized channel reaches of two different widths of same length are considered, which have very mild slope. Hydraulic and sedimentological parameters, and geometry of the model channels are taken here in conformity to some typical subchannels of Jamuna River, and its high flow condition is considered. The flow and channel parameters considered in the model reaches are presented in **Table 7.1**, where the simulation no.1 is for alternate bar, and no. 2 for multiple bars, and 'Sine' in the table means that initial bed level Z_0 is set to be a sinusoidal shape.

Table 7.1 Flow and channel parameters of the schematized channels

Simulation No.	**1**	**2**
Water discharge Q (m^3/s)	1280	2400
Domain B (m) x L (m)	160 x 4500	300 x 4500
Slope S (cm/km)	7.5	7.5
Sediment Diameter d (mm)	0.2	0.2
Initial bed type Z_0	Sine	Sine

As large sandbars generally exist in the lowland rivers, these are provided in the model reach at natural scale as an initial condition; which can be formed under some strict initial and boundary conditions, as discussed in the preceding chapter (not included herein). The bedforms considered here are available in almost all flow conditions in the river, but in simplified form. Then the groynes are placed in a series on one side (right bank) of each channel, one for alternate bars and the other for multiple bars, with a length L_g of 30.0 m and 40.0 m, respectively, and interval S_g of 150.0 m for each, i.e., groyne length-channel width (L_g/B) and groyne aspect (S_g/L_g) ratios for both channels are 1/5.33 and 1/7.5, and 5 and 3.75, respectively. For better understanding the effect of groynes on the sandbars, the channels are considered for both without and with groynes. Thus, four sets of simulation conditions are fixed in the study: the channels with alternate bars for both without and with groynes, and the channels with multiple bars for both without and with groynes; these are termed here as sim1_ngr and sim1_gr, and sim2_ngr and sim2_gr, respectively.

The numbers of cells in longitudinal and transverse directions are 360 and 32, and 360 and 30, in simulation no. 1 and no. 2, respectively. Simulations are made for the duration of 7 days for alternate bars and 14 days for multiple bars, when the temporal variations of variables are considerably reduced, and in this study we use a computational time step of 0.2 sec. Water level at the downstream open boundary, as required by the subcritical state of flow, and also initial water surface are set by the uniform flow condition. Sediment discharge per unit width is calculated by using the local hydraulic conditions, with the sediment transport formula. For better response of the channels periodic conditions in the streamwise direction have been applied for the computation of both flow and bed topography that describes the fluvial processes pass an infinite series of emerged groynes.

7.3 Results and Discussions

As in no-groyne case, the flow is not controlled and hence, no influence in accelerating the flow in the main channel, almost same geometry of bars, i.e., bar

length, bar mode, and so on, is maintained, except a little change in altitude. Due to high flood flow condition as considered in this study in the straight regular channels, initial configurations of bed with large bars move downstream and altitude of these bars is reduced a little, slowly with time. However, intrusion of groynes in the channels diverted the flow toward the main channel from the near bank regions where the groynes installed, and hence, flow is accelerated there. Transverse distributions of streamwise velocities for the channels with alternate and multiple bars, and with and without groynes have been presented in **Fig. 7.1** (for the middle section, and 5th day results).

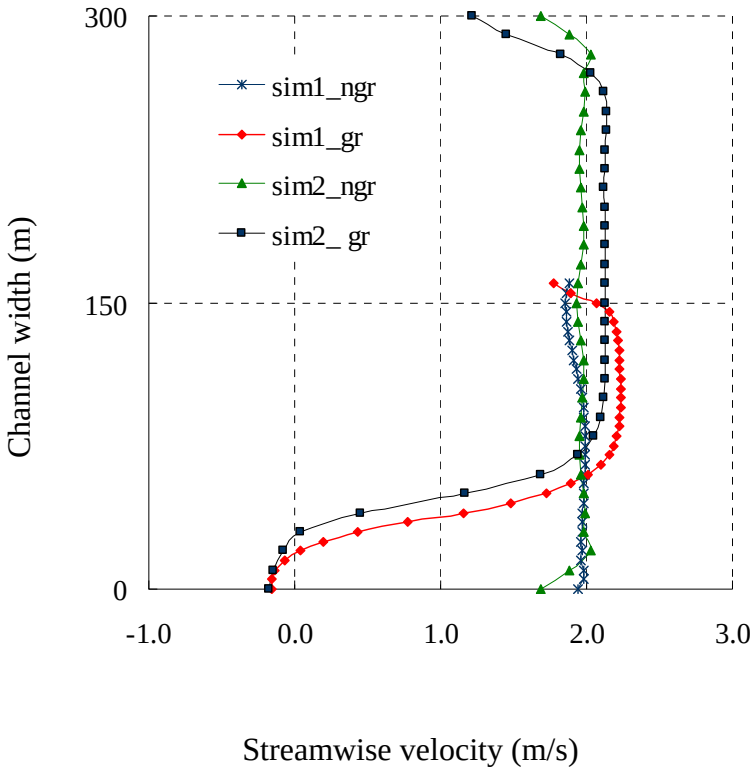

Fig. 7.1 Streamwise velocity profiles for both channels (without and with groynes: sim1_ngr, sim1_gr, and sim2_ngr, sim2_gr) (5th day, at mid-section)

Therefore, the arrangement of a series of groynes decreases the effective width of channel, triggers the sediment movement, and restores the morphology almost in the whole channel. With the progress of time, bars change their forms, and move towards

downstream, gradually reducing these changes from the main channel region to the region close to the opposite side of the groyne embayments. These may due to the effect of less influence of groynes on the flow there.

These responses are found for both cases of alternate and multiple bars. Thus, due to the interaction of groynes, regular patterns of pool-bar complex get very irregular form, and even finally the bars disappear from the main channel as well as other regions with relatively less impact to the area close to opposite bank. This is also seen here that a channel-like formation is made near the normal line of groynes. Time sequences of the changes in bed topographies found from the simulations have been presented in **Fig. 7.2**, where a part of the channel reach has been shown, as the similar responses are recognized by the periodic boundary conditions. This may, however, differ in nature where irregularity (contraction, expansion, bend, and so on) in channels are present, due to some other local hydraulic phenomena, and so on. It is also checked with numerical simulation, not shown herein.

The reduction of altitude of bars is very high, and the change is very rapid when reacted against the series of groynes compared with that of without groyne case. The reduction of bar height (H_b) with respect to time (t) is presented with **Fig. 7.3** for the case of multiple bars, where the bar height is defined as the difference between the elevations of the crest and the trough in a wavelength of bars. Bar height is suppressed due to the decrease of channel width by a series of groynes. It can also be recognized from the criterion of bar evolutions, as proposed by Fujita *et al*. (1983) (**Fig. 7.4**); where higher width-depth ratio in respect of h/Δ (Δ is roughness height and related to sediment size; it is $\Delta = 100\ d$ for rippled bed) favors the formation of bars with various modes, and vice versa. In the figure, the channel conditions for both without and with groyne cases are also marked to understand the channel responses from the numerical simulation as mentioned above. It can be mentioned here that for the flow condition considered here, the shear velocity (u^*) exceeds the fall velocity (w_f) (ratio is 1.4); therefore, suspended mode of sediment transport prevails, and it is considered in the computation scheme.

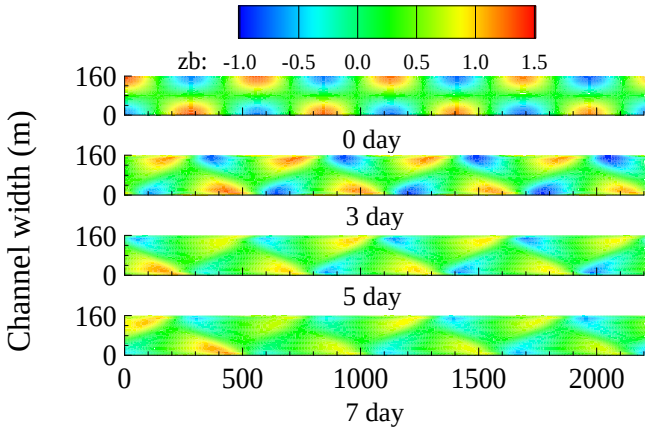
zb: -1.0 -0.5 0.0 0.5 1.0 1.5
Channel width (m)
160
0
0 day
3 day
5 day
7 day
0
500
1000
1500
2000
Longitudinal distance (m)

(a)

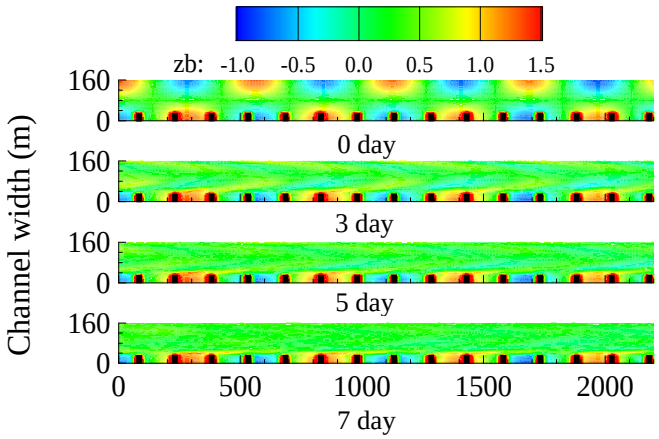
zb: -1.0 -0.5 0.0 0.5 1.0 1.5
Channel width (m)
160
0
0 day
3 day
5 day
7 day
0
500
1000
1500
2000
Longitudinal distance (m)

(b)

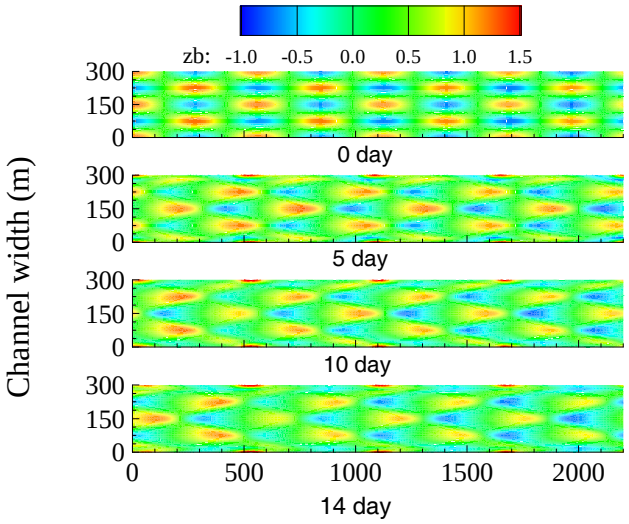

(c)

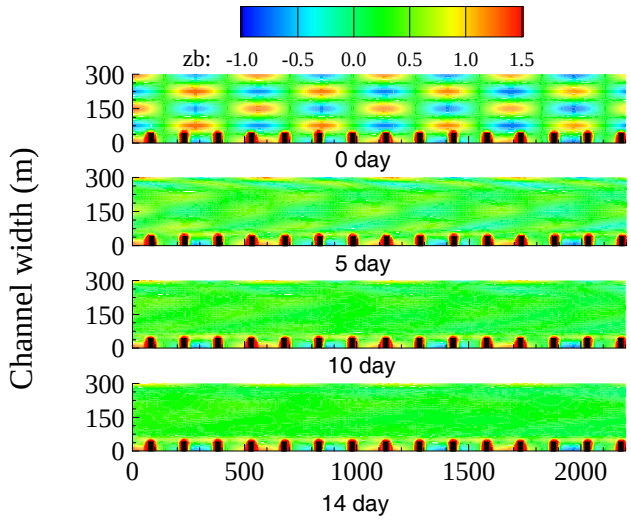

(d)

Fig. 7.2 Bed topographies: alternate bars (a) without and (b) with groynes; multiple bars (c) without and (d) with groynes

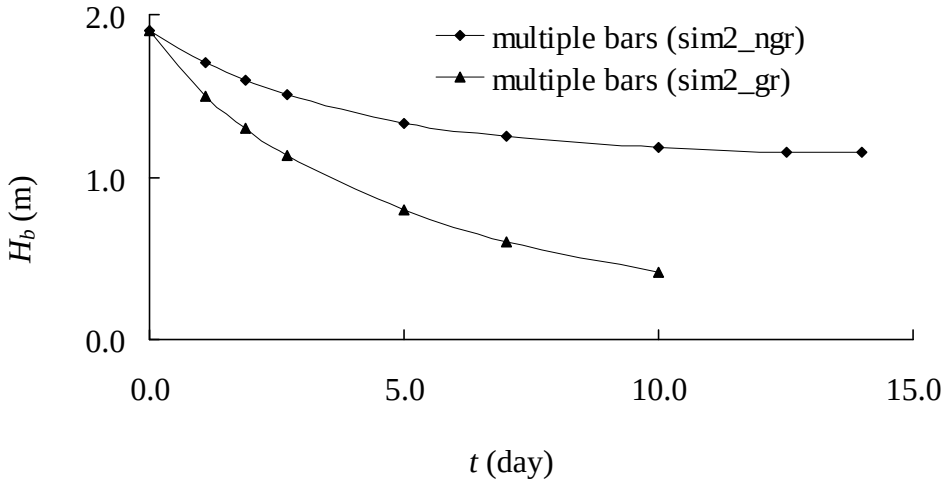

Fig. 7.3 Reduction of bar-height (H_b) with respect to time (t) for multiple bars (without and with groynes: sim2_ngr, sim2_gr)

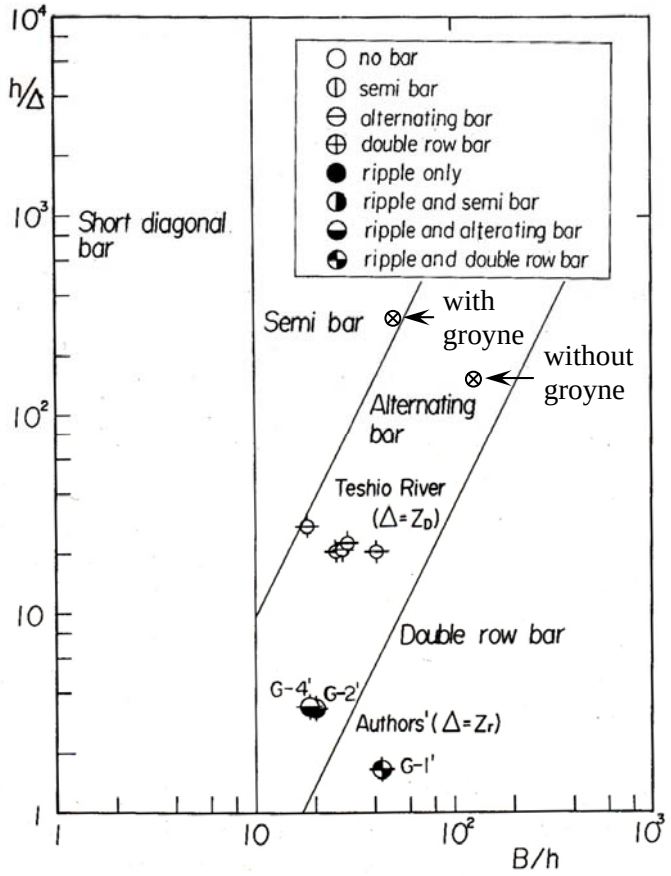

Fig. 7.4 Criterion for the formation of meso-scale bed configuration (Fujita *et al.*, 1983)

The bars adjacent to the banklines are not considered in estimating their heights, and calculation is made up to 10 days duration with groyne case, due to much irregularity of bedforms afterwards. The migration velocity of the bars is estimated by tracking a selected bar crest over time; and for the bars with groynes, this is done at initial stages due to getting very irregular forms later on. This celerity is found around 3.2 m/hr in the case of no-groynes, and 4.3 m/hr with groynes with almost similar values for alternate and multiple bars.

7.4 Conclusions

The responses of schematized lowland river channels with alternate and multiple bars at natural scale against a series of groynes are investigated here with a 2D numerical model. From the computation results, it can be concluded that placing of groynes accelerates the flow in the main channel, hence triggers the sediment transport there, and suppresses the bar height reducing the channel width. Accordingly, bar movement is increased changing their forms, and finally they disappear from the main channel for both alternate and multiple bar cases. Whereas this is not the case if groynes are not placed; at very high flow, only they change altitude a little keeping their regular forms unchanged. However, due to very irregular pattern of channels, this may differ for the involvement of some other local hydraulic factors in nature.

Different lengths of groynes in respect of channel width and different aspect ratios of groynes should be considered to determine the degree of impact in details from the groynes, to know to what extent groynes affect the bars and to what distances. Also irregularity of the channels must be considered in dealing with the field problem along with various flow conditions.

CHAPTER 8

CONCLUSIONS AND RECOMMENDATIONS

8.1 General

Under the present research, the interactions of groynes with various arrangements in both alignment and permeability, along with the characteristics of bedforms without and with groyne cases are investigated in straight lowland river reaches with primary focus on the morphological consequences. Both experiments and numerical simulations have been carried out in considering many aspects in the analyses.

First, numerical investigations are made to examine the influence of various orientations, and thus to identify the suitable alignment of groynes. Then, for some selected alignments of groynes, further modifications in the groyne configuration are made with various combinations of permeability, and detailed laboratory experiments are conducted to investigate the fluvial responses against the structures. The characteristics of the bedforms, very common features in alluvial rivers, are examined by numerical simulations; their interactions with groynes are then investigated utilizing the same numerical model.

The present research approached towards a sustainable solution for lowland river dynamics. In view of that, the following objectives were formulated in Section 1.3:

- Suitable orientation of straight groynes for lowland rivers,
- Optimum alignment of groynes for lowland rivers,
- Configurations of groynes modified with both alignment and permeability for the most suitable design for lowland river problems,

- Characteristics of sandbars in both experiment and prototype scales, and
- Interactions of groynes with sandbars in lowland rivers.

The overall conclusions drawn from the analyses presented in the preceding chapters are summarized in the following section. The final section gives some recommendations for implementation and future research.

8.2 Conclusions

The following conclusions can be drawn from the present research as presented in this dissertation:

8.2.1 Alignments of Groynes

First, the functions of straight groynes with various orientations (100^0, 90^0, 80^0, 70^0) are evaluated. The conclusions drawn from the numerical investigations are summarized as follows:

Larger angled (100^0, 90^0) groynes favor deposition in the groyne field to provide safety to the bank at high flow, but they do not favor rightly establishment of thalweg for navigation at low flow. Moreover, high separation of flow near groyne head, and hence huge scour are expected. Whereas, smaller angled (80^0, 70^0) groynes are functioning better in respect of deepening the channel bed at low flow, except that deposition near bank reduces; even near bank erosion occurred at high flow for 70^0 impermeable groyne. Thus the 80^0 angled groyne can be the suitable one in consideration of both navigation and bank erosion problems in sand-bed alluvial rivers.

Based on the results from the various orientations as discussed above, three modified alignments are designed such as 100^0-80^0, 90^0- 70^0, and a parabolic one with average angle 80^0, which are denoted in Chapter 4 as m1, m2, and m3, respectively. The

analyses from the numerical investigations for these modified alignments are concluded as follows:

The groynes of modified alignments function better compared with the conventional straight ones in consideration of both high flow and low flow problems, and no near bank erosion is present from any of the modified groynes. Among the three groynes (m1, m2, m3), m2 favors higher erosion in channel bed at both high flow and low flow conditions, and protects the channel bank from erosion at high flow as well. Furthermore, depth of scour near groynes is found negligibly small in the case of groyne m2; it is relatively higher for m1, and for m3, in between these two.

Thus, the modified groyne m2 can be recommended to optimize the problem of navigation and bank erosion both in sand-bed alluvial rivers.

8.2.2 Configurations of Groynes

Detailed laboratory experiments have been conducted for finding the most suitable configuration of groynes for lowland river problems. Various combinations of pervious portions are considered in the groyne structures, and some selected alignments are taken, which demonstrated better functions over other alternatives (discussed in the preceding section) along with the straight conventional one. From the fluvial responses against the structures, the following conclusions are drawn:

Flow separation is moderate in optimum aligned impermeable groyne (OA_Imp) and hence, local scour is reduced in area and magnitude both compared with the straight conventional one (St_Imp) due to its modification in alignment. Optimum aligned combined groyne (OA_com) favors much lower local scour to occur than all other models; also deposition in the groyne field as well as erosion in the main channel are relatively regular, but moderate in magnitude. Local scour is found higher in the case of modified bandal structure (OA_MBS) in area and magnitude both compared with the models, St_com and OA_com; however, two other important features: erosion and deposition are better responded.

Therefore, modified configurations, OA_com and OA_MBS, minimize flow separation and improve erosion in channel bed. Although OA_MBS is advantageous in respect of anti-erosion of bank and maintenance of navigation channel, much attention should be paid for structural safety at high flood. However, OA_Com offers more gradual transition from main channel to land, which favors ecological connectivity through better migration of species, thus an increase in biodiversity of bed fauna is to be expected. Also the less turbulent flow climate in the groyne field further enhances ecological potential.

The features explored from the laboratory investigations imply that further modification in the lower permeable portion in OA_MBS can be made with the arrangements for permeability of OA_com, so that the modified structure can serve optimal function both at high flow and low flow conditions to address the lowland river problems; however, scour condition by downflow at upstream side of the structure needs further investigations. Moreover, the combined structures (St_com, OA_com, and OA_MBS) minimize scour near groynes and strong return currents, so the aspect ratio could be increased, thus a cost-effective design approach can be expected.

8.2.3 Formation of Sandbars and their Interactions with Groynes

Numerical simulations of sandbars in both experiment and prototype scales are made in the straight channels to examine their formation processes and characteristics as concluded here as follows:

The method of describing bar formation processes by numerical simulation shows reasonably good agreement when compared with theoretical and experimental results. The multiple bar patterns present in the nature are reproduced by the numerical simulation in this study, where the evolution of bars with a pool-bar complex can be observed; but the bar heights and irregularities in bar evolutions with different wavelengths are not reproduced rightly; variation in discharges with some other local hydraulic factors may be responsible for these in nature. The discrepancies between

experiment and prototype scales are: bar irregularities and time to equilibrium state, which may due to differences in bed slope, and dimension scale, respectively.

Interaction of groynes with the sandbars in the schematized channels is investigated with 2D numerical model; the channels are considered for both without and with groyne cases for both alternate and multiple bars, to understand the effect of groynes rightly. The following are the conclusions drawn from the investigations:

Intrusion of groynes accelerates the flow in the main channel, and hence increases the sediment transport there. Accordingly, bar movement is increased changing their forms, and finally they disappear. Whereas this is not the case if groynes are not placed; at very high flow, only they change altitude a little keeping their regular forms unchanged.

8.3 Recommendations

The following recommendations can be made for future research:

- The analyses were based on the schematic river channels, i.e., idealized flow and sediment conditions were considered. It is recommended to use the procedures presented in this dissertation in a real-life situation. In this case, the behavior of the groynes is not only a function of the discharge, but also is of the location along the river. Groyne field located in a straight reach would behave differently from that located in a bend.
- In this study, morphological consequences of groynes were focused in evaluating their performances with a little discussion on hydraulics behind these. More detailed investigations on the hydrodynamics can be done, including three dimensional flow structures near groynes with corresponding measurements, to understand rightly the interactions of groynes with the flow, and modification of flow patterns from their various arrangements.
- In conducting the laboratory experiments, clear-water-scour conditions are maintained for all of the test runs, in which sediment transports and bed changes occurred in the control area, and scour phenomena is resulted rightly; detailed

laboratory experiments are recommended considering the sediment mobility throughout the channel for the proposed groyne design. Moreover, for the general applicability of the design, pilot projects in the field are very important to execute.

- Different lengths of groynes in respect of channel width, and different aspect ratios of groynes should be considered to determine the degree of impact on the bedforms in details, to know to what extent groynes affect the bars and to what distances. Also irregularity of the channels must be considered in dealing with the field problems along with varying flow conditions.

REFERENCES

Abe, S., 1982. On the effects of cross dykes on alternate bars, *Proc. of the Exeter symposium*. IAHS Publ. no. 138.

Alauddin M. and Tsujimoto T., 2010a. Alignment of groynes for bank protection and maintaining thalweg for navigation in alluvial river with fine sediment. *Proc. Int. Conference on Hydro-Science and Engineering*, Chennai, India, pp.51-60.

Alauddin, M. and Tsujimoto, T., 2010b. Interaction of groynes with large-scale sandbars at lowland rivers. *Proc. Int. Conference on Modern Hydraulic Engineering,* London Science Publishing Limited, pp. 51-54.

Alauddin, M. and Tsujimoto, T., 2011a. Optimum design of groynes for stabilization of lowland rivers. *Annual Journal of Hydraulic Engineering, JSCE*, Vol.55, pp.145-150.

Alauddin, M. and Tsujimoto, T., 2011b. Optimum configuration of groynes for stabilization of alluvial rivers with fine sediment. *Int. Journal of Sediment Research,* Vol.26, No.3, World Association for Sedimentation and Erosion Research (in printing).

Alauddin, M., Tashiro, T., and Tsujimoto, T., 2011c. Experimental investigation of channel responses against different configurations of groynes. *Advances in River Engineering, JSCE,* Vol.17 (in printing).

Alauddin, M., Tashiro, T., and Tsujimoto, T., 2011d. Design of groynes modified with both alignment and permeability for lowland river problems. *Journal of Applied Mechanics, JSCE,* Vol.67 (in printing).

Alauddin, M., Tashiro, T., and Tsujimoto, T., 2011e. Formation and characteristics of sandbars at both experiment and prototype scales. *International Review of Civil Engineering,* Vol.2, No.3, Praise Worthy Prize Publishing House (in printing).

Alvarez, J. A. M., 1989. Design of groins and spur dikes. *Proc. 1989 National Conf. on Hydraulic Engineering, ASCE,* New York, pp.296–301.

Ashida, K. and Michiue, M., 1972. Studies on bed load transportation for nonuniform sediment and river bed variation. *Disaster Prevention Research Institute Annuals,* Kyoto University, No. 14B, pp.259-273 (in Japanese).

Aya, S., Fujita, I., and Miyawaki, N., 1997. 2D models for flows in river with submerged groins. *In: Proc. 27th IAHR Congress*, San Fransisco, CA. USA, pp.829-837.

Bahar, S.M.H. and Fukuoka, S., 1999. The influence of submersible groins in series on bed geometry. *Annual Journal of Hydraulic Engineering, JSCE*, vol. 43, pp. 671-676.

Bradford, S. F. and Sanders, B. F., 2002. Finite volume model for shallow-water flooding arbitrary topography. *Journal of Hydraulic Engineering*, 128(3), pp.289–298.

Bristow, C.S., 1993. Sedimentary structures in bar tops in the Brahmaputra River, Bangladesh, *In: Braided Rivers* (Ed. By J.L. Best and C.S. Bristow), Spec. Pub. Geological Society, 75, pp.277-289.

CEGIS (Center for Environmental and Geographic Information Services), *Monitoring and prediction of bank erosion report series*, 2004, 2005, 2006, and 2007.

Chen, F. Y. and Ikeda, S., 1997. Horizontal separation in shallow open channels with spur dikes. *Journal of Hydroscience and Hydraulic Engineering*, 15(2), pp.15-30.

Church M, Jones D. 1982. Channel bars in gravel-bed rivers. *In Gravel-Bed Rivers: Fluvial Processes, Engineering and Management*, ed. RD Hey, JC Bathurst, CR Thorne, pp.291–338.

Coleman, J.M., 1967. *Deltaic Evolution.* Fairbridge (ed.), Encyclopedia of Earth Sciences, Reinhold, New York, NY. pp.255-261.

Coleman, J.M., 1969. Brahmaputra River: channel processes and sedimentation, *Sedimentary Geology*, 3, pp.129-239.

Colombini, M., Seminara, G., and Tubino, M., 1987. Finite amplitude alternate bars. *Journal of Fluid Mechanics*, 150, pp.213-232.

Cunge, J. A., Holly, F. M., and Verwey, A., 1980. Practical *Aspects of Computational River Hydraulics*, Pitman, USA.

Dalrymple, R. A. 1985. *Introduction to Physical Models in Coastal Engineering, in Physical Modeling in Coastal Engineering*. Rotterdam, Netherlands, pp.3-9.

Dean, R. G., 1985. Physical Modeling of Littoral Processes, in Physical Modeling in Coastal Engineering. Rotterdam, The Netherlands, pp.119-139.

Delft Hydraulics and DHI, 1996. FAP24 River Survey Project, Special Report 6, Floodplain Levels and Bankfull Discharge (prepared for FPCO), Dhaka, Bangladesh.

DeVries, M., Klaassen, G. J., and Struiksma, N., 1989. On the Use of Movable Bed Models for River Problems: State of Art. *Symp. River Sedimentation*, Beijing, China.

Duan, J.G., Li He, Fu, X., and Wang, Q., 2009. Mean flow and turbulence around experimental spur dike. *Advances in Water Resources*, Vol. 32(12). pp.1717-1725.

Elahi, K.M., Ahmed, Q.S., and Mafizuddin, M. (eds.), 1991. Riverbank erosion, flood and population displacement in Bangladesh, Riverbank Erosion Impact Study, Jahangirnagar Univ., Savar, Dhaka.

Engelund, F., 1974. Flow and bed topography in channel bends, *Journal of Hydraulic Division, ASCE*, Vol. 100, No. 11, pp.1631-1648.

FAP 21, 2001. *Guidelines and Design Manual for Standardized Bank Protection Structures*, Bank Protection Pilot Project, Govt. of Bangladesh, December, pp. 1.1-4.21.

Fazli, M., Ghodsian, M., and Neyshabouri, S.A.A.S., 2008. Scour and flow field around a spur dike in a 90° bend, *Int. Journal of Sediment Research*, Vol. 23, No. 1, pp.56-68.

Flood Forecasting and Warning Centre (FFWC), 2010. (http://www.ffwc.gov.bd/).

Fujita, Y., Muramoto, Y., and Furukawa, T., 1983. Formative conditions of meso-scale river bed configuration, *Annuals of disaster prevention research institute, Kyoto University*, Vol.25, No.B-2, pp.429-449.

Fujita, Y., 1989. Bar and channel formation in braided streams, River meandering, *Water Resources Monograph 12*, pp.417-462.

Fujita, Y. and Muramoto, Y., 1985. Studies on the process of development of alternate bars, *Bulletin of the disaster prevention research institute 35, Kyoto*, pp.55-86.

Fukuoka, S. and Yamasaka, M., 1985. Equilibrium height of alternate bars based on non-linear relationships among bed profiles, flow and sediment discharge, *Proc. of JSCE*, No. 357, pp.45-54 (in Japanese).

Ghodsian, M. and Vaghefi, M., 2009. Experimental study on scour and flow field in a scour hole around a T-shape spur dike in a 90° bend, *Int. Journal of Sediment Research*, Vol. 24, No. 2, pp.145-158.

Hansen, E., 1967. *The formation of meanders as a stability problem*, Hydraulics Lab., Tech. Univ. Denmark Basic Res. Prog. Rep. 13.

Halcrow, Sir William and Partners, DHI, EPC, and DIG, 1994. *River training studies of the Brahmaputra river*, Prepared for BWDB.

Halcrow and Hasconing, 1999. *River bank protection project, evaluation of the performance of hard points*. Review of damage during 1999 flood season, and recommended remedial works.

Hasegawa, K., 1983. *Hydraulic research on planimetric forms, bed topographies and flow in alluvial rivers*. PhD Dissertation, Hokkaido University.

Hudson, R. Y., Herrmann, F. A., Sager, R. A., Whalin, R. W., Keulegan, G. H., Chatham, C. E., and Hales, L. Z., 1979. Coastal Hydraulic Models, Special Report No. 5. *US Army Corps of Engineers*, Waterways Experiment Station, Vicksburg, MS.

Ikeda, S., 1974. On secondary flow and dynamic equilibrium of transverse bed profile in alluvial curved open channel. *Proc. of the Japanese Society of Civil Engineers*, No. 229,1974, pp.55-65.

Ikeda, S., 1984. Flow and bed topography in channels with alternate bars. In: River Meandering. *Proc. of the Conf. Rivers '83*. (ed. by CM. Elliott), ASCE, pp.733-746.

Ishii, C., Asada, H., and Kishi, T., 1983. Shape of separation region formed behind a groyne of non-overflow type in rivers. *XX IAHR Congress*, Moscow, USSR, pp.405-412.

Itakura, T. and Kishi, T., 1980. Open channel flow with suspended sediments. *Proc. of ASCE*, HY8, pp.1325-1343.

Izumi, N. and Pornprommin, A., 2002. Weakly nonlinear analysis of bars with the use of the amplitude expansion method. *Proc. of JSCE*, 712, pp.73-86 (in Japanese).

Jansen, P.P., van Bendegom, J., van den Berg, J.H., de Vries, M., and van Zanen, A., 1979. *Principles of river engineering – The non tidal alluvial rivers.* Delftse Uitgeversmaatschappij, Delft, The Netherlands.

Jackson, R.G., 1975. Hierarchical attributes and unifying model of bed forms composed of cohesionless material and produced by shearing flow. *Geological Society of America Bulletin 86*, pp.1523–1533.

Jia, Y. and Wang, S. Y., 1999. Numerical model for channel flow and morphological change studies. *Journal Hydraulic Engineering*, 125(9), pp.924-933.

Kang, J.G., Yeo, H.K., Kim, S.J. and Ji, U., 2011. Experimental investigation on the local scour characteristics around groynes using a hydraulic model. *Water and Environment Journal*, Vol. 25(2), pp.181-191.

Kishi, T., Yamazaki, S., and Enoki, K., 1966. Suspension of bed materials by water waves. Proc. *21st Annu. Conference of Japan Society of Civil Engineers* (in Japanese).

Kitamura, K., 2003. Experimental Study on Flow and Bed Deformation around a series of Spur Dykes. *Bachelor's Thesis*, Kyoto University (in Japanese).

Klaassen, G. J. and Vermeer, K., 1988. Channel characteristics of the braiding Jamuna river, Bangladesh. *Int. Conference on River Regime*, Published by John Wiley & Sons. Ltd, pp.173-189.

Klaassen, G.J., Douben, K., and van der Waal, M., 2002. Novel approaches in river engineering. *River Flow 2002* (eds., Bousmar and Zech), pp.27-43.

Klingeman, P.C., Kehe, S.M., and Owusu, Y.A., 1984. *Streambank erosion protection and channel scour manipulation using rockfill dikes and gabions*. Rep. No. WRRI-98, Water Resources Research Institute, Oregon State Univ., Corvallis, Ore.

Krebs, M., Zanke, U., and Mewis, P., 1999. Hydro-Morphodynamic modelling of groin fields. *In: Proc. 28th IAHR Congress*, Graz, Austria.

Kuhnle R.A., Alonso C.V., and Shields Jr F.D., 2002. Local scour associated with angled spur groynes. *Journal of Hydraulic Engineering*, ASCE, Vol. 128, No. 12, pp.1087-1093.

Kurabayashi, H. and Shimizu, Y., 2002. Numerical calculation of bed deformation in braided stream with emerged mid-channel bars. *Annu. Journal of Hydraulic Engineering, 46, JSCE*, pp.743-748 (in Japanese).

Martin, J. L. and McCutcheon, S. C., 1999. *Hydrodynamics and Transport for Water Quality Modeling*. Lewis Publications, Boca Raton, Florida.

McCoy, A., Constantinescu, G., and Weber, L. J., 2008. Numerical investigation of flow hydrodynamics in a channel with a series of dykes. *Journal of Hydraulic Engineering*, 134(2), pp.157–172.

Mojtaba, G.K. and Abbas, B.G., 2009. Effect of groynes opening percentage on river outer bank protection. *Journal of Applied Science*, 9(12), pp.2325-2329.

Mosselman, E., 2005. Bank protection and river training along the braided Brahmaputra-Jamuna River, Bangladesh. *Braided Rivers* (eds., Smith, Best, Bristow and Petts), Blackwell Publishing, pp.270-281.

Muraoka, H., Fushimi, T., Kadota, A., and Suzuki, K., 2009. Changes of bed configuration caused by a permeable groyne of stone gabion. *33rd IAHR Congress: Water Engineering for a Sustainable Environment*, pp.1364-1371.

Muto, Y., Imamoto, H., and Ishigaki, T., 2000. Turbulence characteristics of a shear flow in an embayment attached to a straight open channel. *Proc., of the 4th Int. Conf. on HydroScience and Engineering, IAHR*, Seoul, Korea, 232.

Muto, Y., Kitamura, K., Khaleduzzaman, A.T.M., and Nakagawa, H., 2003. Flow and bed topography around impermeable spur dykes. *Advances in River Engineering, JSCE*, Vol.9 (in Japanese).

Nakayama, K., Sato, K., and Horikawa, Y., 1998. Numerical calculation of shallow water flow using CIP method. *Annu. Journal of Hydraulic Engineering, JSCE,* No. 42, pp.1159-1164 (in Japanese).

Nazim Uddin M., Hoque. M. M., and Rahman, M. M., 2010. Flow field around bank protection structures along the Jamuna River. *17th Congress IAHR APD 2010,* 21st to 24th February, Auckland, New Zealand.

O'Connor, B. A. and Nicholson, J., 1988. *A Three-Dimensional Model of Suspended Particulate Sediment Transport*, Coastal Engineering 12.

Ohmoto, T., Hirakawa, R., and Ide, K., 1998. Responses of secondary currents and sediments to submerged groynes. Annual *Journal of Hydraulic Engineering, JSCE*, vol.42, pp.1003-1008 (in Japanese).

Ouillon S, Dartus D., 1997. Three-dimensional computation of flow around groyne. *Journal of Hydrological Engineering, ASCE,* **123**(11), pp.962–970.

Parker, G., 1975. On the cause and characteristic scales of meandering and braiding in rivers. *Journal of Fluid Mechanics*, 76(3), pp.457-480.

Peng, J., Kawahara, Y., and Tamai, N., 1997. Numerical analysis of three-dimensional turbulent flows around submerged groynes. *In: Proc. 27th IAHR Congress,* San Francisco, USA.

Pornprommin, A. and Izumi, N., 2001. Nonlinear stability analysis of alternate and multiple bars. *2nd Proc. RCEM2001, IAHR*, Japan, pp.693-702.

Pornprommin, A., Teramoto, A., Izumi, N., Kitamura, T., and Tsujimoto, T., 2002. Numerical simulation of bar formation in straight channels by the NHSED2D model. *Journal of Applied Mechanics, JSCE*, pp.629-938.

Przedwojski, B., Blazejewski, R., and Pilarczyk, K.W., 1995. *River training techniques-fundamentals, design and application*. Balkema, Rotterdam, Netherlands.

Rahman, M.M., Nakagawa, H., Khaleduzzaman, A.T.M., Ishigaki, T., and Muto, Y., 2004. On the formation of stable river course. *Disaster Prevention Research. Institute Annuals*, Kyoto Univ., No. 47B, pp.601-616.

Rajaratnam, N. and Nwachukwu, B., 1983. Flow near groin-like structures. *Journal of Hydraulic Division,* 109(3), pp.463–480.

Rhie and Chow, 1983. A numerical study of the turbulent flow past an isolated airfoil with trailing edge separation. AIAA J., 21, pp.1525-1532.

Richardson, E. V., Stevens, M. A., and Simons, D. B., 1975. The design of spurs for river training. *Proc. 16th, IAHR Congress*, São Paulo, Brazil, pp.382–388.

Rozovskii, I.L., 1961. *Flow* of *Water in Bends* of *Open Channels.* Israel programme for scientific translations, Jerusalem, pp.224-231.

Rubey, W.W., 1933. Settling velocities of gravel, sand and silt particles. *American Journal of Science*, 25, pp.325-338.

Schumm S.A. and Winkley B.R., 1994. The character of large alluvial rivers. *In: The Variability of Large Alluvial Rivers* (Ed. by S.A. Schumm and B.R. Winkley), American Society pf Civil Engineers, New York, 1-13.

Sharmin, R., Rahman, M.M., Martin, A., Haque, E., Hossain, I., and Razzak, A., 2007. Effectiveness of bandalling and dredging for the maintenance of navigation channel in the Jamuna River. *Int. Conference on Water & Flood Management*, March 12-14, Dhaka, Bangladesh, pp.125-133.

Shields, F.D.Jr., Cooper, C.M., and Knight, S.S., 1995. Experiment in stream restoration. *Journal of Hydraulic Engineering, ASCE*, Vol. 121(6), pp.494-502.

Shimizu, Y. and Itakura, T., 1991. Calculation of flow and bed deformation with a general non-orthogonal coordinate system. *Proc. of XXIV IAHR Cong.*, Madrid, Spain, Vol. C, pp.241-248.

Smith, T. J., and O'Connor, B. A., 1977. A Two-Dimensional Model for Suspended Sediment Transport. *IAHR Congress*, Baden-Baden, West Germany.

SOS-arsenic.net, 2006. *Combat Arsenic Crisis in Ganga-Meghna-Brahmaputra (GMB) Plain*. http://www.sos-arsenic.net/english/bengal.html.

Takebayashi, H., Egashira, S., and Okabe, T., 2001, Stream formation process between confining banks of straight wide channels. *2nd Proc. RCEM2001, IAHR*, Japan, pp.575-584.

Teramoto, A, Nakamura, S., and Tsujimoto, T., 2003. Bank erosion with bar migration. *Int. Symp. Disaster Mitigation & Basinwide Water Management*, Niigata, Japan, B06, CD-ROM.

Thorne, C.R., Russell, A.P.G., and Alam, M.K., 1993. Planform pattern and channel evolution of the Brahmaputra River, Bangladesh. *In: Braided Rivers* (Ed. by J.L. Best and C.S. Bristow), Spec. Publ. Geological Society, 75, pp.257-276.

Tingsanchali, T. and Maheswaran, S., 1990. 2D depth-averaged flow computation near groyne. *Journal Hydraulic Engineering*, 116(1), pp.71-85.

Tominaga, A., Ijima, K., and Nakano, Y., 2001. Flow structures around submerged spur dikes with various relative height. *Proc., 29th IAHR Congress*, Beijing, 421–427.

Tsujimoto, T., Toda, Y., Furuhata, H., and Shionoya, H., 2010. Ecological function of series of groins and induced morphology in estuary segment of river with tidal motion - downstream reach of the Kiso River, Japan. *8th Int. Simp. Ecohydraul. 2010*, COEX, Seol, Korea, paper no. 274.

Uddin, M.J., 2007. RCC spurs in Bangladesh: Review of design, construction and performance. *MSc Thesis*, UNESCO-IHE, The Netherlands.

Uijttewaal, W. S. J., Lehmann, D., and van Mazijk, A., 2001. Exchange process between a river and its groyne fields - model experiments. *Journal of Hydraulic Engineering, ASCE*, 127(11), pp.928-936.

Uijttewaal, W.S.J., 2005. The effects of groyne layout on the flow in groyne fields: laboratory experiments. *Journal of Hydraulic Engineering*, Vol. 13(9), pp.782-791.

Uijttewaal, W.S.J., 1999. Groyne field patterns determined with particle tracking velocimetry. *Proc. 28th IAHR Congress*, Graz, Austria.

Van Heereveld, M.A. and Zijlstra, R.O.T., 2007. River Groynes for the Future - Harmonising today's demands in innovative groyne design. *In: Proc. the 32nd Congress of IAHR*. CORILA (ISBN 88-89405-06-6).

van Rijn, L.C., 1987. Mathematical modeling of Morphological processes in the case of Suspended Sediment Transport. *PhD Thesis*, Delft Tech. Univ., Delft, The Netherlands.

van Rijn, L. C., 1989. *The State of the Art in Sediment Transport Modeling, in Sediment Transport Modeling*, edited by Sam S.Y. Wang, 1989. American Society of Civil Engineers, New York.

van Rijn, L.C., Van Rossum, H., and Termes, P.P., 1989. Field Verification of 2D and 3D Suspended Sediment Models, *Journal of Hydraulic Engineering, ASCE*.

Watanabe, A., Fukuoka, S., Yasutake, Y., and Kawaguchi, H., 2001. Groin arrangements made of natural willows for reduction bed formation in a curved channel. *Advances in River Engineering, JSCE*, Vol.7, pp.285-290 (in Japanese).

Wikipedia, 2011. *Ganges-Brahmaputra-Meghna basins*. http://en.wikipedia.org/wiki/File:Ganges-Brahmaputra-Meghna_basins.jpg**.**

Yabe, T., Ishikawa, T., Kadota, Y., and Ikeda, F., 1990. A numerical cubic-interpolated pseudoparticle (CIP) method without time splitting technique for hyperbolic equations. *Journal of the Physical Society*, 59(7), pp.2301-2304.

Yossef, M.F.M. and de Vriend, H.J., 2010. Sediment exchange between a river and its groyne fields: mobile-bed experiment. *Journal of Hydraulic Engineering*, 136(9), pp.610–625.

Zhang, H., Nakagawa, H., Muto, Y., and Baba, Y., 2006. Numerical simulation of flow and local scour around hydraulic structures. *Int. Conf. on Fluvial Hydraulics*, Lisbon, Portugal, pp.1183-1693.

Zhang, H., Nakagawa, H., Kawaike, K., and Baba, Y., 2009. Experiment and simulation of turbulent flow in local scour around a spur dyke. *Int. Journal of Sediment Research*, Vol. 24, No. 1, pp.33-45.

Zhang, H., Nakagawa, H., Baba, Y., Kawaike, K., and Teraguchi, H., 2010. Three-dimensional flow around bandal-like structures. *Annu. Journal of Hydraulic Engineering, JSCE*, vol. 54, pp.175-180.

Zhao, D. H., Lai, J. S., Shen, H. W., Tabios, G. Q., III, and Tan, W. Y., 1994. A finite-volume two-dimensional unsteady flow model for river basins. *Journal Hydraulic Engineering*, 120(7), pp.863–883.

Zhou, W. and Chen, J., 1998. River morphology and channel stabilization of the Brahmaputra River in Bangladesh. Int. *Journal of Sediment Research*, Vol. 13, No.4, pp.44-58.

Zimmermann, C., 1977. Roughness effects on the flow direction near curved stream beds. *Journal of Hydraulic Research*, 15, pp.73-85.

LIST OF FIGURES

LIST OF TABLES

LIST OF SYMBOLS

Roman Symbols

$a^{'}$	$a' = B^{*}/\tau_{*} - 1/\eta_0$ = parameter in Eq. (56)	
B	channel width	m
B_{*}	parameter in Eq. (56)	
c	local concentration of suspended sediment	-
c_b	reference concentration at $z = 0.05h$	-
C	depth-averaged concentration	-
C_d	bed friction coefficient	-
C_{dv}	drag coefficient of vegetation	-
d	sediment diameter	m
d_v	cylinder diameter	m
D_x,D_y	diffusion terms in x and y directions, respectively	
Fr	Froude number	
g	acceleration due to gravity g = 9.81 m/s^2	m/s^2
h	depth of flow	m
h_l	flow-depth at low flow	m
h_{imp}	depth of flow in impermeable groyne case	m
H	water surface elevation	m
H_b	height of bar	m
I_e	Energy slope	
k	turbulence kinetic energy	m^2/s^2
K_v	permeability factor	-
K_c	coefficient in Eq. (55)	
L	length of channel reach	m
L_g	length of groyne	m
n	transverse direction perpendicular to streamline	
N_a	density of cylinder in permeable groyne	-
n_m	Manning's roughness coefficient	s/m$^{1/3}$
n_b	bar mode	
N_{*}	coefficient to describe the intensity of secondary flow	
q_b	bedload transport rate in the depth-averaged velocity direction	m^2/s

q_{su}	rate of entrainment of suspended sediment	m/s
q_x	bedload transport rate per unit width in *x*- direction	m^2/s
q_y	bedload transport rate per unit width in *y*- direction	m^2/s
Q	water flow rate (discharge)	m^3/s
r	normalized hydrodynamic forrce	
r'	fluctuation component of r	
r_s	radius of curvature of a streamline	m
Re	Reynolds number	
s_g	specific gravity of sediment	
s	streamline direction	
S	bed slope	
S_g	spacing of groynes	m
t	time	s
u	depth-averaged velocity components in *x*- direction	m/s
u_{bn}	near-bed velocity in *n*- direction	m/s
u_{bs}	near-bed velocity in *s*- direction	m/s
u_w	slip velocity at wall	m/s
u_*	shear velocity	m/s
u_{*c}	critical shear velocity	m/s
U_{imp}	mean velocity from impermeable groynes	m/s
v	depth-averaged velocity components in *y*- direction	m/s
V	total velocity of flow	m/s
V_b	total flow velocity at bottom	m/s
V_n	sediment movement velocity component in *n*- direction	m/s
V_s	sediment movement velocity component in *s*- direction	m/s
w_f	settling velocity of sediment	m/s
x	component of the Cartesian coordinate in streamwise direction	
X_g	downstream distance of scour hole from the groyne	m
y	component of the Cartesian coordinate in transverse direction	
Y_{ch}	distance of main channel from the bankline	m
Y_g	distance of scour hole from the bankline	m
z	component of the Cartesian coordinate in vertical direction from initial bed	
z_b	bed elevation	m
z_0	initial bed elevation	m

Greek Symbols

α_*	coefficient in Eq. (55)

β	angle of sediment transport direction with *x*-axis	
β_s	$\beta_s = w_f h/\varepsilon_s$ = parameter in Eq. (53)	-
β_v	parabolic function for velocity distribution $\beta_v = 3(1-\sigma_v)(3-\sigma_v)$	
β_b	channel aspect ratio = B/h	
β_g	groyne aspect ratio = S_g/L_g	
δ	angle between main stream direction and flow near bed	
Δ	roughness height in rippled bed	m
Δ_g	submerged specific gravity of sediment $\Delta_g = (\rho_s - \rho)/\rho$	
Δt	time step	s
ΔZ_{ch}	erosion in channel bed	m
ΔZ_g	scour near groyne	m
ΔZ_{gf}	deposition in groyne field	m
ε	dissipation rate of the turbulence kinetic energy	m^2/s^3
ε_s	sediment diffusivity	m^2/s
ϕ	angle between the sediment movement direction and streamline	
ϕ_0	velocity coefficient (= V/u_*)	
η	transverse component of general coordinate	
η_0	coefficient in Eq. (56)	
γ	angle between *x*- and *s*-axis	
κ	Von Karman constant $\kappa = 0.4$	
λ	porosity of bed materials	
λ_b	bar wave length	m
λ_g	adjustment coefficient for slope gravitational effect	
μ_k	kinetic friction coefficient of bed materials	
μ_s	static friction coefficient of bed materials	
ν	kinematic viscosity	m^2/s
ν_t	eddy viscosity	m^2/s
θ	angle between *x*- and ξ–axis	
θ_c	critical angle of repose	
θ_s	angle of mainstream direction with *x*-axis	
ρ	density of water	kg/m^3
ρ_s	density of sediment	kg/m^3
σ_v	$\sigma_v = \dfrac{3}{\phi_0\kappa + 1}$	
σ^2	variance of hydrodynamic force	-

τ_{bx}	*x*- component of bottom-friction	N/m^2
τ_{by}	*y*- component of bottom-friction	N/m^2
τ_{vx}	*x*- component of vegetation drag	N/m^2
τ_{vy}	*y*- component of vegetation drag	N/m^2
τ_w	wall shear stress	N/m^2
τ_x, τ_y	*x* and *y* components of resistance to flow	N/m^2
τ_*	dimensionless shear stress on the bed	
τ_{*c}	dimensionless critical shear stress	
ς	z/h	
ξ	streamwise component of general coordinate	
Ω	parameter in Eq. (56)	
ζ	dummy variable = $= r^{'} \big/ \sqrt{2}\,\sigma$	

ACKNOWLEDGMENTS

The completion of this thesis owes the generous support received from many individuals whose contribution this dissertation possible, which I am indebted to. First, and foremost, my utmost gratitude goes to my honorable advisor, Prof. Tetsuro TSUJIMOTO for allowing me to conduct this research under his auspices, for his kindness, and most of all, for his patience in giving me constant support and advice throughout my research. Besides my advisor, I am deeply grateful to other members of the jury: Prof. Yuichiro FUJITA of Gifu University, Prof. Norimi MIZUTANI, Assoc. Prof. Yuji TODA, and Assoc. Prof. Takashi TASHIRO, for their encouragement and insightful comments.

I owe to the Monbukagakusho (Ministry of Education, Culture, Sports, Science and Technology, Japan) for providing me with this opportunity to acquire the knowledge and to expertise in River Engineering in order to contribute to the best possible way of overcoming the alluvial river problems of my country and the world.

I would like to thank once again to Dr. Takashi TASHIRO for his constructive comments, continual encouragement, and untiring help during my difficult moments. His endless patience in both research and many other things are strongly impressed on my memory. I extend my sincere thanks to Dr. Makiko OBANA, and all other members of my laboratory including Ms. Fumi YAMAMORI, who contributed directly or indirectly to this dissertation. In particular, experimental work was an important part of this study, where many of the friends, especially Mr. Yoshimoto and Mr. Ma, graduate students, engaged and helped me to advance the work.

My warm thanks are due to Prof. B. C. Basak of DUET; his knowledgeful encouragement and way of thinking made a good basis for my high-level research.

Also sincere thanks and appreciations are expressed to Dr. Md. Nazim Uddin of DUET, who provided me with much information related to this study.

Last but not the least, I express my personal indebtedness and my loving thanks to my beloved wife, for her support, motivation, and sacrifices; and for being a wonderful wife and a mother for our sons Jonayed and Jobayer. My special gratitude is due to my elder brother for his constant spiritual encouragement and moral teaching.